ABSTRACT

Title of Dissertation:	STRATEGIES TO ENHANCE THE STABILITY AND POTENCY OF EXTRACELLULAR VESICLE THERAPEUTICS
	Anjana Jeyaram Doctor of Philosophy, 2019
Dissertation directed by:	Associate Professor, Dr. Steven M. Jay, Fischell Department of Bioengineering

As key mediators of intercellular communication, extracellular vesicles (EVs) have emerged as a new therapeutic modality, specifically via a microRNA (miRNA) transfer mechanism. Unlike synthetic carriers and liposomes, EVs can evade endosomal degradation, show low immunogenicity, and are able to cross biological barriers. Despite the advantages of using EVs as therapeutic carriers, there remain several obstacles to clinical translation. Intrinsic RNA levels in EVs are low and current exogenous loading methods are inefficient and may damage EVs or their nucleic acid cargo, which can ultimately impair bioactivity. Even if the therapeutic cargo can be loaded effectively, the stability of these formulations must be evaluated and improved to preserve potency after storage for use in clinical settings. Thus, we hypothesize that studying and developing new methods to load and store EVs can enhance our understanding of EVs and improve the delivery of nucleic acid cargo. Here, we develop two techniques for loading nucleic acid cargo into extracellular vesicles and assess the impact of different storage conditions on EV stability. Sonication was shown to be a viable method for cargo loading without inducing cargo and vesicle aggregation. Next, the stability of both endogenously therapeutic EVs and those loaded with cargo via sonication was assessed. -80°C storage preserved EV activity and -20°C or lyophilized EVs stored at room temperature were shown to be comparable. However, EVs loaded via sonication saw a loss in cargo retention within a week of storage. Lastly, we developed a novel method for loading based on the creation of a pH-gradient within EVs. This allowed for enhanced passive incorporation of negatively charged cargo into vesicles without perturbing the membrane. Collectively, the work in this dissertation improves our understanding of the methods used to preserve and enhance the potency of extracellular vesicle therapeutics. This information provides new knowledge on the nature of EVs and their durability, enhancing their potential as an important delivery vehicle.

STRATEGIES TO ENHANCE THE STABILITY AND POTENCY OF EXTRACELLULAR VESICLE THERAPEUTICS

by

Anjana Jeyaram

Dissertation submitted to the Faculty of the Graduate School of the
University of Maryland, College Park, in partial fulfillment
of the requirements for the degree of
Doctor of Philosophy
2019

Advisory Committee:
Associate Professor Dr. Steven Jay, Chair
Associate Professor Dr. Christopher Jewell
Assistant Professor Dr. Huang Chiao Huang
Professor John Fisher
Professor Peter Kofinas, Dean's Representative

Dedication

To my parents and my sister, Archana, for their continuous love and support, regardless of whether or not they understood my work.

And to the people who were with me for the ups and downs of research. Imaly, John, Leo, and George, I couldn't have done it without you.

Acknowledgements

I could not have done any of the following work without my incredible support system. First and foremost, I would like to thank my advisor Dr. Steven Jay for his guidance over the past five years. He has given me the opportunity to grow as a scientist and the independence to pursue a wide range of project areas. I am truly grateful to have joined his research group and glad to call him my mentor.

My experience would not have been the same without the original members of the lab, Tek, John, Divya, and Eli. It was a pleasure to build the lab together. In particular, Dr. Tek Lamichhane provided invaluable mentorship. Tek was always available for discussing new ideas and greeted any obstacle with a positive outlook. Also, I would be remiss if I did not thank the high school and undergraduate students who made this work possible: Bryana Rowley, Meghna Bhatt, Cristina Tous, Christopher Kuffner, and Leigh-Anne Worthington. Eli and Chris were essential in discussions to develop our idea for depot delivery of EVs and contributed essential knowledge of protein engineering. I look forward to seeing how you carry on and further develop our idea with future members of the lab. And a big thank you in advance to Louis Born and Stephanie Kronstadt for working with me to finish up the loose-ends of my projects.

I have been lucky to work with great collaborators who have contributed to the research in my dissertation. Samm Stewart and Dr. Xiaoming He provided input on stability studies and preservation strategies for biologics. Dr. Sheng Wang, Dr. Lin

Zou, and Dr. Wei Chao from the University of Maryland School of Medicine have helped greatly with performing *in vivo* studies and provided essential knowledge about sepsis and inflammatory diseases. I also have had the pleasure of working with a number of other collaborators on projects not directly part of my thesis. Though not included in my dissertation, these experiences helped to broaden my research expertise.

My committee members, Dr. Christopher Jewell, Dr. Huang Chiao Huang, Dr. John Fisher, and Dr. Peter Kofinas have generously put in the time and effort to help me produce a quality dissertation. Also thank you to Dr. Kimberly Stroka for serving on my proposal committee and providing feedback.

Lastly, this work was supported in part by a predoctoral fellowship from the Pharmaceutical Researchers and Manufacturers of America (PhRMA) Foundation.

Table of Contents

List of Tables

List of Figures

List of Commonly Used Abbreviations

EV: Extracellular vesicles

NTA: Nanoparticle tracking analysis

BCA: Bicinchoninic acid

qPCR: Quantitative polymerase chain reaction

ESCRT: Endosomal sorting complex required for transport

MVE/MVB: Multivesicular endosome/body

Nucleic acids

DNA: Deoxyribonucleic acid

ss DNA: single stranded DNA

ds DNA: double stranded DNA

RNA: Ribonucleic acid

miRNA: MicroRNA

ss miRNA: single stranded miRNA

ds miRNA: double stranded miRNA

siRNA: Short/small interfering RNA

Cell types

HEK293T; Human embryonic kidney cells

BDMSC: Bone marrow derived mesenchymal stem cells

HUVEC: Human umbilical vein endothelial cells

MCF-7: Michigan Cancer Foundation-7

Chapter 1: Introduction

Nucleic acid-based therapies, including DNA and various types of RNA, have emerged as a promising therapeutic approach [1–3]. However, unprotected nucleic acids quickly face degradation, ultimately limiting therapeutic outcomes [4]. A number of approaches have been explored to protect and delivery nucleic acid cargoes including viral and non-viral vectors. Yet, these approached still face a number of challenges in overcoming physiological barriers and ensuring effective delivery [5]. One potential way to address many of these challenges is through the use of extracellular vesicles (EVs).

EVs are natural carriers of information between cells and have demonstrated an ability to cross biological barriers, avoid endosomal degradation, and have low immunogenicity. Thus, EVs can combine the benefits of cell therapies and an advanced drug delivery system while avoiding many of the limitations of both. Thus, there has been an exponential increase in research focused on ways to use EVs as a therapeutic device (**Figure 1.1**). However, there remain many open questions and obstacles to eventual large-scale clinical translation of this technology.

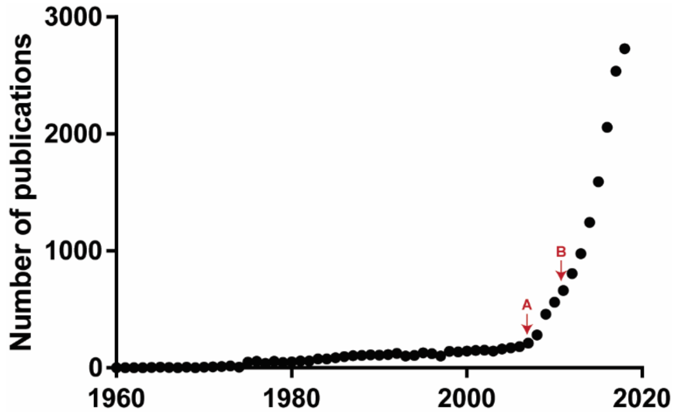

Figure 1.1. Extracellular vesicle publications indexed on PubMed each year. (A) In 2007, Valadi et al. published the first report of EVs mediating the transfer of RNA between cells (B) In 2011, Alvarez-Erviti et al. demonstrated the first proof of concept study for delivery of exogenous siRNA via EVs.

For example, therapeutic activity of EVs is often attributed to a microRNA (miRNA) transfer mechanism [6,7]. However, miRNA content in EVs may conform to a low occupancy model [8], potentially resulting in limited potency or an issue with dosage consistency upon clinical translation. By actively loading EVs with cargo, we can controllably deliver therapeutically relevant amounts of cargo and achieve a therapeutic effect with lower EV dosages. Further, it is unclear how stable EV-associated miRNAs are, with prior experience with cell-based products suggestive of specialized storage needs for preservation of function. If EV formulations are not stable in more conventional methods of storage than -80°C, then this technology cannot become widespread. Further, due to the nature of shipping and handling of materials, EVs may undergo an undetermined number of freeze-thaw cycles. Understanding the effects of these conditions as well as improving the stability is essential for clinical translation. Without improved stability, EV therapies will remain limited.

Thus, better ways to enhance and preserve the potency of these vesicles can improve their clinical relevance. The work in this dissertation combines molecular biology and engineering techniques in both cell and animal models to study methods of enhancing EV potency. Knowledge from lipid-based drug delivery and cell therapies were used to develop novel modes of cargo loading and evaluate storage conditions.

The following chapter, **Chapter 2**, provides an overview of extracellular vesicles, beginning with their innate functions in physiological processes and reviewing studies taking advantage of EV properties for therapeutic applications. **Chapter 3** investigates the use of sonication as a method to load cargo, in particular nucleic acids, into EVs. **Chapter 4** evaluates the potency of innate and loaded EV function after storage at various conditions to determine the optimal storage conditions for eventual clinical use. **Chapter 5** explores a novel loading method based on creating a pH-gradient in EVs. This method removes the need for a harsh physical force for cargo loading, consequently limiting the potential for cargo degradation. **Chapter 6** provides a summary of the work accomplished in this dissertation, the contributions to the field, and the future research directions necessary to further the field before EVs become a clinically viable therapy. Lastly, the **Appendix** contains ongoing work addressing EV delivery.

Chapter 2: Function and therapeutic potential of extracellular vesicles

Biotherapeutics, including proteins, nucleic acids, and cells, have emerged as powerful players in treating numerous diseases. However, due to their labile nature, these molecules require protection to ameliorate the risks of degradation upon administration. Thus, delivery systems such as liposomes and polymer carriers have been successfully developed; for example, there are currently 15 liposomal drug formulations approved for clinical use [9–11]. Yet, even these established approaches must overcome hurdles including cytotoxicity, immunogenicity, endosomal degradation, and biological barriers [5]. Once these concerns are addressed, it is still a monumental challenge to achieve therapeutic delivery in sufficient quantities at the correct target sites of action in the desired time frame to induce the desired effect [5]. Thus, there remains a significant need for developing effective delivery systems for biotherapeutics.

Many of these obstacles can be addressed by extracellular vesicles (EVs), which have emerged as promising alternatives to synthetic drug delivery systems. Studies have shown that EVs mediate the paracrine activity of cell therapies by transferring nucleic acids and proteins protected by a lipid membrane [12]. Due to this natural function of cargo transport, EVs may not require any engineering to promote endosomal escape [13] and can surmount biological barriers to delivery [14,15]. EVs have also been shown to have low toxicity and immunogenicity [14,16]. Certain EVs, such as those derived from antigen presenting cells, have been shown to avoid complement-mediated EV lysis [17], improving their circulation time.

However, EVs have weaknesses of their own – including low levels of endogenous cargo and unknown stability. Addressing these weaknesses will allow for production of EVs as a promising therapeutic delivery system. To consider how to accomplish this, it is useful to first assess the physiological function of EVs to understand how these characteristics contribute to their advantages as delivery vehicles and then explore the current state of research pertaining to cargo loading and EV storage.

2.1 EVs and their functions in the body

Extracellular vesicles (EVs) are cell-derived lipid vesicles that play a major role in cell-cell communication. They were first described in 1983 as part of a disposal mechanism to discard unwanted materials from cells [18], but later determined to be important mediators of intercellular communication in normal physiological processes and disease progression [19]. The term extracellular vesicles encompasses a number of vesicles secreted by cells, including apoptotic bodies, microvesicles, and exosomes (**Figure 2.1**). Apoptotic bodies originate from the outward blebbing of apoptotic cell membranes and range from 500-2000nm [20]. These vesicles contain nuclear fractions and organelles of the apoptotic cell. Microvesicles are also believed to originate from the cell surface, but of non-apoptotic cells. While some report microvesicles to range 50-1000 nm in size [20], others report 200-1000 nm [21]. This inconsistency is partly due to lack of established methods for isolation and incomplete studies of EV subpopulations. The smallest and most studied of these vesicles are exosomes, which are estimated to range 50-200 nm. Both microvesicle and exosome populations have been investigated for therapeutic interest. Although certain markers are enriched in particular EV groups, they may still be present in other types of vesicles as well, making them difficult to differentiate. Due to the unclear composition of purified vesicle populations, we cannot confirm a homogenous population of EV group only. Thus, I will refer to the vesicles used in this dissertation by the broader term extracellular vesicles, unless referring to a specific mode of biogenesis.

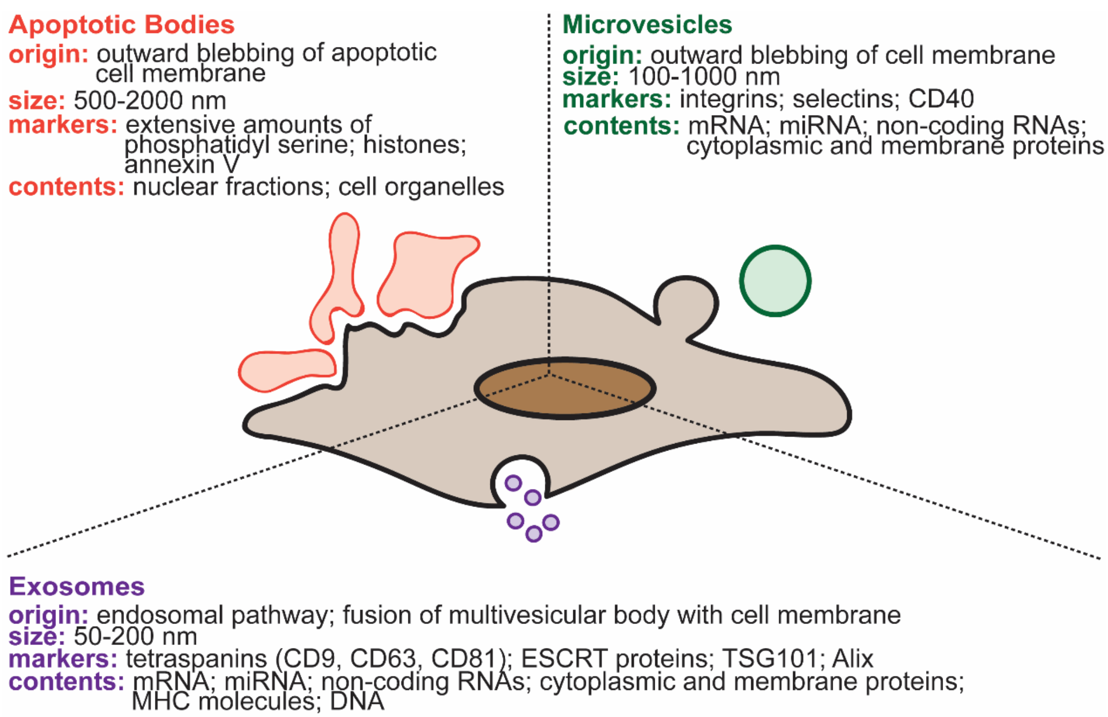

Figure 2.1. Types of extracellular vesicles and their characteristics. The term EV encompasses apoptotic bodies, microvesicles, and exosomes. They can be distinguished by their origin and particular markers.

2.1.1 Biogenesis and release

Although extracellular vesicle classification is based on mode of biogenesis, these mechanisms are not fully understood [22,23]. In general, exosomes are formed by inward-budding within the endocytic system, while microvesicles are formed from the outward budding from the plasma membrane [22–27].

Exosome biogenesis begins with the inward budding of an endosome membrane to form intraluminal vesicles (ILVs). At this point the endosome is termed a multivesicular endosome (MVE) or multivesicular body (MVB) due to the presence of multiple vesicles within the endosome. Finally, the fusion of the MVEs with the plasma membrane releases the contents – exosomes. Several mechanisms have been described to explain the mechanisms of exosome biogenesis, but none are fully understood. The best characterized method of biogenesis involves the endosomal sorting complex required for transport (ESCRT) [28]. ESCRT machinery is an assembly of protein sub-complexes that along with accessory proteins mediates the scission of cellular membranes into vesicles [29]. ESCRT-0 is involved in MVE formation and the recruitment of the ESCRT machinery. Binding of the ESCRT-0 protein HRS to phosphatidylinositol 3-phosphate (PI3P) initiates ESCRT activity. ESCRT-I and -II mainly function in protein sorting and the recruitment of ESCRT-III. ESCRT-III coordinates the membrane severing which results in vesicle formation. Depletion of ESCRT components in cells via silencing mechanisms has shown impaired exosome release confirming their role in exosome biogenesis [30]. However, a number of studies show that inhibiting ESCRT components does not prevent the formation of MVEs [31] or the release of exosomes, indicating that other mechanisms may be at play as well. These mixed results could be due to limitations of isolation methods and characterization techniques in differentiating between EV populations. Additionally, these results suggest that there may be multiple modes of exosome release within a cell population. Less characterized modes of biogenesis involve methods mediated by lipids and tetraspanins. Lipids can self-organize into specific subdomains on cellular membranes, including that of MVEs. The endosomal pathway for proteolipid protein (PLP) packaging into Oli-neu cell derived exosomes does not require ESCRT and is instead mediated by ceramide, which can induce the coalescence of small microdomains into larger domains. This consequently produces domain-induced budding of vesicles [32]. Tetraspanins are proteins with four transmembrane domains, that have both amino- and carboxyl- termini facing the cytoplasm. They can interact with themselves and other proteins to organize tetraspanin-enriched microdomains (TEMs). Certain tetraspanins have been shown to be required for the incorporation of certain cargo into exosomes and thus it is believed that they play a role in biogenesis [33], but the exact mechanism is unknown. Exosomes are released upon MVE fusion with the cell’s plasma membrane. The Rab family of small GTPase proteins mediate the steps of intracellular vesicle trafficking that ultimately lead to docking of the MVEs to the plasma membrane [27,30,34]. After docking, SNARE (soluble NSF-attachment protein receptor) complexes may allow fusion of the MVB to the membrane and facilitate release [30].

The mechanisms behind microvesicle biogenesis are even less studied than those responsible for the formation of exosomes. One potential pathway begins with the clustering of transmembrane proteins and lipids in distinct domains. Tetraspanins may be involved in sorting of components similarly to exosomes. The accumulation of calcium ions and a degradation of cytoskeletal components while phosphatidylserine moves to the extracellular domain promotes an outward budding of the membrane. Budding and pinching off of the membrane may occur via the ESCRT machinery described above or by a signaling cascade initiated by the GTP-binding domain protein ARF6 [26].

It still remains to be determined whether the specific steps and components involved in exosome and microvesicle biogenesis are conserved across cell-types or function specific [22]. Studies suggest that the mode of biogenesis is likely a factor in determining EV cargo content [23]. Alix, an accessory protein of ESCRT involved with biogenesis, has been shown to be integral to exosomal miRNA enrichment of adult human liver stem-cell-like cells [35]. The RNA binding protein SYNCRIP (synaptotagmin-binding cytoplasmic RNA-interacting protein) shuttles miRNA with a specific motif into hepatocyte exosomes, but does not indicate any dependence with biogenesis pathway [36]. Further research is necessary to elucidate how different types of EVs are formed and the impact that this has on the cargo. As mentioned before, due to uncertainty in the purity of EV populations we cannot accurately use the terms exosome or microvesicle for the vesicles used in the project until this is well understood.

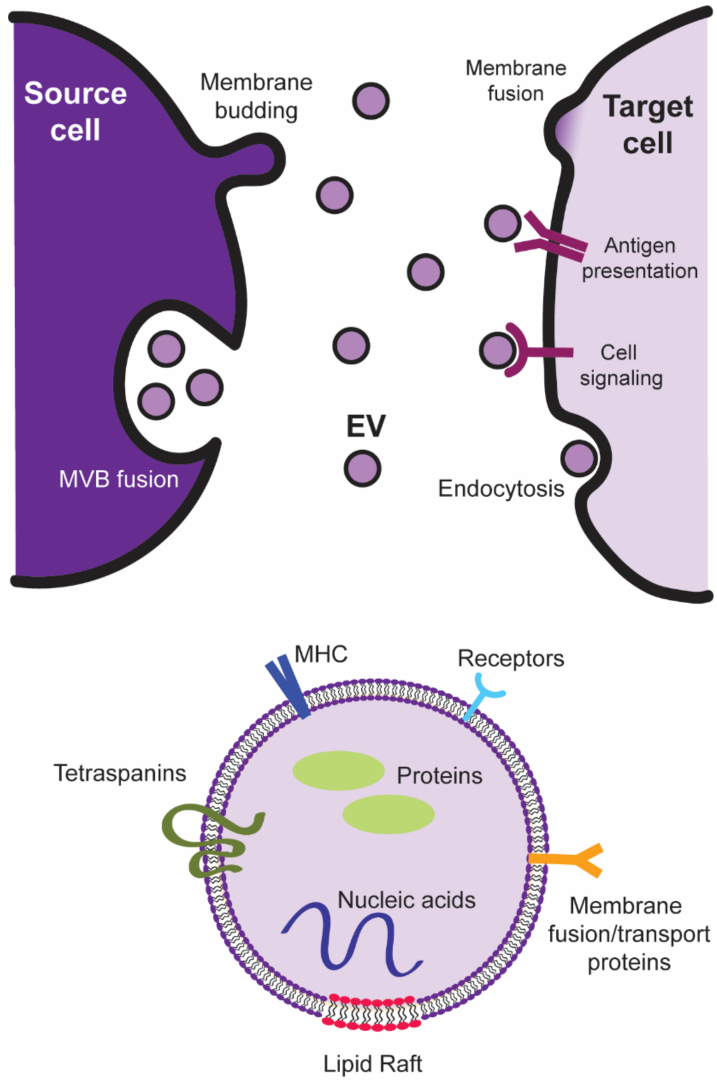

Figure 2.2. Biogenesis, uptake, and contents of extracellular vesicles. (A) EVs are released either from budding of the plasma membrane or through the fusion of a multivesicular body to the plasma membrane. Once they reach a target cell, EVs can interact with cell surface receptors or delivery cargo to the interior of the cell via membrane fusion or endocytosis. (B) EVs are composed of a lipid bilayer containing various membrane proteins. They can also contain protein as well as nucleic acids in their interior.

2.1.2 EV components

Although the source cell can dictate EV composition, the two are not identical. [36,37]. In general, particular proteins, lipids, and nucleic acids are enriched or not present in EVs compared to cells. The contents of EVs can reflect the nature and state of the parent cell. The specific sorting of protein and RNA into exosomes is controlled by several pathways which are not fully understood. As shown in **Figure 2.2**, once released from the source cells, the EVs impart an effect on the target cell either by delivering internal cargo or by interacting via surface proteins. Thus, exosome composition determines the outcome of communication.

Proteins

EVs contain a specific subset of cellular proteins, some of which depend on the cell type that secretes them, while others are found in most EVs regardless of cell type. Since exosomes originate via the endocytic pathway, they have been shown to contain proteins involved in MVE formation in various cell types. [26]. Microvesicle-enriched proteins have been less studied than exosomes and are largely cell type dependent. They include matrix metalloproteinases (MMPs), glycoproteins, and integrins [22]. Many use CD63, CD9, TSG101 and Alix as exosomal markers. However, while these proteins are enriched in exosomes, it may not be accurate to call them markers since different subsets of EVs may contain common markers. Due to overlap and discrepancies in the protein content of exosomes and microvesicles, proteins specifically expressed in one class versus the other have yet to be identified. Thus there is no consensus on markers to distinguish the classes of vesicles once they have been secreted by cells [38]. Therefore, the International Society of Extracellular Vesicles recommends reporting the amount of three or more proteins expected to be present in the EV population of interest [39].

Lipids

Though there appear to be differences in lipid composition among EVs derived from different cell types, most exosomes seem to be enriched in phosphatidylserine, sphingomyelin, and saturated fatty acids [26] as well as GM3 and ceramide in comparison to source cells [19]. The lipid composition of the vesicles as well as lipid-raft-associated proteins provide the EVs with structural stability. Additionally, they can be involved in the biological activity of EVs. The angiogenic activity of tumor derived EVs can be mediated by sphingomyelin levels [40].

Nucleic acids

It was not until 2007 that it was discovered that EVs carry nucleic acids, namely mRNA and microRNA (miRNA) [41]. Further, Deregibus et al. showed that the angiogenic functional activity of endothelial progenitor cell-derived EVs is dependent upon the RNA they contain [7]. This shed new light on EVs as carriers of genetic information between cells. Among the molecules carried by EVs, miRNA have gained increasing attention due to their role in regulatory roles in gene expression. Some of these miRNAs were not expressed in the donor cell indicated that the RA was specifically targeted to EVs through a selective mechanism [41]. Some studies claim that a specific motif (GGAG) controls the loading of miRNAs into exosomes by binding to the heterogenous ribonucleoprotein A2B1 [37]. Annexin-2 is an alternative mechanism believed to sort specific miRNAs into EVs [42–44]. Like in the case of biogenesis, these mechanisms have not been fully understood and are not the only ones. Further research is necessary to determine the involvement of additional RNA-binding proteins and specific RNA motifs that facilitate this transfer.

2.1.3 EV uptake

Just as there are many modes of biogenesis, there exist several methods of EV uptake by recipient cells. The uptake mechanism of EVs appears to be dependent on the mode of biogenesis. Protein interactions between the EVs in part mediate their uptake. These proteins include tetraspanins, integrins, immunoglobulins, proteoglycans, and lectins. After these interactions, EVs are taken up by either fusing with the cell membrane of by endocytosis. Upon endocytosis, the EVs fuse with the endocytic membrane, releasing their contents into the cytoplasm.

2.1.4 EV function in normal physiological and pathophysiological processes

By being taken up by recipient cells, EVs transfer their nucleic acid and protein content, which in turn affects the target cell. These vesicles have been extensively studied in the context of cancer progression. The communication of cancer cell-derived EVs with local and distant microenvironments plays a role in developing a pre-metastatic niche [45,46] in addition to promoting cancer cell growth and survival [47]. These EVs can also mediate chemoresistance by the transfer of particular miRNAs [48]. Beyond cancer, EVs have been shown to mediate airway inflammation and allergic reactions in the lungs [49] and are involved in regulating asthma. RNA transfer mediated by EVs in the brain Is believed to be involved in neurodegenerative disease [50]. Not only do EVs promote disease progression, but also, they play a prominent role in maintaining normal physiological processes. EVs have been implicated in neuronal development, synaptic activity, and nerve regeneration They are also able to mediate cardiovascular health [51]. Due to these wide range of EV roles in the body, they have great potential in both diagnostics and therapeutics.

2.2 Isolation and characterization of EVs

Exosomes can be isolated using various techniques, but there is no established gold standard for isolation. The most common method of isolation is differential centrifugation [38,52]. In this process, cellular debris, apoptotic bodies, and microvesicles are removed in succession as they are pelleted in increasing centrifugal speed spins. Lastly, exosomes are believed to be pelleted using high speed ultracentrifugation. However, since this isolation method is based on size, smaller microvesicles as well as other contaminants (proteins, viral particles, etc.) may also be isolated along with exosomes. Thus, it is inaccurate to claim pure isolation of EVs until confirmation of biogenesis mode. Additionally, this procedure may result co-precipitation of protein aggregates and there are risks of EV aggregation, fusion, or disruption [53,54]. An alternative method to isolate based on size is size exclusion via the use of filters or chromatography [53,55]. One study demonstrates that using ultrafiltration combined with size exclusion liquid chromatography results in EVs with a different *in vivo* biodistribution than EVs isolated by ultracentrifugation due to a decrease in aggregates [53]. Further studies are necessary to develop a reproducible protocol. EVs can also be isolated by using flotation density gradients of either sucrose or commercial gradients. This will allow the separation of vesicles from protein and RNA aggregates based on their buoyancy. Immunoaffinity isolation is based on using characteristic surface proteins on certain EV classes to isolate that group of vesicles. In this method, antibodies for surface proteins are used to select the desired EV population or trap unwanted populations. These antibodies are generally associated with beads or other matrices to facilitate physical separation. While immunoaffinity isolation has the potential for high EV specificity and purity, better characterization of EV populations and knowledge of what population is desired is necessary. Polymeric precipitation mixtures, such as the commercial ExoQuick system, are relatively simple to perform, but there are concerns about the purity of the product like other methods. Microfluidics have also recently been studied as a method of EV isolation, but yield is a limitation [56].

Despite all these studies, to date there exists no isolation method which guarantees isolation of a pure single class of EVs. Thus, it is important to be precise when describing the isolated EV population. The subsequent work in this dissertation will use differential centrifugation since it the best characterized isolation method and most widely used.

2.3 EVs as therapeutics

2.3.1 Endogenous bioactivity of EVs

Due to the presence of numerous bioactive molecules mentioned previously, some EVs have the intrinsic potential to modulate the phenotype and function of a recipient cell. This can be exploited for therapeutic functions. EVs can have an effect based on (1) receptor-ligand interactions at the cell surface which can trigger a cell signaling pathway and (2) transfer of contents after cell uptake.

Cardiovascular and immune therapies are two areas of great interest in EV therapeutics research. EVs present an alternative for dendritic cell-based vaccinations against cancer. One of the first therapeutic applications of EVs was in the form of a cancer vaccine [56,57]. Antigen presenting cells, including dendritic cells (DCs), have antigen-loaded MHC I and II complexes as well as co-stimulatory factors that can activate T cells. DC-derived exosome therapies are in clinical trials for cancer immunotherapies [58]. The therapeutic potential of EVs in the heart was highlighted by reports of bioactivity from cardiac progenitor cell-derived EVs [59] as well as identification of EVs as the key bioactive factors of CD34+ angiogenic cells responsible for promoting vascular regeneration [12]. Other work has shown therapeutic bioactivity of EVs isolated from other cell types of interest for cardiac therapy, such as mesenchymal stem cells [60–62].

2.3.2 Delivering exogenous therapeutic cargo via EVs

The natural involvement of EVs in cell-to-cell communication makes them attractive carriers of exogenous therapeutic molecules. The structure of EVs can protect encapsulated cargo and their size minimizes recognition by the phagocytic cells of the immune system. Further, their lipid composition stabilizes the vesicles in blood circulation and improves uptake by cells in comparison to many synthetic particles.

They also have a natural ability to pass through biological barriers. Thus, there is interest in incorporating cargo into these vesicles for drug and gene delivery.

2.3.3 Modulating EV cargo by manipulating source cells

EVs can be loaded with exogenous cargo either before or after isolation from cells, as illustrated in **Figure 2.3**. Mesenchymal stem cells incubated with the chemotherapeutic Paclitaxel can produce EVs loaded with the drug, preserving its anti-tumor properties [63]. While simple incubation is enough to load some molecules into cells (and subsequently EVs), incorporating nucleic acids requires an active approach. One such method is simple overexpression of desired cargo by transfection [64]. This can be done by either transfecting the desired oligonucleotides or a plasmid that will express them in the cells. The main obstacle to this approach is that the mechanisms of cellular sorting into EVs are not fully understood. To overcome this, some groups have identified particular motif sequences that are enriched in miRNAs highly expressed in EVs. Thus, transfecting cargo with these sequences added can enhance cargo loading in EVs. Alternatively, targeted loading can be achieved by fusion of cargo with constitutive EV proteins. Transfection of a plasmid can also be used for loading a desired protein, by fusion of a desired protein with constitutive EV proteins [14,65–67]. However, this requires making a vector for each fusion protein and thus can be laborious if loading various different proteins.

2.3.4 Loading cargo into EVs after isolation

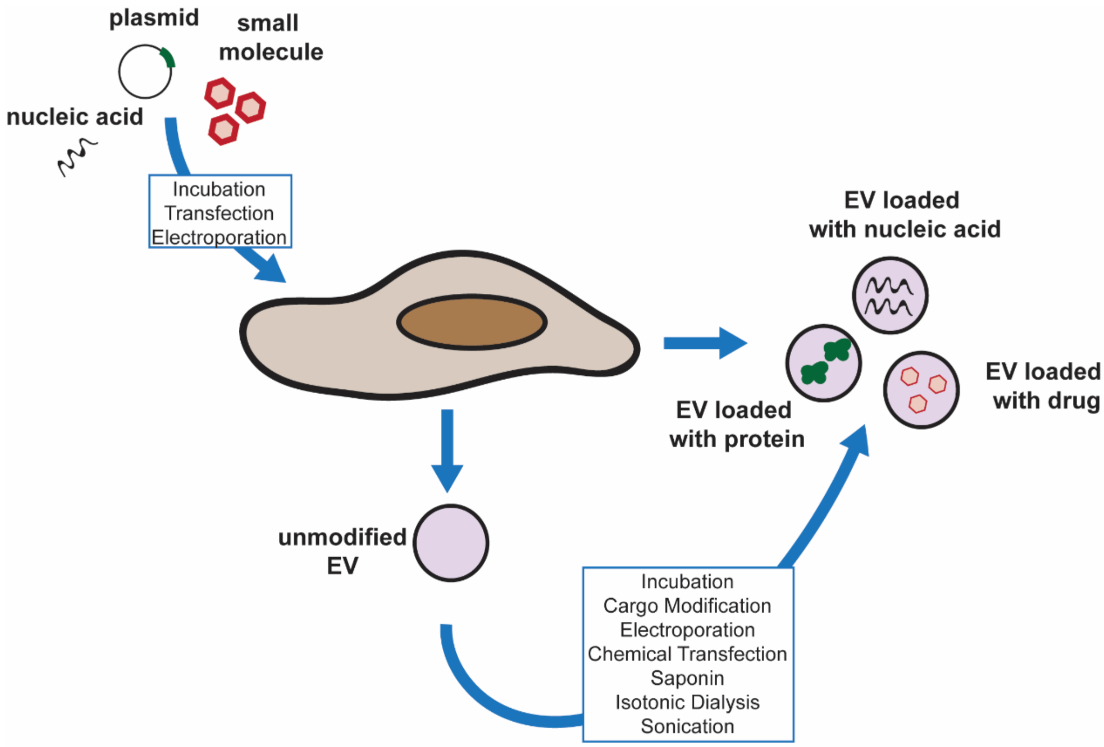

Figure 2.3. Extracellular vesicle cargo loading techniques. EVs can be loaded either by manipulating the source cell or by modifying EVs after isolation. Both techniques can be used to load nucleic acids, proteins, or small molecules.

Passive incubation

As the sorting and packaging mechanism of cargo into EVs is not fully understood, there is interest in post-isolation loading of EVs. In the cases of some hydrophobic cargos, EVs can be loaded by incubation with the cargo [68,69]. Curcumin, doxorubicin, and paclitaxel have been successfully loaded into EVs and delivered as therapeutics [68–70]. However, this method is not applicable to hydrophilic compounds, including nucleic acids, which cannot spontaneously cross the lipid bilayer.

Cargo modification

Nucleic acid cargo can be modified to promote EV loading. Cholesterol conjugation involves covalently bonding cholesterol to the therapeutic oligonucleotide. In this case, the nucleic acids are associated on the outside of the EVs. Chemically modifying huntingtin gene (Htt) siRNA to conjugate with cholesterol improved association with the EV membrane [71]. Cholesterol-conjugated siRNA was loaded into glioblastoma cells by incubation at 37°C for 90 minutes [72]. Another study showed that although cholesterol-tagged siRNA can be effectively loaded onto EVs, functional siRNA could not be delivered *in vitro* [73]. Although this is a simple and effective method of loading, the cargo is still exposed and subject to degradation. Thus, it is preferable to ensure loading of the cargo within the vesicle.

Electroporation

Most studies with exogenously loaded EVs employ electroporation as a means to incorporate cargo into the vesicles [14,74,75]. In this method, EVs are mixed with the therapeutic cargo in an electroporation buffer and then electroporated to disrupt the EV's surface structure. The formation of pores in the membrane allow cargo to be incorporated into the EVs. Electroporation was used to successfully load siRNA into dendritic cell derived exosomes for delivery to the brain and showed a comparable efficiency to commercial cationic liposome transfection reagent, Lipofectamine [14]. Our lab has demonstrated that various nucleic acids can be loaded into EVs at, on average, hundreds of molecules per vesicle. The loading efficiency is dependent on both nucleic acid and EV size [76]. Despite some successes, groups have demonstrated that electroporation may not work well in all cases [77]. Also, while electroporation may not significantly damage ligands and receptors on the EV surface or the membrane [78] it induces significant aggregation of RNA cargo (**Figure 2.4**) and changes EV morphology [79]. As with liposomes, electroporation can also induce aggregation and fusion of EVs [78]. Thus, there is a need for improved methods of loading.

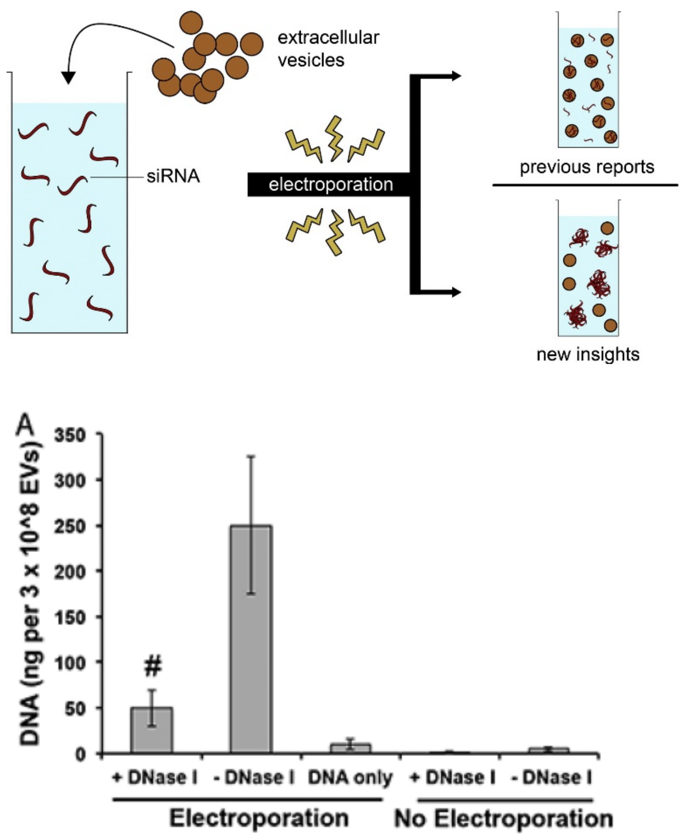

Figure 2.4. Aggregation of nucleic acid after electroporation may lead to falsely high loading efficiencies. (A) While previous reports suggested that electroporation can be an effective method for loading nucleic acids into EVs, Kooijmans et al. demonstrated that aggregation led to inaccurate quantification of loading. Reprinted with permission from Kooijmans et al. Journal of Controlled Release. Copyright 2013. (B) Lamichhane et al. demonstrated that treating EVs with DNase I after electroporation loading shows that 80% of the DNA quantified was not adequately protected by EVs. Reprinted with permission from Lamichhane et al. Molecular pharmaceutics. Copyright 2015. American Chemical

Chemical transfection

Commercial reagents have been shown to have improved loading of siRNA compared to electroporation [80]. However, purchasing reagents can be expensive and a limiting factor for scale-up. Additionally, depending on the commercial reagents used it may be unfeasible to separate the EVs from the micelles of the transfection reagent that contain the desired RNA [75]. Thus, in these cases it is difficult to distinguish which component is leading to the functional result [81].

Saponin

Other methods of permeabilizing the EV membrane include saponin-mediated loading and hypotonic dialysis. The addition of saponin [82,83], a detergent-like molecule that removes cholesterol from the membrane, results in pore formation. This is performed by incubating the EVs and cargo with saponin. While saponin loading has demonstrated high loading efficiency without compromising drug delivery abilities *in vitro* [82,83], difficulty in removing the molecule from EV preparations could pose problems in uptake and stability.

Hypotonic dialysis

In the hypotonic dialysis method, EVs are disperse in a hypotonic solution, causing them to swell and form pores, making the membrane permeable for soluble therapeutic molecules to enter the vesicles via osmosis. After this step, the loaded vesicles are then put in an isotonic solution restoring EVs and resulting in cargo encapsulation. While this method has shown a higher loading than passive incubation or electroporation, its modifies EV size and charge, which ultimately inhibited cellular uptake [83]. The results from this study convey the importance of preserving EV integrity after loading cargo. EV integrity is also modified extrusion and freeze-thaw loading methods.

2.3.5 Limitations and areas for improvement

While there are a number of methods used for loading cargo into extracellular vesicles, there is no consensus on the best method of loading for nucleic acids. Many researchers have explored loading cargo into cells before EV isolation; however, loading may vary greatly for each producer cell type and each cargo due to variations in biogenesis among cell populations. This may also contribute to increased variation in loading efficiency. Further, this requires modification of source cells each time loading a different cargo molecule is desired. Thus, in such cases, loading EVs after isolation is advantageous. Although, scalability of EVs loaded by cell manipulation can be achieved using techniques for mass production of EVs, scalability for loading post-isolation will vary with method and must be considered. While many methods have emerged for loading, purifying the sample is a problem with chemical transfection and saponin loading. Though cargo modification has emerged as an effective method of nucleic acid loading, each type of cargo would have to be modified before being able to load and adds an extra step of complexity to the process. Electroporation is a simple and straightforward processes, but it has been shown to induce aggregation of RNA cargo leading to misleading results of loading efficiency. Thus, there is a need to develop easy to use and scalable methods of loading that do not degrade nucleic acid cargo.

2.4 Preservation and storage stability of extracellular vesicles for therapeutic applications*

As with cells and other cell-derived products (proteins, etc.), maintenance of EV biological activity during storage is both critical and challenging. Yet, little has been reported about EV preservation. Though storage of EV-based therapeutics is not expected to be as difficult as cell-based therapy preservation, some limitations will undoubtedly apply. Ultimately, effective preservation and storage of EVs will be critical in determining the scope of their therapeutic application. Here, I summarize current knowledge of EV preservation and storage techniques in the context of their uses as primary biotherapeutics as well as drug carriers. I further highlight critical areas for future study towards overcoming current limitations to enable effective preservation and storage of therapeutic EVs.

2.4.1 EVs as primary biotherapeutics – EVs isolated from biofluids

As EVs are released in the body as a form of cell-cell communication, they can be isolated from biofluid samples for therapeutic applications. In many cases, it is not practical or most useful to isolate EVs from a patient sample immediately after biofluid collection. Studies have shown that the biofluid storage method can impact EV yield, composition, and function (summarized in **Table 1**). It is important to understand what

* Adapted by permission from Springer Nature The AAPS Journal: **Jeyaram A**, and Jay SM. "Preservation and storage stability of extracellular vesicles for therapeutic applications." *The AAPS journal* 20.1 (Copyright 2018): 1.

these changes are and how to avoid them for reproducible therapeutic outcomes, which are essential for clinical translation.

Table 2.1. Summary of tested storage conditions for various biofluid samples and the impact on EVs.

Biofluid	Storage	Time	Physical features	Contents	Activity	Other
Semen	-80°C	2 years	No change [84]	No change [84]	No change [84]	-
		30 years	No change [84]	↓AChE activity [84]	↓ HIV-1 inhibition [84]	-
Urine	RT	2 hr, 1 day, 1 week	↓ EV yield over time [85]	-	-	-
	-20°C	1 week	-	↓ EV associated protein recovery (27.4%) [86]	-	-
	-80°C	1 week	-	87.4% EV associated protein recovery [86]	-	-
	4°C + vortexing	2 hr, 1 day, 1 week	↓ EV yield over time [85]	-	-	-
	-20°C + vortexing	2 hr[9], 1 day[9], 1 week[9,10]	↓ EV yield over time [85]	86% EV associate protein recovery [86]	-	-
	-80°C + vortexing	2 hr[9], 1 day[9], 1 week[9,10]	↓ EV yield over time [85]	100% EV associated protein recovery [86]	-	-
	-80°C + protease inhibitors	2 hr, 1 day, 1 week	↓ EV yield over time (higher yield than without inhibitors) [85]	-	-	-

Milk	4°C	2 hr	-	-	-	Contamination by stress-induced EVs [87]
	-80°C	2hr [87], 4 weeks [88], 6 months [89]	No change [90]	-	No change [90]	Contamination by stress-induced EVs [87]
	-80°C (no cells or cream)	2-8 weeks	-	No change in CD63 and CD9 expression [87]	-	Less contamination by stress-induced EVs [87]
Blood (general)	RT - 160°C	Short term (days), Long term (months)	-	-	-	Varying EV signal intensity (most stable in heparin blood collection tubes) [91]
Serum	RT	6,12,24, 28 hr	-	No change in CD63, TSG101[92]; Stable DNA; Decrease in DNA concentration after 24 hr [92]	-	-
	4°C	24,72,168 hr	-	No change in CD63, TSG10 [92]; Stable DNA; Relatively stable DNA concentration with slow decrease after 72 hr [92]	-	-
	Freeze thaws	1, 3, 5 cycles	-	No change in CD63, TSG101 [92]; Stable DNA; Dramatic decrease in	-	-

				DNA concentration [92]		
Platelets	-80°C + DMS0	1 hr	↑EVs [93]	-	↑procoagulant activity [93]	-
Plasma	RT	0-42 hr	-	No change in RNA levels [94]	-	-
	4°C	2 weeks	-	No change in RNA levels [95]	-	-
	-20°C	2 weeks	-	No change in RNA levels [95]	-	-
	-80°C	2 weeks	-	No change in RNA levels [95]	-	-
		1 month	No change in yield [96]; Increase in EV yield [97]	No change in CD63, miRNA expression, or protein content [96]	-	-
		20 months	Decrease in EV yield [97]	-	-	-
		7 years[24]; 12 years[22]	No change in morphology [98]	No RNA degradation [94]; ↑Total protein [98]; ↑Protein/nucleic acid aggregation [98]	-	-

Broncheoa-lveolar Lavage Fluid (BALF)	4°C	4 days	↑ Size; ↓Zeta potential [99]	Change in protein composition [99]	-	-
	-80°C	4 days	Multilamellar vesicles; ↑ Size; ↓ zeta potential [99]	Change in protein composition [99]	-	-

RT = room temperature

Semen

Seminal EVs have been demonstrated as potentially useful in the development of new prostate cancer diagnostics [100] and have recently been shown to possess anti-HIV-1 activity [101]. However, it is often not possible to isolate EVs immediately upon collection of clinical samples, thus studies investigating sample storage methods are vital to enabling therapeutic use of semen-derived EVs. To this end, Madison et al. showed that human seminal plasma or blood serum samples could be stored at -80°C for short periods of time without significantly impacting EV yield or bioactivity [101,102]. Welch et al. showed preservation of semen EV physical properties, including morphology, concentration, and size after short (2 years) and prolonged freezing (30 years) at -80°C [84]. The prolonged freezing of the semen also did not significantly alter EV total RNA content. The protein concentrations and proteome profiles of these EVs as determined by Bradford analyses and protein-footprinting (silver stain), respectively, were also independent of length of freezing.

However, while semen EV morphology remained preserved, there was a significant decrease of EV-associated acetylcholine-esterase (AChE) activity after prolonged freezing. AChE is a plasma membrane protein incorporated into EVs during biogenesis, making AChE enzymatic activity a commonly used marker for EVs. This decrease in AChE activity may have important functional and biological effects. Welch et. al. demonstrated that while freezing for two years did not significantly impact semen EV bioactivity, prolonged freezing of the semen before EV isolation impaired the ability of EVs to prevent HIV-1 infection of cells [84]. The significant correlation between decreased AChE activity and absence of HIV-1 inhibition suggests that prolonged freezing of biofluids can impair critical therapeutic bioactivity of isolated EVs, depending on the mechanism of action. Although the small sample size limits conclusions, this report suggests the need for additional studies on the effects of biofluid storage prior to EV isolation.

Urine

EV collection from urine is of great interest for biomarker development, and this biofluid may also serve as a convenient medium for collection of EVs to be re-tasked for therapeutic purposes via drug loading methods [103–105]. Zhou and colleagues showed that storage temperature is critical; EVs were effectively preserved at -80°C, whereas storage at -20°C resulted in a significant loss of EVs compared to fresh urine. EV recovery after freezing could be maximized by intensive vortexing of the samples after thawing, resulting in 87.4% and 100% recovery from -20°C and -80°C storage, respectively [86]. Further studies suggest EV degradation can occur within two hours of urine collection and confirmed that the optimal storage of urine samples for EV preservation is -80°C with the addition of protease inhibitors [85].

Milk

Milk-derived EVs have already been utilized as drug carriers and are also reported to have intrinsic therapeutic properties [89,90,106]. Bovine milk-derived EVs have been stored at -80°C for four weeks without any changes in physical properties, and percent loading of paclitaxel in these EVs also remained stable over this time [88]. Milk EVs stored at -80°C also remained mostly free of coagulation for several months and showed minimal loss of activity [90]. Others have found that storing unprocessed breast milk at -80°C or 4°C causes the death of cells present in breast milk and results in contamination of the breast milk EV population, with the majority EVs formed after storage-induced stress on the cells [87]. These findings are particularly critical given the surge of interest in the potential therapeutic applications of milk-derived EVs.

Blood components

EVs isolated from various components of the blood, including plasma, platelets, and serum, have been employed for a variety of diagnostic and therapeutic purposes [91,107]. In contrast to other biofluids, one study showed that long-term storage and freeze-thaw have been reported to not have a critical impact on EV yield [108], while another demonstrated that platelet samples stored as a liquid at room temperature yielded less EVs with decreased procoagulant activity than those frozen with 6% DMSO as a cryoprotectant [93]. This effect may be due to effects on EV-associated proteins, which are reported to be sensitive to acute sample storage temperature as well as the period of time before initial sample processing [108]. Interestingly, separate studies showed that storage of plasma at 4°C,-20°C, or -80°C as well as two freeze-thaw cycles, did not result in significant degradation of EV-associated RNA [95,96]. An additional report detailed that even after storage of plasma samples at room temperature for over 42 hours or -80°C for 12 years, EVs could still be isolated without degraded RNA levels [94]. DNA contained in serum EVs also remained stable in different environments, including one week at 4°C, one day at room temperature and after repeated freeze-thaw cycles [92]. Despite this apparent stability of blood component EV-associated nucleic acids after freezing, fresh plasma yielded a more pure sample of EVs than those isolated from frozen and thawed plasma samples [98] as well as a higher yield of vesicles [97]. Additionally, protein and nucleic acid aggregation was observed after 7 years of storage at -80°C [98]. Kalra et al. took a different approach to evaluating the stability of EVs in plasma [109]. LIM 1863 colorectal cancer cell-line derived EVs were spiked into plasma and stored at 4°C, -20°C, and -80°C, with or without protease inhibitors. Immunoblotting showed the EV marker TSG101 to be present up to 90 days at all storage conditions, but varying intensities indicate greater stability at -80°C. Samples stored at 4°C had a decreased yield in EVs compared to both -20°C and -80°C. While protease inhibitor did not impact protein expression in this study, it did reduce EV aggregation.

Saliva

Studies have emerged suggesting that saliva can be a non-invasive alternative sample for diagnostics. Kechik et al. demonstrated that salivary EVs can be stable when stored without protease inhibitor [110]. However, the different storage temperatures were not compared at the same time points. Samples were evaluated at either 4°C for 1 hour, -20°C for 1 week, or -80°C for 1 month. Total protein concentration of the samples was the same at all of these conditions, but at -20°C for 1 week, there is decreased intensity of CD63 expression, as shown via immunoblotting. To better understand the effect of storage on salivary EVs, samples at each temperature need to be analyzed at the same time. Understanding the effect of storage on the RNA content and additional proteins will also be important for evaluating if storage can impair the use of these EVs in diagnostics.

Broncheoalveolar lavage fluid (BALF)

There is growing interest in the use of airway EVs for treating pulmonary diseases, including asthma and chronic obstructive pulmonary disease (COPD), Airway EVs can be isolated from BALF, however, as with other biofluids, there is limited knowledge on the effect of storage conditions on the integrity of these EVs. Maroto et al. concluded that storage conditions can significantly destabilize surface characteristics, morphological features, and protein content of BALF derived EVs [99]. Importantly, this study demonstrates that storage conditions impact the proteomic content of the EVs, with distinct populations being lost during storage at 4°C as well as -80°C. Maroto et al. hypothesized that these differences are most likely due to the dissociation of membrane-integrated proteins, rather than the loss of internal EV proteins. This change in protein composition and morphology after -80°C is contradictory to the results of studies in frozen whole plasma [96], likely due to concentrated plasma proteins minimizing freezing effects. Overall, this study highlights the importance of understanding the impact of storage of different biofluids on EV populations.

2.4.2 EVs as primary biotherapeutics – EVs isolated from conditioned medium

In addition to biofluids, EVs can also be isolated from conditioned medium of cell cultures. To our knowledge, there are no studies reporting the impact of storage of conditioned medium before EV isolation, although it is notable that the International Society for Extracellular Vesicles (ISEV) recommends storage of EVs in phosphate buffered saline at -80°C in siliconized vessels to prevent adherence of EVs to surfaces [38]. There have, however, been some studies on the impacts of storage conditions on EVs after isolation from conditioned medium. In a patent owned by Capricor Therapeutics detailing the process for producing EV formulations from cardiosphere-derived cells [111], EV concentration was determined to remain stable after one week of storage at 4°C, -20°C, and -80°C, as quantified by Nanoparticle Tracking Analysis. Despite this stability in size over one week, miRNA levels decreased during this period when EVs were stored at 4°C or -20°C and continued to decrease over 90 days. Within 30 days, the EV miRNA content dropped to below 50% of the initial amount at both 4°C and -20°C. miRNA levels when stored at -80°C showed little change over 90 days. The reduction of miRNA when stored at lower temperatures was ameliorated by using Plasmalyte A, Ringers, and Plasmalyte A + Dextrose, although initial buffer content was not reported. The Plasmalyte A-containing buffer yielded EVs with the highest bioactivity, as assessed by changes in macrophage phenotype after treatment with EVs. While lyophilization was not directly compared to storage in the various buffers, the process did not cause any significant reduction in *in vitro* or *in vivo* bioactivity in comparison to EVs that had not been lyophilized. Further, lyophilization and rehydration of EVs did not result in substantial losses of miRNAs. While this patent includes some of the most extensive studies on EV stability reported to date, it remains unknown whether this information can be translated to EVs from other source cells,

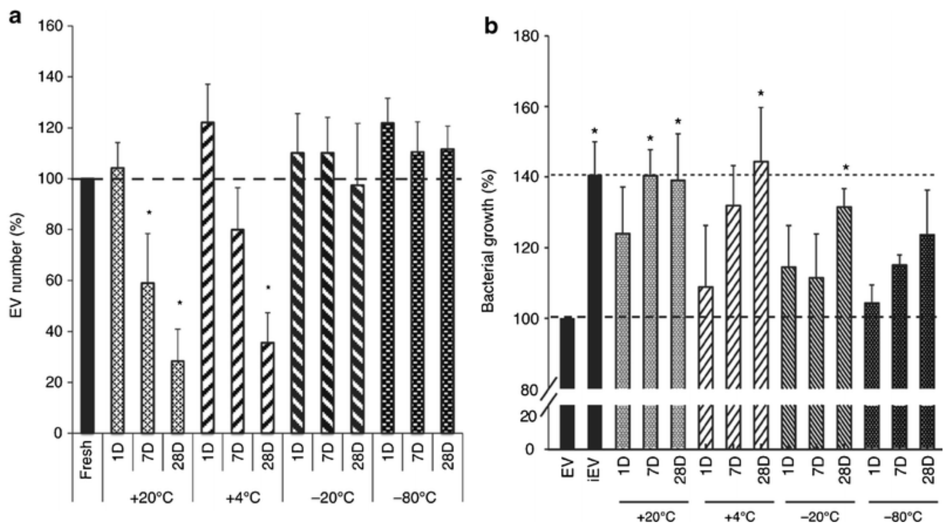

Figure 2.5. Effect of storage conditions on number and antibacterial capacity of neutrophilic granulocyte-derived EVs. (A) Changes in EV number after storage in comparison to a fresh sample were evaluated by flow cytometry. EVs were stored at + 20, + 4, − 20, or at − 80°C for up to 28 days ($n = 4$–8, *$p < 0.05$ by *t* test). EV number decreased significantly at + 20 and + 4°C, but not at − 20 or at − 80°C. (B) Bioactivity after storage was evaluated by incubating bacteria with either fresh or stored samples of EVs. Heat-denatured EVs (iEV) were used as a negative control. Storage conditions of + 20, + 4, − 20, and − 80°C were assessed up to 28 days, with a decrease in bioactivity observed with increased length of storage. ($n = 4$–6, *$p < 0.05$ by *t* test). Adapted via open access from © 2014 Ákos M. Lőrincz et al.

which will vary in surface lipid and protein composition as well as cargo content. This potential variability is reinforced by studies of liposome stability, which show that the specific surface composition has a critical role [112]. Further, it would be useful to determine if the EV concentrations and overall bioactivity remain stable beyond seven days.

Lőrincz et al., provide a convincing argument that storage significantly alters both the physical and functional properties of antibacterial EVs derived from human neutrophilic granulocytes [113]. Storage at 4°C for just a single day was shown by flow cytometry to result in significantly decreased EV number and antibacterial effect. Upon storage at -20°C, EV number was preserved, but a shift in size as well as almost complete loss of antibacterial function by 28 days were observed. In contrast, storage at -80°C prevented significant changes in physical and functional properties at 28 days (**Figure 2.5**).

In total, these studies confirm that storage conditions are critical to EV function. Specifically, they agree that -80°C storage is optimal for preserving isolated EV samples, which is unfavorable due to increased costs and limitations in transportation. Also, the mechanism of storage-induced changes in EV bioactivity remains unclear. Further understanding of this mechanism may allow for rational design of improved strategies to prevent loss of function of EVs in storage, which would significantly broaden the potential therapeutic applications for EVs.

2.4.3 EVs as drug delivery vehicles

Most methods of exogenous EV loading involve manipulation of the EV structures to introduce cargo into the vesicles, potentially altering the stability of these vesicles in comparison to those that are endogenously bioactive. Currently, to our knowledge, there are no published studies on the storage stability of exogenously loaded EVs and their cargo. However, there is evidence that the mechanism of loading can alter EV properties. A commonly used method of cargo loading for EV-based gene and drug delivery is electroporation [114], a process in which the temporary formation of pores in the EV membranes allows for cargo diffusion into the vesicles. Although this method is widely used, it has been shown to induce precipitation of nucleic acids, such as siRNA, and yield low siRNA incorporation into EVs [79]. While endogenous *in vitro* functionality of the EVs remains unchanged, Johnsen et al. reported that electroporation can induce EV aggregation [115]. This same study also demonstrated that RNA may appear to be released from the EVs or degraded after electroporation based on buffer choice, but further studies are necessary to confirm this and to clarify the dynamic nature of any cargo loss or degradation. These effects also remain to be characterized for additional methods of EV loading. Overall, potency and morphology of cargo-loaded EVs after storage must be evaluated prior to their translation as drug delivery vehicles.

2.4.4 Future directions

EVs have tremendous potential to alter the biotherapeutic landscape and impact treatment of myriad diseases and injuries. However, before this potential can be realized, a systematic understanding of how to best preserve the function of EVs during storage must be developed. Adverse effects of storage on EV function reported in the studies cited herein suggest the need for controlling and improving storage conditions to preserve EV therapeutic utility. One potential approach to accomplish this is the use of disaccharide stabilizers in EV storage buffers [116,117]. For example, trehalose is a natural, non-toxic sugar widely used as a protein stabilizer and cryoprotectant by both the food and drug industries and has been validated as a cryo-preservative for labile proteins, vaccines, and liposomes as well as cells and organs for transplant. It works by decreasing intracellular ice formation during freezing and preventing protein aggregation [118]. Bosch et al. have demonstrated that 25mM of trehalose in PBS (TRE) may be an attractive way to protect EVs during storage [119]. TRE itself was shown to not alter any physical characteristics of the EVs, the RNA or protein profiles, or typical EV markers. However, there was a significantly higher particle count in TRE compared to PBS, along with reduced mean size and size distribution. This translated into higher purity (ratio of particle to protein concentration) of reconstituted EV formulations with TRE, possibly via reduced EV aggregation as the result of trehalose interference with interparticular attractive forces. This report indicates that further study of trehalose and related stabilizers, such as sucrose, is warranted.

To date, a primary limitation to studying EV storage effects and mechanisms has been inconsistency in EV characterization and analysis. While one study showed that NTA and electron microscopy analysis illustrated no change in vesicle size from 1 to 10 freeze-thaw cycles (-20°C) [120], another reported that once isolated, a single freeze-thaw cycle lowered the EV count by 10-15%, as detected via flow cytometry [121]. Elsewhere, Almizraq et al. demonstrated that red blood cell-derived EV characteristics varied after storage based on the method of detection [122]; a comparison of tunable resistive pulse sensing, flow cytometry, and dynamic light scattering showed varying changes in EV concentration after storage. Thus, utilization of standardized EV characterization methods, such as those recommended by ISEV [38], would aid progress in this area.

2.4.5 Conclusions

The most promising mode of storage remains -80°C; however, availability may be limited by cost [95,123] and poses challenges in transportation. Thus, alternatives such as lyophilization and the incorporation of additives may be necessary to improve EV storage stability. Without advances in this area, EV therapies will be limited to personalized settings requiring expensive preparation processes by highly skilled personnel. Increased understanding of how to best store therapeutic EVs would allow EV-based approaches to meet their full versatile potential as a new class of promising therapeutics and drug carriers.

2.5 Clinical outlook for EV therapeutics

EVs have the potential to join antibodies and cell therapies as the next breakthrough in medical treatment [124]. As mentioned, they have shown great promise, both due to their innate therapeutic activity and as delivery vehicles. There are currently seven clinical trials either active, recruiting, or not yet recruiting that are focused on using extracellular vesicles as a therapeutic intervention. Of these seven studies, one is using EVs that are loaded with exogenous nucleic acid. This group from MD Anderson Cancer Center has engineered EVs to delivery siRNA against oncogenic $KRAS^{G12D}$. *In vitro* and *in vivo* studies in mice have shown the ability to inhibit metastasis and increase survival in a mouse model of pancreatic cancer [125,126]. Additionally, three phase I trials have been completed using either autologous EVs from immature dendritic cells and ascites and two phase 2 trials have been completed using autologous EVs from mature dendritic cells and allogenic EVs from mesenchymal stem cells [124]. There are also a number of companies that have emerged with either unmodified or engineered EVs as their therapeutic platform. For these technologies to reach the patients and be widespread, many challenges remain to be addressed. Such challenges include manufacturing, characterization, delivery, cargo loading, stability, and cell culturing conditions among others. In the following chapters we focus on cargo loading and EV stability.

Chapter 3: Active loading of nucleic acid cargo into extracellular vesicles by sonication †

3.1 Introduction‡

Extracellular vesicles have emerged as potential drug carriers for a wide variety of therapeutic applications. These cell-derived lipid vesicles play critical roles in intercellular communication by acting as vehicles for biomolecule transfer between cells [20,103,127] and may overcome biological hurdles that hinder the effectiveness of synthetic drug delivery systems[128]. In particular, EVs have been identified as potential therapeutics via an RNA transfer mechanism [6,7], leading to their emergence as promising vehicles for therapeutic RNA delivery. However, intrinsic RNA levels in EVs are relatively low, raising questions about EV therapeutic potency and sparking investigations into methods to increase levels of specific RNAs in EVs.

To enhance therapeutic RNA levels in EVs, approaches have focused on modification of parent cells as well as exogenous loading of fully formed EVs after isolation, as mentioned in **Chapter 2**. The former has been successfully employed [64,67,129–131], however this general strategy may hinder translation due to safety and scalability

---

† A portion of this work is adapted with permission from Springer Nature Cellular and Molecular Bioengineering: Lamichhane TN, **Jeyaram A**, Patel DB, Parajuli B, Livingston NK, Arumugasaamy N, Schardt JS, Jay SM. "Oncogene knockdown via active loading of small RNAs into extracellular vesicles by sonication." *Cellular and molecular bioengineering*. Copyright 2016 Sep 1;9(3):315-24.
‡ The introduction is adapted from **Jeyaram A**, Lamichhane TN, Wang S, Zou L, Dahal E, Parajuli B, Knudsen DR, Chao W, Jay SM. "Enhanced loading of functional miRNA cargo via pH-gradient modification of extracellular vesicles." *Molecular Therapy*. (Submitted 2019)

concerns and also would not be applicable for EVs isolated from blood or biological fluids. Several exogenous loading techniques have been reported, including active methods such as electroporation and sonication. In particular, electroporation remains amongst the most commonly reported approaches to EV loading [14,74,75,125,126,132]. However, literature reports of successes with this method must be balanced against studies noting limitations such as induction of significant aggregation of RNA cargo and changes to EV morphology [76,79]. Moreover, as with liposomes, electroporation can also induce aggregation and fusion of EVs [78]. Additionally, heat shock has been used to enable functional miRNA mimic loading [133], but this may also lead to nucleic acid destabilization and could impact EV membrane fluidity. Passive loading methods that do not involve exposing EVs and nucleic acid cargo to external force have also been explored. Notably, chemical modification of siRNAs [71,134,135] has enabled high levels of functional loading. This approach is promising, but requires specific modification of each prospective cargo molecule. Each of these strategies has strengths and weaknesses, but none has been established as universally applicable for unlocking the full therapeutic potential of nucleic acid delivery via EVs. Therefore, there remains a need to develop additional nucleic acid loading methods for EVs.

In this study, we explored sonication as a method for loading nucleic acids, in particular small RNAs, into EVs. While this technique has been used successfully to load small molecule drugs, such as paclitaxel, into EVs [136], its effectiveness for loading nucleic acid cargo remains unknown. Here, we demonstrate the ability to load various nucleic acid cargos into EVs by sonication and evaluate functionality in multiple *in vitro* assays using different cargos. Further, we explore the impact of sonication on the endogenous function of EVs and evaluate the potential to load multiple cargos simultaneously.

3.2 Methods

3.2.1 EV isolation and characterization

EVs were isolated from either HEK 293T cells (ATCC CRL-3216), MCF-7 (ATCC), or bone marrow-derived MSCs (ATCC PC-500-012). Cells were cultured in EV depleted media until 90% confluency, when the conditioned media was collected and subjected to differential centrifugation as described previously. After spinning at 300xg for 10 min, the supernatant was then centrifuged at 2000 x *g* for 20 min followed by 10,000 x *g* for 30 min. Lastly EVs were pelleted by spinning for 2 hours at 118,000 x *g* using Optiseal tubes (Beckman Coulter) in a Type 70 Ti ultracentrifuge rotor (Beckman Coulter). All centrifugation steps were carried out at 4 °C. EVs were then resuspended in 1X PBS and washed using 300 kDa MWCO filters and. Total protein concentration was measured by bicinchoninic acid (BCA) assay. EV size and concentration were assess by nanoparticle tracking analysis (NTA) via NanoSight. Isolated EVs were diluted 20-fold in PBS before analysis in three different fields of view (1 min acquisition time with at least 100 particle tracks) and analyzed with NTA 2.1 software. All experiments were independently replicated with n = 3.

EVs were also assessed via immunoblotting using standard approaches to determine the presence of EV-specific markers (Alix and TSG101). RIPA buffer was used for EV lysis and a 1:1 ratio of PBS to Odyssey Blocking Buffer reagent was employed as the blocking buffer. Antibodies were obtained from Cell Signaling Technologies unless indicated; primary antibodies anti-Alix (2171) and anti-TSG101 (sc-7964; Santa Cruz Biotechnology) were used at a 1:500 dilution; anti-GAPDH (2118) was used at a 1:2000 dilution. The secondary antibody was goat anti-rabbit IRDye 800CW (956579-01-4; LI-COR), used at a dilution of 1:10,000. Bands were detected with a LI-COR Odyssey CLX Imager and the data were quantified using its associated software.

3.2.2 Sonication parameter optimization and EV loading

siRNA sequence: 5′-GGUGCCAGUUCUCCAAGAUUdTdT-3′ (Dharmacon GE Life Sciences CTM-120916)

miRNA sequence: 5′-CAA AGU GCU GUU CGU GCA GGU AG-3′ (Dharmacon GE Life Sciences CTM-197815)

ssDNA sequence: 5′-TGCTAGCTATCTAGTAGCCTAGTTA-3′ (Integrated DNA Technologies)

For cargo loading, 1000 pmole of nucleic acid cargo was incubated with 100 µg of EVs (as determined by BCA) in 100 µL total volume. The samples were incubated at room temperature for 30 minutes before sonication in a water bath sonicator VWR® symphony™; cat# 97043-964, 2.8 L capacity, dimensions 24 L x 14 W x 10 D cm) at

35 kHz for 30 s total duration unless otherwise indicated. For each indicated time, the samples were placed on ice for 1 min halfway through the total sonication duration.

In quantification experiments, nucleic acids were labeled before loading by mixing with dye reagent according to the manufacturer's instructions for Quant-iT PicoGreen Assay Kits (ThermoFisher Scientific, cat# P11496) or Quant-iT™ microRNA Assay Kits (ThermoFisher Scientific, cat# Q32882). Nucleic acid loading was quantified using Quant-iT™ kits following extensive washing using a 300 kDa MWCO filter to remove excess unincorporated nucleic acids as previously described [76]. Samples were compared to a standard curve to quantify EV-associated cargo. In the case of DNA oligo encapsulation, samples were digested with DNase I prior to extensive washing and inactivation as described in our previous work [76]. However, this step was unable to be carried out for RNA encapsulation due to inability to successfully inactivate RNase A, potentially due to a high binding affinity of this enzyme to EV lipids.

3.2.3 Electroporation

Electroporation of EVs was carried out as previously described [76]. EVs were mixed with cargo in electroporation buffer (1.15 mM potassium phosphate, pH 7.2, 25 mM potassium chloride, 21% Optiprep) and electroporation was carried out at 400 V and 125 µF with two pulses using Gene Pulser/Micropulser Cuvettes (Bio-Rad #165-2089) in a GenePulser Xcell electroporator (Bio-Rad). Samples were then washed (300 kDa MWCO; Pall #OD300C33) to remove free cargo and buffer components and 1 mM

EDTA was added [79]. After incubation at room temperature for 15 min, samples were washed again in 300 kDa MWCO filters.

3.2.4 Nucleic acid aggregation

Fluorescently labeled ssDNA (sequence above in section 3.2.2) was either sonicated or electroporated as described above. To assess aggregation, the samples were then washed in 300 kDa MWCO filters with 1XPBS to remove unaggregated ssDNA. The aggregates of size greater than 300 kDa were left behind in the filter. Aggregation level was quantified using a SpectraMax Gemini plate reader (excitation = 480 nm; emission = 520 nm).

3.2.5 EV uptake analysis by flow cytometry

Uptake was assessed for unmodified, sonicated, and electroporated. HEK293T-derived EVs were labeled with the green fluorescent membrane dye PKH67 (Sigma-Aldrich). EVs were loaded with Cy3- labeled siRNA. EVs were resuspended in diluent C solution (Sigma-Aldrich). PKH67, diluted to 4 μM in diluent C, and EVs (800 μg/mL) were combined at 1:1 ratio for 5 min with frequent mixing, followed by the addition of EV-depleted FBS at a 1:2 ratio of FBS to PKH67-EV mixture for 1 min. Labeled EVs were filtered again using Nanosep 300 kDa spin columns and resuspended in PBS.

PKH67-labeled EVs (25 μg) were added to 100,000 HEK293T cells in a 12 well plate in 1 mL DMEM supplemented with 10% EV-depleted FBS for 22 h at 37 °C. Unlabeled

EVs and siRNA alone were used as negative controls for PKH67 and Cy3 labeling, respectively. Unloaded PKH67-labeled EVs and transfected Cy3-labeled siRNA were used as positive controls. HEK293T cells incubated with Cy3-siRNA loaded PKH67-labeled EVs or appropriate controls were collected from the wells using 500 µL of 5 mM EDTA for 2 min and collected in 1.5 mL centrifuge tubes. Cells were washed twice with FACS buffer (0.5% BSA in 1X PBS) at 200×g for 2 min each and resuspended in FACS buffer. The samples were run on a FACSCanto II Cell Analyzer (BD Biosciences) and analyzed by FlowJo Single Cell Analysis Software. Gating was done first on live cells in forward light scatter/side scatter. PKH67 + and Cy3 + populations were gated from the live cell population.

3.2.6 Gene knockdown via siRNA-loaded EVs

GAPDH: Dharmacon, ON-TARGETplus GAPDH Control siRNA, Catalog # D-001830-01-20

HER2: Cell Signaling, SignalSilence® HER2/ErbB2 siRNA II, Catalog #6283

Scrambled siRNA: Sigma Aldrich, MISSION® siRNA Universal Negative Control #1; SIC001

GAPDH knockdown experiments were performed by loading HEK293T EVs with GAPDH siRNA and HER2 knockdown experiments used MCF-7 EVs loaded with HER2 siRNA. The EV types chosen in these studies are the same as the cell line which they are treating. 100 µg/mL EVs were added to the cells in 12 well plates to achieve the indicated final concentrations of siRNA based on calculated loading amounts.

HiPerFect transfection of the siRNA was used as a positive control with unloaded EVs and scrambled siRNA as negative controls. Knockdown was evaluated by qPCR and immunoblotting. Using the iScript cDNA Synthesis Kit (Bio-Rad), cDNA was created from cellular RNA (isolated via Qiagen RNeasy Mini Kits). Quantitative PCR (ABI 7900 Fast HT) using SsoAdvanced Universal SYBR Green Supermix (Bio-Rad) was used to detect RNA levels, with settings as recommended for the Supermix reagent. The real time PCR data were analyzed using the ΔΔCt method. Target genes GAPDH and HER2 were assessed using gene specific primers, with β-actin and p53 mRNAs selected as controls that were not expected to be affected by the siRNA treatment. The sequences of the primers used for this study are listed below:

GAPDH F: 5′-TGTTGCCATCAATGACCCCTT-3′

GAPDH R: 5′-CTCCACGACGTACTCAGCG-3′

p53 F: 5′-GTC CCA AGC AAT GGA TGA TTT GAT GC-3′

p53 R: 5′-GGC ATT CTG GGA GCT TCA TCT GG-3′

HER2 F: 5′-CAA CTG CAC CCA CTC CTG TGT GGA CC-3′

HER2 R: 5′-CGC TTG ATG AGG ATC CCA AAG ACC ACC C-3′

β-actin F: 5′-CTG TGG CAT CCA CGA AAC TA-3′

β-actin R: 5′-CGC TCA GGA GGA GCA ATG-3′

Protein isolation and immunoblotting were carried out using standard methods as described previously; additional antibodies for these studies included anti-β-actin

(8457; 1:2000 dilution) and anti-HER2 (2165; 1:500 dilution). Densitometry was performed using LI-COR Odyssey software.

3.2.7 Measuring endogenous nucleic acid levels

Endogenous levels of nucleic acid within EVs was measured by adding SYTO™ 60 Red Fluorescent Nucleic Acid Stain (Thermo Fisher, S11342) at a 1 uM concentration to equal amounts of passive and sonicated EVs (based on BCA protein content) for 20 min at 37°C. After labelling EVs were washed three times using 300 kDa MWCO filters and resuspended in 1 X PBS. Fluorescence levels were measured at excitation 652 nm and emission 678 nm.

3.2.8 Hoescht stain proliferation assay

P5 HUVECs (Lonza) were plated in a black-walled 96-well plate at 5,000 cells/well the day before treatment. Cells were washed and serum starved in endothelial cell basal media (PromoCell). Treatments were added in basal media supplemented in 0.2% FBS and incubated for 4 days at 37°C. Cells were then washed with 1XPBS and 50 uL of 0.1 ug/mL Hoescht stain (Thermo Scientific 33342; Rockford, IL) was added per well. After 30 min incubation at room temperature, the wells were washed with 1XPBS. Fluorescence was measured at excitation 362 and emission 486, with 12 readings per well. Data is reported as fold change compared to the control cells treated with basal media supplemented with 0.2% FBS.

3.3.9 Gap closure assay

P5 HUVECs were plated in 48-well plates at 40,000 cells/well the day before the assay so that the cells are at 100% confluency at the time of inducing the gap. On the day of the experiments, cells were scratched using a P200 pipette tips (Mettler Toledo, Rainin 30389243; Columbus, Ohio) to create a gap in the cell monolayer. Then cells were serum starved for 2 hrs in basal media. After serum starving, cells were washed and treatments were added in basal media, with basal media and endothelial growth media as negative and positive controls, respectively. Images were taken at 0 hr and 11 hrs. The area of the denuded areas at each time point were measured using Image J. Data is shown as % closure in the gap area.

3.3.10 Statistical Analysis

Parametric statistical tests (one-way analysis of variance (ANOVA) with Bonferroni post hoc test, 2-sample t test) were used as appropriate and statistical significance level is indicated for each figure where it was calculated. Statistical significance was shown with the following notation: ns (not significant), $p > 0.05$, * or # $p \leq 0.05$, ** or ## $p \leq 0.01$, *** or ### $p \leq 0.001$, **** or #### $p \leq 0.0001$. Data are plotted as mean ± standard deviation.

3.3 Results

3.3.1 The effects of sonication on EVs and nucleic acids

To ensure the integrity of EVs after sonication, we evaluated them via nanoparticle tracking analysis and western blotting. HEK293T EVs were sonicated for durations up to 180 seconds either with or without siRNA. The size distribution and concentration were then measured via NTA. The size distribution and mean diameter remained similar for each of the conditions suggesting that there is minimal aggregation or rupture of the EVs (**Figure 3.1A**). Western blotting for markers specific to EVs showed that the protein integrity was preserved (**Figure 3.1B**).

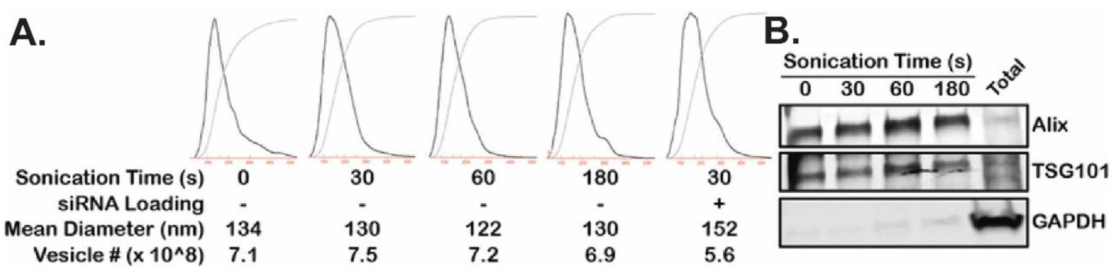

Figure 3.1. EV characterization after sonication. (A) Concentration and size distribution of EVs were measured via NTA for the indicated duration of sonication. Representative data from 3 independent trials shows no significant difference in samples. (B) Levels of EV markers Alix and TSG101 remain unchanged after sonication as shown by immunoblot. Total refers to total cellular lysate. GAPDH was used as a control cellular marker.

Next, the impact of sonication on nucleic acid cargo was evaluated. An agarose gel showed increased degradation of plasmid DNA after 30 s of exposure (**Figure 3.2A**). Thus, all subsequent experiments used 30 s sonication time. Another potential concern was cargo aggregation. As mentioned in Chapter 2, prior reports indicated that electroporation results in siRNA aggregation. Here, we assessed the potential for sonication-induced aggregation by filtering sonicated siRNA through 300 kDa MWCO filters. Sonication resulted in ~12 fold less siRNA aggregation than electroporation (**Figure 3.2B**).

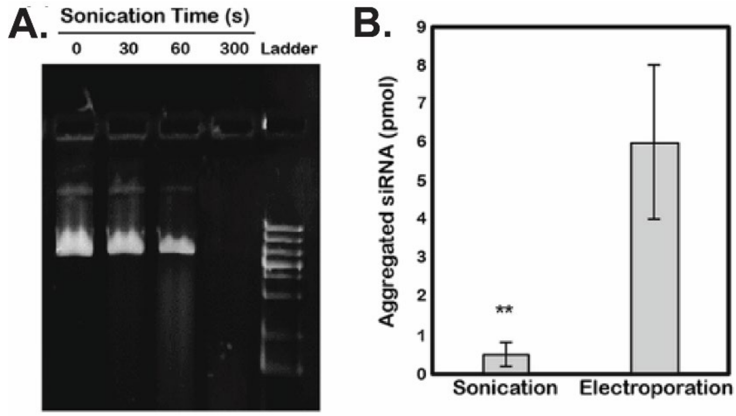

Figure 3.2. The effect of sonication on nucleic acid integrity. (A) Plasmid DNA integrity was evaluated by running samples through agarose gel electrophoresis (0.6% agarose) for durations up to 300 s and staind with SYTO-60. (B) Equal amounts of siRNA were either sonicated (30 s) or electroporated (2 pulses) and washed with 300 kDa MWCO filters. The amount of siRNA aggregation larger than 300 kDa were quantified after labeling with PicoGreen dye.

3.3.2 Quantification of cargo loading and function in sonicated EVs

Once the preservation of EV and nucleic acid integrity was evaluated, levels of cargo loading were quantified (**Figure 3.3**). Comparing siRNA, miRNA, and ssDNA, miRNA showed the highest total cargo loading into the EVs after sonication. All three were more effectively loaded into EVs after sonication than by passive incubation.

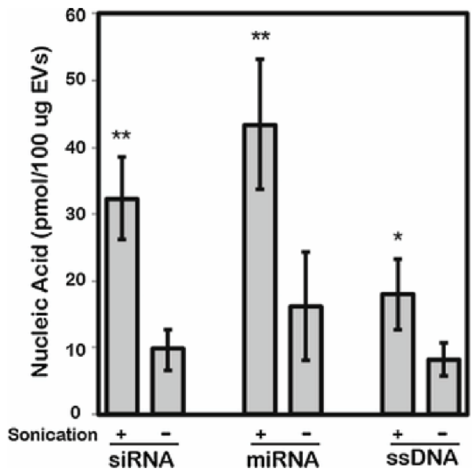

Figure 3.3. Loading various nucleic acids via sonication. siRNA, miRNA, and ssDNA encapsulation were evaluated for EVs loaded via sonication or passive incubation after washing unincorporated nucleic acids. **p < 0.01, *p < 0.05 by t test compared to passive incubation; n = 3

Cellular uptake of EVs was then assessed to ensure that sonication did not impair siRNA delivery (**Figure 3.4**[§]). HEK293T cells were treated with PKH67-labeled HEK293T EVs loaded with Cy3-labeled GAPDH siRNA. After 22 hours of incubation, flow cytometry showed a decrease in cellular uptake of sonicated EVs (84.86%) compared to EVs that were not sonicated EVs (95.03%). However, siRNA delivery was higher in EVs that were loaded by sonication (2.96%) than for EVs passively incubated with siRNA (0.16%) or electroporated (0.16%).

[§] Figure 3.4 courtesy of Divya B. Patel

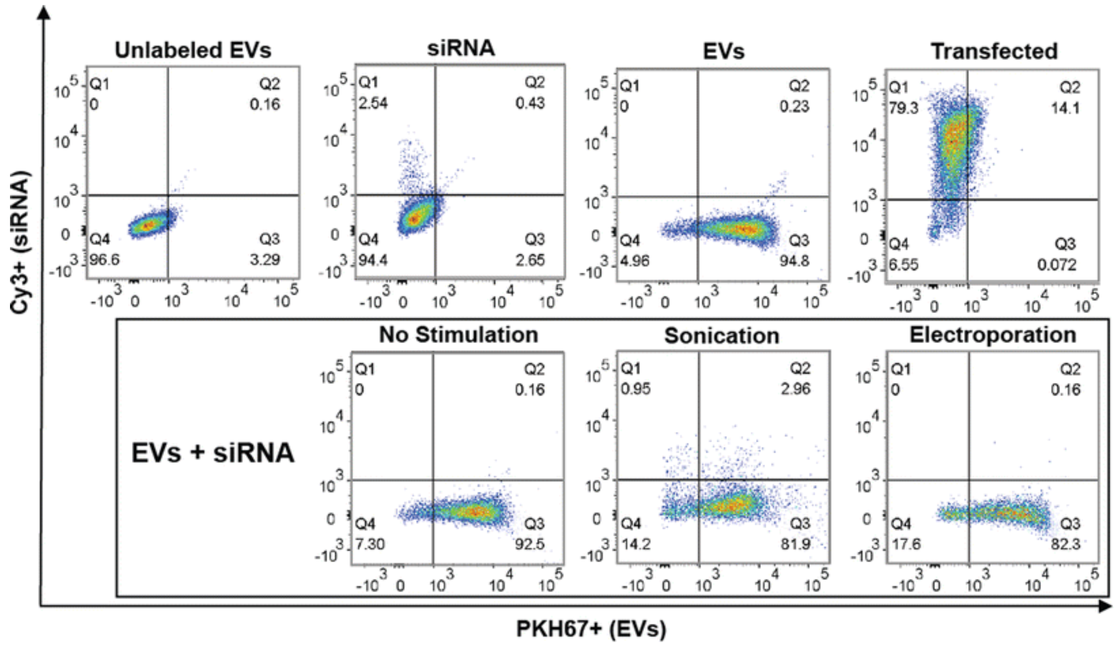

Figure 3.4. EV uptake and siRNA delivery. PKH67+ and Cy3+ populations were gated from live cells, with Q2 showing cells containing both labeled EVs and labeled siRNA. The upper four panels show cells incubated with unlabeled EVs (unlabeled EVs), Cy3-siRNA (siRNA), PKH67 labeled EVs (EVs), or transfected with Cy3-siRNA (transfected). The lower three panels represent cells incubated with PKH67 EVs loaded with Cy3-siRNA by different methods: passive incubation (no stimulation), sonication, or electroporation.

After confirming delivery of siRNA into the cells we needed to ensure functional integrity of the cargo being delivered. Knockdown of GAPDH, an enzyme involved in glycolysis, was used as a proof-of-concept study to evaluate function. HEK293T cells were treated with HEK293T EVs loaded with siRNA targeted to GAPDH at different concentrations for 24 h. Diminished mRNA levels (down to 33.3% of control levels; **Figure 3.5A**) and downregulation of GAPDH protein expression (**Figure 3.5B, C**). Upon validating the functional activity of siRNA delivery with sonicated EVs, we then proceeded to a therapeutically relevant siRNA cargo, HER2 siRNA. This will target a critical oncogene target that is overexpressed in an aggressive form of breast cancer

[137]. MCF-7 breast cancer cells were treated with MCF-7 EVs loaded with HER2 siRNA to achieve a final siRNA concentration of 20 nM. The loaded EVs achieved 59.2% knockdown of HER2 mRNA compared to control levels (**Figure 3.5D**), with a similar level of protein knockdown observed by immunoblot (**Figure 3.5E, F**)[**].

[**] Figure 3.5 courtesy of Tek N. Lamichhane

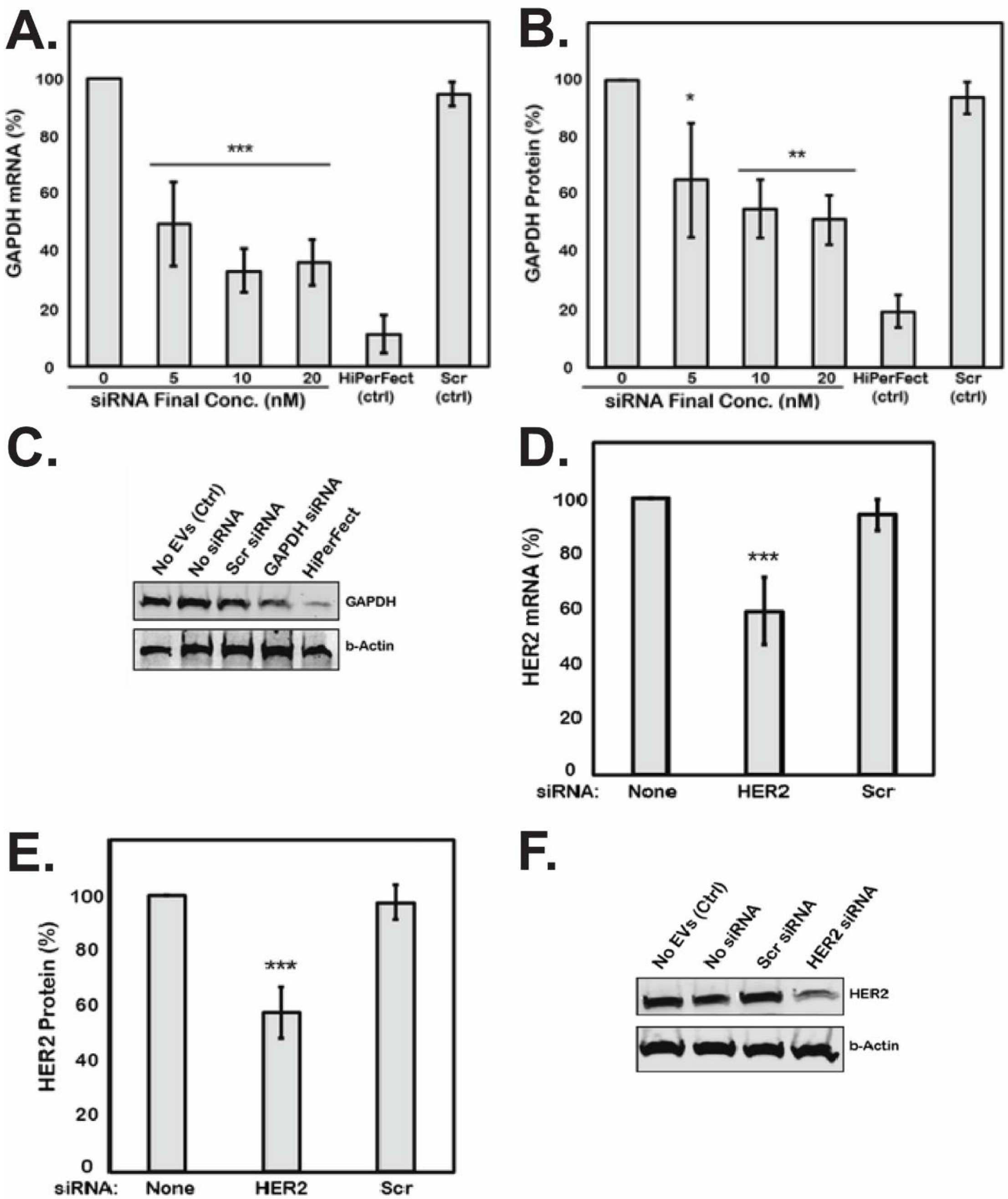

Figure 3.5. Functional delivery of siRNA via sonication loaded EVs. (A) Delivering GAPDH siRNA to HEK293T cells via sonication loaded HEK293T derived EVs shows a dose dependent decrease of GAPDH mRNA in the cells as shown by qPCR. GAPDH mRNA level is shown as a percent of the levels in EVs without any treatment. HiPerfect transfection used 5 nM siRNA. (B) Densitometry measurements from 3 independent immunoblots also reflected a dose dependent decrease in GAPDH protein levels compared to the untreated control. (C) Representative immunoblot used to generate data in panel B. β-actin was used as a housekeeping control protein. (D) Delivering HER2 siRNA to MCF-7 cells via sonication loaded MCF7 derived EVs resulted in decrease of HER2 mRNA levels in cells as shown by qPCR and (E) a decrease in protein levels as shown by densitometry measurements from 3 immunoblots. (F) Representative immunoblot used to generate data in panel E. EVs loaded by sonication with a scrambled siRNA sequence (Scr (ctrl)) were included (20 nM final siRNA concentration) as a control.

3.3.2 Evaluating the impact of sonication on endogenous EV function

While sonication loading is promising for EV function, it remains unknown how this loading method impacts endogenous function. As mentioned, this is done by temporarily porating the membrane and allowing for the diffusion of cargo into the vesicle. Since this method is based on diffusion, there is potential for cargo within the EV to also escape by this same mechanism. Thus, we investigate here the potential of sonication to lead to a loss in endogenous therapeutic cargo and function of EVs.

Figure 3.1 shows that the size distribution and EV-associated markers Alix and TSG101 remain preserved after sonication. The impact of sonication on protein content was also more broadly evaluated by looking at potential changes in total protein concentration via BCA (**Figure 3.6A**). As expected, there is minimal change in the protein level or content after sonication.

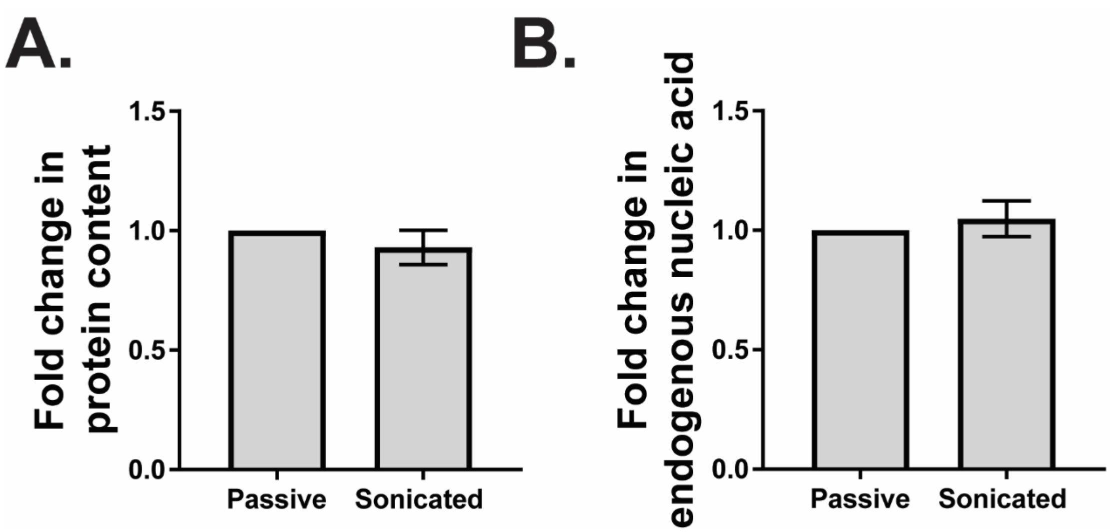

Figure 3.6. Protein and nucleic acid levels in EVs after sonication. Total protein content of BDMSC EVs after sonication as shown by (A) BCA and (B) a total protein gel. (C) Endogenous nucleic acid levels in EVs normalized to the levels in passively incubated EVs. (n = 3)

To assess any loss of endogenous nucleic acids, passively incubated EVs and sonicated EVs were labeled with a cell permeable nucleic acid stain, SYTO™ 60 Red Fluorescent Nucleic Acid Stain and washed extensively. There was no difference in the levels of nucleic acids measured (**Figure 3.6B**), suggesting that sonicating using the parameters described does not result in outward diffusion of a significant amount of nucleic acid cargo.

To confirm that there are limited effects on the endogenous therapeutic effects of EVs after sonication, the pro-vascularizing activity of BDMSC EVs was evaluated using gap closure and proliferation assays (**Figure 3.7**) Both showed no statistical significance between passive and sonicated treatments.

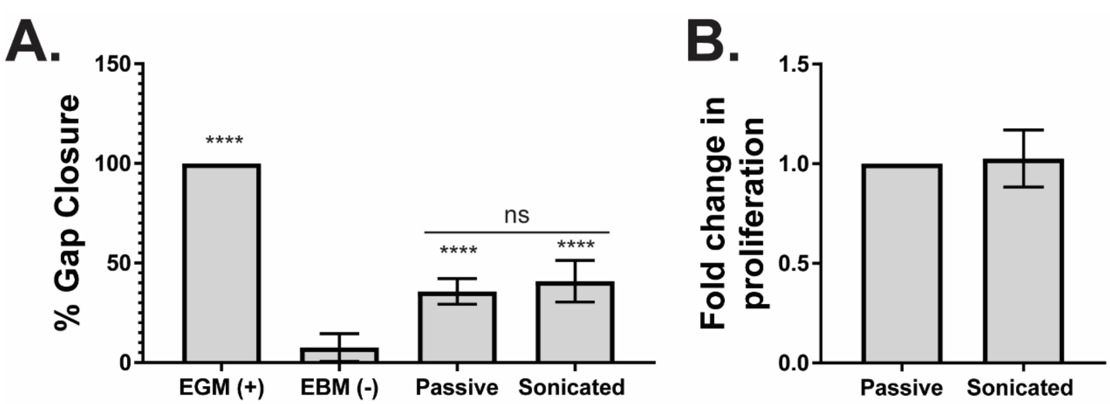

Figure 3.7. Functional activity of sonicated BDMSC EVs. (A) EV function is expressed as a percent closure of gap area after introducing a scratch in a monolayer of HUVECs. EGM and EBM are the positive and negative control treatments, respectfully. (B) Proliferation was measured using a Hoescht stain after incubating HUVECs with BDMSC EVs. Data is shown as fold change with respect to proliferation induced by passively incubated EVs. (n =3)

3.3.2 Co-loading cargo for simultaneous delivery

Combination therapies have shown to be beneficial over targeting a disease with just one molecule by acting on multiple targets [138]. miRNA combination therapies have been gaining traction in cancer [139] and cardiovascular applications [140]. While delivering two different treatments may show a benefit in vitro, to have similar benefits in vivo we will need to deliver these components in the same vehicle to make sure they are being taken up in similar amounts. Co-loading ensures spatiotemporal uniformity between the multiple components. The ability to controllably co-load two different miRNA cargos into a single EV population was determined by loading Cy3-labeled miR-93 and Cy5 labeled miR-126 in varying proportions. Results show that despite variations in replicates, on average we are able to achieve close to the intended ratio (**Figure 3.8**). Further studies will determine the reproducibility and functional benefits.

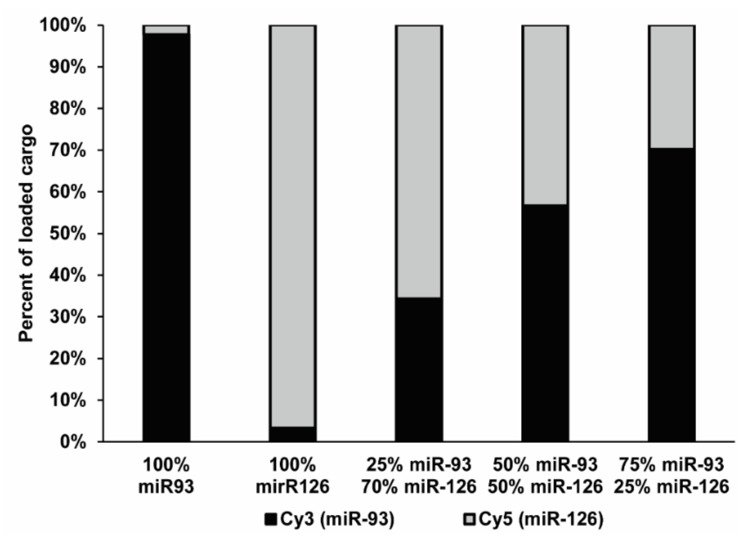

Figure 3.8. Co-loading fluorescently labeled miRNAs into an EV population via sonication. Cy3 labeled miR-93 or Cy5 labeled miR-126 were added to the loading solutions at the indicated volumes before sonication. Data is shown as the percent of the total loaded RNA content that was quantified to be either miR-93 or miR-126 using a standard curve. N=3

3.4 Discussion

Sonication has previously been evaluated as a potential method for loading small molecule drugs into EVs[136]; however, it was unknown whether this technique would be feasible for loading labile nucleic acid cargoes. The results described here demonstrate that sonication can be used to effectively load various small nucleic acids (miRNA, siRNA, ssDNA) into EVs and may be a potential alternative to electroporation.

In this study, we have shown that sonication results in minimal aggregation compared to electroporation [115] (**Figure 3.2**) and enhanced siRNA delivery (**Figure 3.4**). However, the technique used here only measured aggregates greater than 300 kDa and did not investigate the presence of smaller aggregates. Furthermore, while we showed increased uptake of sonicated EVs compared to electroporated EVs, the delivery of labeled siRNA using sonicated EVs was still very low (2.96%). Despite low levels of siRNA delivery, we still observed an encouraging functional effect in knocking down GAPDH and HER2 levels *in vitro*. Thus, we have demonstrated a method with minimal aggregation of nucleic acids in comparison to electroporation, but still has comparable function.

Though we showed the ability to enhance the presence of a particular nucleic acid cargo in EVs, it is also important to understand the effect of loading on endogenous cargo present in the EVs. This information is vital to choosing the appropriate cell source to obtain EVs to be therapeutic carriers. There is great intersest in using already therapeutic EVs, such as those derived from BDMSCs, as carriers to enhance their existing function. However, if the loading technique used diminishes this effect, then the more practical choice would be a source which is cost-effective and easy to culture with high yield rather than one which is therapeutic but requires more maintenance. Here, we have shown that the process of sonication does not lead to a decrease in endogenous nucleic acid (**Figure 3.6**). It is important to note that here we only observed changes induced by sonication and not any changes to endogenous nucleic acid levels due to the introduction of a new cargo. It has been shown previously that genetically perturbing EV content through cellular overexpression can decrease endogenous levels in immortalized bone marrow derived macrophage cells [141]. Thus, there is a potential for changes in endogenous levels after enhancing a particular cargo level in EVs via sonication. We were also able to confirm, via two different functional assays that the BDMSC EVs retained their vascularization bioactivity. These results suggest that sonication can be used to load relatively inert EVs (such as those derived from HEK293T cells [142]) or to enhance already therapeutic EVs (such as those derived from BDMSCs) without losing innate function. This is important for the advancement of EV therapeutics because knowing that sonication does not impair endogenous benefit expands the potential for EV sources.

Despite these advantages of sonication, we have also shown that prolonged exposure to sonication will degrade nucleic acid cargo (**Figure 3.2**). This degradation poses concerns for the scalability of this method since nucleic acid is added in considerable excess for the loading method. Any remaining nucleic acid cargo in the loading volume could not be used in subsequent loading of fresh EV samples due to the potential for degradation.

3.5 Conclusion

Although high duration of exposure can lead to nucleic acid degradation, sonication enables effective cargo loading into EVs without inducing aggregation or reducing the innate therapeutic function of EVs. An additional advantage to this method is its simplicity, but the damaging effects to nucleic acids after repeated exposure limit its scalability potential. In summary, this method is a viable alternative to electroporation, but leaves room for improvement in nucleic acid stability.

Chapter 4: Evaluating the impact of storage conditions and duration on extracellular vesicle characterization and function††

4.1 Introduction

Stability of a therapeutic after storage is critical to defining shelf-life and potential applications; however, studies characterizing the stability of EVs are limited. Further, understanding EV responses to storage is essential to how and where EV-based therapies will be used to ensure that they retain their potency. This remains a significant obstacle to the translation of EV-based approaches.

Prior work has focused predominantly on storage of bodily-fluid derived EVs [85,88,99,143], but in recent years studies have emerged investigating the effects on cell-culture derived EVs [113], which have the most relevance for large-scale therapeutic development. Only recently have studies emerged observing the impact of storing EVs post-isolation [144–146]. Currently, standard protocol is to store EVs at -80°C as a precaution to prevent any degradation [38]; however, requiring constant -80°C storage will decrease the clinical appeal of EVs. Further, a clearer understanding of the effects of various storage conditions and the effects of freezing and thawing these samples is necessary. There is a clear need for a systematic investigation of storage parameters. In this study, we set out to study the physical and functional effects of

†† **Jeyaram A**, Bhatt M, Stewart S, He X, Jay SM. "Evaluating the impact of storage conditions and duration on extracellular vesicle characterization and function." (In preparation)

storage conditions and freeze-thaw cycles on EV bioactivity, specifically on mesenchymal stem cell (MSC) EVs.

MSC-derived EVs show great promise in therapeutic applications and have been used frequently to illustrate the potential of EVs as cell-free therapeutics [147–149]. These EVs have been demonstrated to promote wound healing [150,151], mitigate acute kidney injury [152], and encourage proper tissue remodeling post-myocardial infarction [62] among other therapeutic outcomes [153–156]. Due to their therapeutic functions, MSC-derived EVs are a promising target for eventual clinical translation. However, no studies have been conducted on the stability of MSC-derived EVs after storage. Therefore, this study aims to understand if storage has an impact on basic EV characterization and more importantly if any changes translate to impairment of vascularization bioactivity.

Furthermore, it remains unknown how well loaded cargo is preserved after storage of exogenously-loaded EVs. Many methods of loading, such as sonication, disrupt the lipid membrane and thus may result in leakage of cargo. Further, if a loading technique does not effectively integrate the cargo within the EV, cargo may be degraded or lost after storage. Understanding the effects of storage on both endogenously therapeutic and cargo-loaded EVs is essential to influencing further work on EV formulation development.

Here we report the effects of storage at various temperatures and freeze-thaw cycles on EV characterization and bioactivity. The use of trehalose as a storage buffer and cargo retention are also studied.

4.2 Methods

4.2.1 Cell culture

Bone marrow-derived MSCs (BDMSCs; ATCC PC-500-012) and HEK293T cells (ATCC CRL-3216) were cultured in Dulbecco's Modification of Eagle's Medium (DMEM) [+] 4.5 g/L glucose, L-glutamine, sodium pyruvate (Corning) supplemented with 10% FBS in T175 tissue culture polystyrene flasks in the presence of EV-depleted serum. The media for BDMSCs also incorporated 1% non-essential amino acids. BDMSCs were used at passage 3 for functional assays and passage 5 for characterization. BDMSC were used to show endogenous functionality, while HEK293T EVs were used for all loading studies. HUVECs (Lonza C2519A) were cultured in flasks coated with 0.1% gelatin prior to cell seeding in endothelial growth media (PromoCell C-22121).

4.2.2 EV isolation

Conditioned media from BDMSCs and HEK293T cells grown in EV-depleted media was collected and subjected to differential ultracentrifugation with a 100,000 x *g* final centrifugation step as previously described [76,104]. Pelleted EVs were resuspended in 1XPBS and washed using Nanosep 300 kDa MWCO spin columns (Pall). The washed EVs were resuspended in 1XPBS and filtered using an 0.2 um syringe filter.

4.2.3 EV storage conditions

After isolation, EVs were characterized and then aliquoted to store at either room temperature (RT), 4°C, -20°C, or -80°C. Separate aliquots were prepared for each storage time length (7 day, 28 days) or for freeze-thaw cycles (1 cycle, 5 cycles). Three replicate samples were prepared for each time point and storage condition. Each freeze-thaw cycle consisted of freezing the samples overnight before thawing.

4.3.4 EV quantification by nanoparticle tracking analysis (NTA)

EVs were quantified by nanoparticle tracking analysis (NTA) via a NanoSight LM10 using NTA analytical software version 2.3. Isolated EVs were diluted to a concentration of 10 ug protein/mL and aliquoted out for each of the time points and storage conditions before loading into the NanoSight analysis chamber at room temperature. Three samples were prepared for each time point. Each sample was analyzed in triplicate using different fields of view with a 60 second video acquisition time. The camera level and threshold were set consistently at 16 and 7, respectively for all samples.

4.2.5 EV quantification by CD63 Exo-ELISA ULTRA

As an alternative to NTA, EV concentration was evaluated by the amount of EV-associated CD63 via ELISA (ExoELISA™-ULTRA CD63, System Biosciences), following the manufacturer's instructions. 50ug of EVs in coating buffer were captured on a high protein binding microtiter plate by incubating at 37°C for 1 hr. After this step, all subsequent washes and incubations were done at room temperature under agitation. After three washes, each five minutes, samples were incubated for 1 hr with an anti-CD63 primary antibody (1:100) that recognizes the protein on the EV surface. Plates were then washed again and incubated 1 hr with a secondary antibody (1:5,000) linked to Horseradish Peroxidase enzyme was then added for signal amplification. After a final washing step, plates ere incubated with extra-sensitive TMB ELISA substrate for 10 minutes. The reaction was stopped using a Stop buffer and quantitated using a spectrophotometric plate reader at 450nm.

4.2.6 Total protein analysis and immunoblots

Total EV protein amounts were determined by bicinchoninic acid assay (BCA) following the manufacturer's protocol. Protein level experiments were performed with three replicate samples for each time point, and each sample was measured in duplicate. Based on the Day 0 protein amount, samples containing 20 ug of protein were aliquoted for each time point for the total protein and western blots. At each time point, samples were prepared and stored until the blot was run. Total protein stains were done using Swift Membrane Stain (G-biosciences). The membrane was imaged using a LI-COR Odyssey CLX Imager. Specific EV protein marker levels were quantified using immunoblot analysis for Alix (Abcam ab186429) at 1:1000, TSG101(Abcam ab125011) at 1:1000, CD63 (Applied Biomaterials Inc Y402575) at 1:200, and GAPDH (D16H11; Cell Signaling, 5174) at 1:2000, incubated over two nights at 4°C while shaking. Goat anti-rabbit IRDye 800CW (925–32210; LICOR) secondary antibody was used at a 1:10,000 dilution. The bands were detected with a LI-COR Odyssey CLX Imager and quantified using LI-COR Image Studio.

4.2.7 Gap closure assay

HUVECs (P5) were seeded in 48 well plates in endothelial growth medium (EGM) and allowed to grow until the formation of a confluent monolayer. The cell monolayer was then disrupted to form a scratch using a pipette tip [157]. After washing, the cells were serum-starved for 2 hours after which the medium was replaced with the treatments. EGM and endothelial basal media (EBM) were used as positive and negative controls, respectively. The experiments with Day 0 EVs were conducted on the day of isolation and the remaining EVs were stored at the indicated conditions or freeze-thaw cycles. After storage, another gap closure assay was performed with the samples at those time points. The gap area was imaged at both 0 hours and 11 hours. The change in denuded area was quantified using ImageJ.

4.2.8 Statistics

Parametric statistical tests (one-way analysis of variance (ANOVA) with Bonferroni post hoc test or 2-sample t test) were used as appropriate and statistical significance level is indicated for each figure where it was calculated. Unless otherwise indicated in the figure captions, ANOVA with Bonferri was used.

4.3 Results

4.3.1 Storage effects on EV size, concentration, and protein markers

After EVs were isolated from conditioned medium of BDMSCs by differential centrifugation, they were aliquoted for each of the storage conditions and time points (n=3). EV size, concentration, and variation in size distribution were assessed using nanoparticle tracking analysis (NTA) by a NanoSight LM10. EV size (as represented by mode and mean) showed a slight increasing trend both over time and with increasing freeze-thaw cycles (**Figure 4.1**). After 28 days of storage at -20°C, statistically significant shifts in EV mean (130 nm to 158 nm, ** $p \leq 0.01$) and mode (113 nm to 143 nm, ** $p \leq 0.01$) were observed. After 5 freeze-thaw cycles at -80°C, there was a 46 nm increase in mean size from 130 nm to 176 nm (** $p \leq 0.01$). The variation in size distribution also increased with storage time, most significantly at RT (* $p \leq 0.05$) and after 5 freeze-thaw cycles at both -20°C and -80°C (* $p \leq 0.05$).

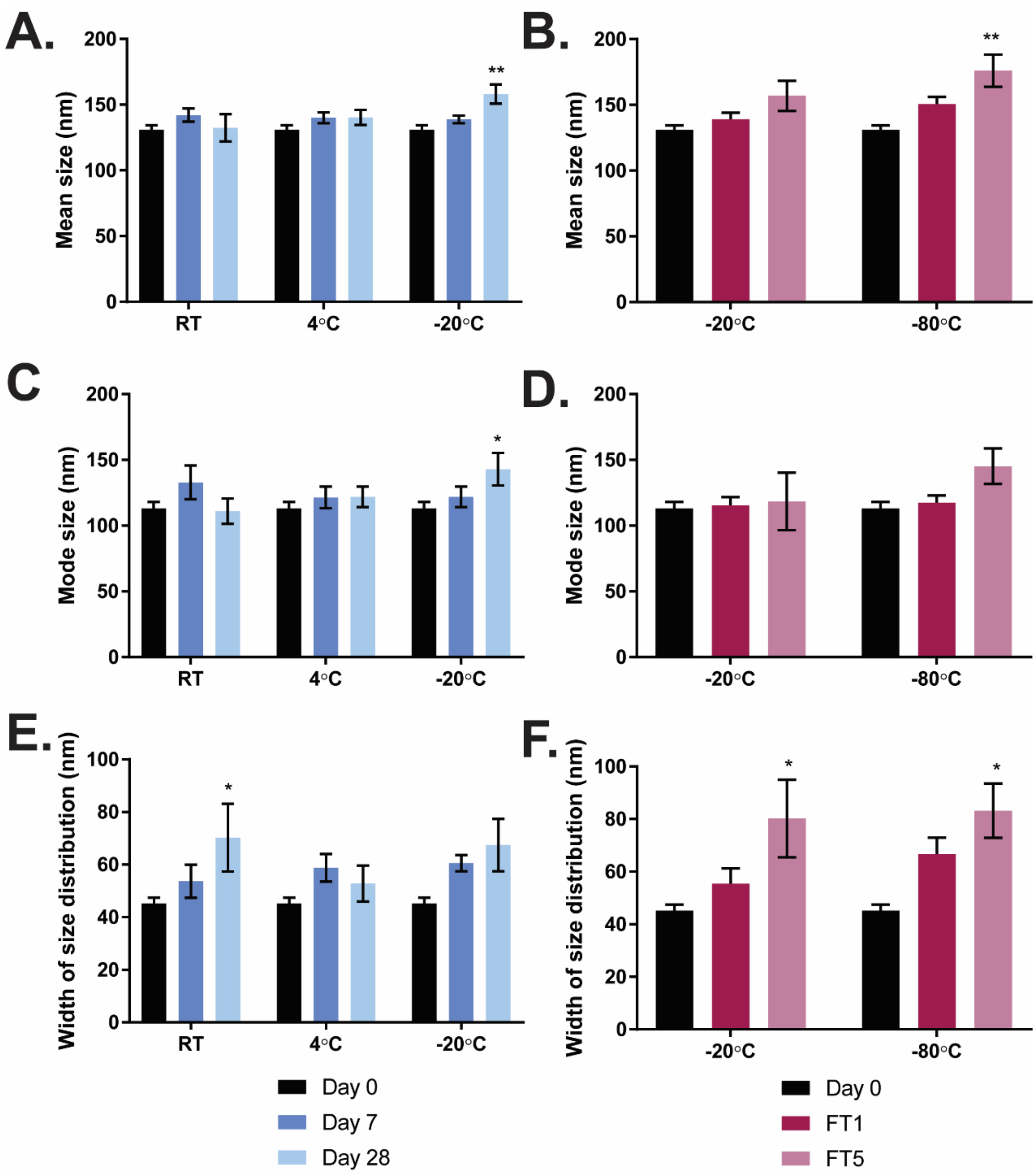

Figure 4.1. Storage effects on size distribution of BDMSC EVs. (A) Mean EV size over 28 days and (B) after freeze-thaw cycles, as well as (C) mode of EV size over 28 days and (D) after freeze-thaw cycles show an increasing trend. (E) The width of the size distribution over 28 days and (F) after freeze-thaws also increases. This variation in size is the standard deviation of the size distribution of each sample reading. N = 3 and each n was measured 3 times at different fields of view. Statistical significance is shown in comparison to the Day 0 (fresh) sample. (2 way ANOVA; no matching; simple effects within rows; Dunnett post hoc. * p≤0.05, ** p≤0.01, *** p≤0.001, **** p≤0.0001)

Surprisingly, the concentration of BMSC EVs also appeared to increase both with storage time and with increasing number of freeze-thaw cycles when using NTA (**Figure 4.2**). If the particle sizes were also decreasing with time and number of freeze-thaw cycles, the change in size could be attributed to EVs rupturing and reforming into smaller vesicles. However, as this was not the case, an alternative method of EV quantitation was necessary.

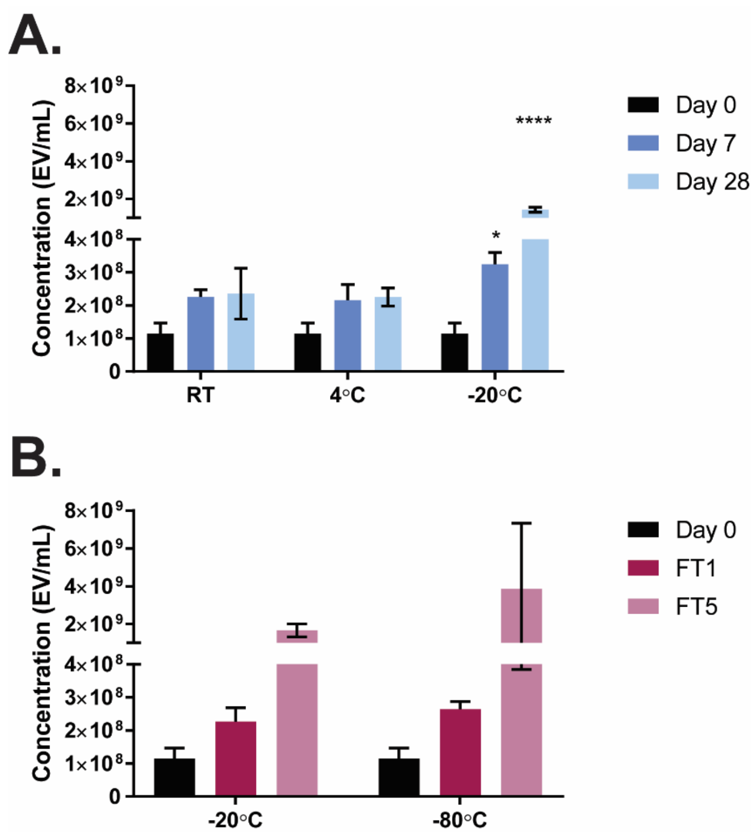

Figure 4.2. Concentration measurements of BDMSC EVs via NTA after storage. Concentration of EV samples after (A) storage up to 28 days and (B) after up to five freeze-thaw cycles. N = 3 and each n was measured 3 times at different fields of view. Statistical significance is shown in comparison with the Day 0 (fresh) sample. (2 way ANOVA; no matching; simple effects within rows; Dunnett post hoc. * $p \leq 0.05$, ** $p \leq 0.01$, *** $p \leq 0.001$, **** $p \leq 0.0001$)

Via Exo-ELISA (**Figure 4.3**), BDMSC EV number remained consistent after 5 freeze-thaw cycles. Day 0 EVs were quantified at 2.05×10^{10}. After the freeze-thaw cycles, EVs at -20°C and at -80°C were quantified at 1.71×10^{10} and 1.93×10^{10} (EV number), respectively.

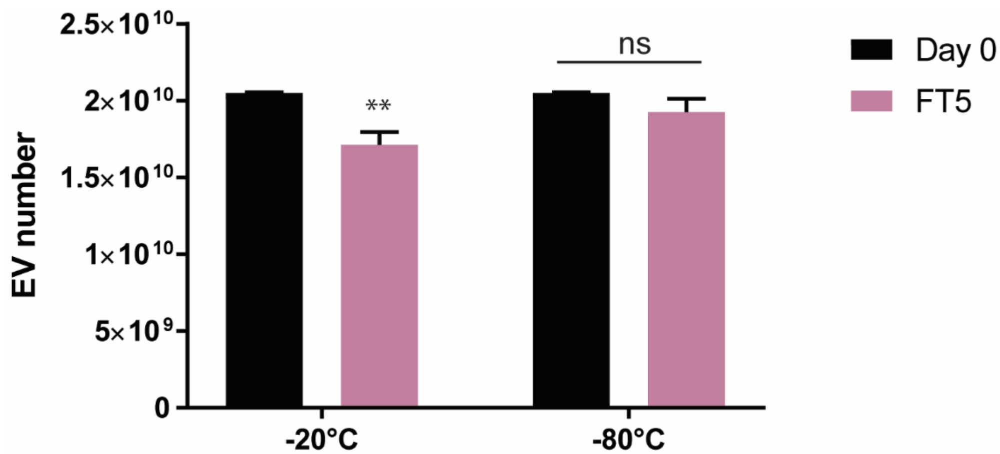

Figure 4.3. BDMSC EV number measurements via ELISA after storage. Measurements of EVs on the day of isolation and after five freeze-thaw cycles via CD63 Exo-ELISA ULTRA shown as total EV number.

To explore potential causes of BDMSC EV concentration increase via NTA, the effects of salt (**Figure 4.4**) and protein concentrations (**Figure 4.5**) were determined. To evaluate the effect of changes in salt concentration of the buffer that may be induced by storage and freeze-thaw cycles, the same amounts of EVs were resuspended in 0.5XPBS, 1XPBS, and 10XPBS solutions. While there was no significant change in size measurements, EVs in 10XPBS showed a significant increase in concentration measurement compared to EVs in 1XPBS.

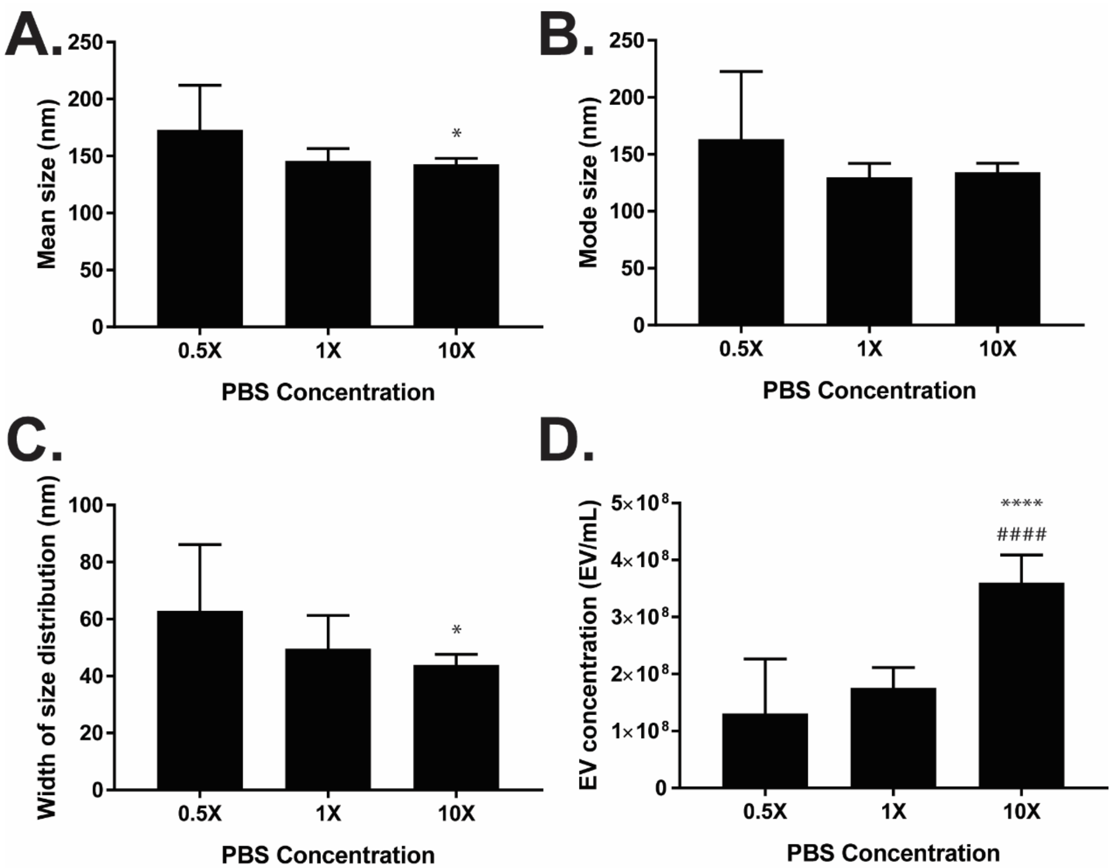

Figure 4.4. Effect of PBS concentration on BDMSC EV characterization via NTA. (A) Mean (B) mode and (C) width of the size distribution as well as the (D) concentration of EVs was measured via NTA. The same number of EVs was resuspended in either 0.5X, 1X, or 10X PBS before measuring. N = 3 and each n was measured 3 times at different fields of view. * = significance with respect to 0.5x; # = significance with respect to 1X.

Alternatively, a potential cause of an increased concentration via NTA could be due to proteins that are dissociating from EVs. To study the impact of free protein concentrations on NTA measurements, 10 ug, 100 ug, or 1000 ug of BSA were added to an EV solution. While there was no significant change in size, the addition of 1000 ug of BSA showed a significant increase in concentration measurement of EVs. This indicated that both changes in buffer salt concentration or detachment of proteins from EVs could cause the apparently artificial increase in EV concentration as measured by NTA.

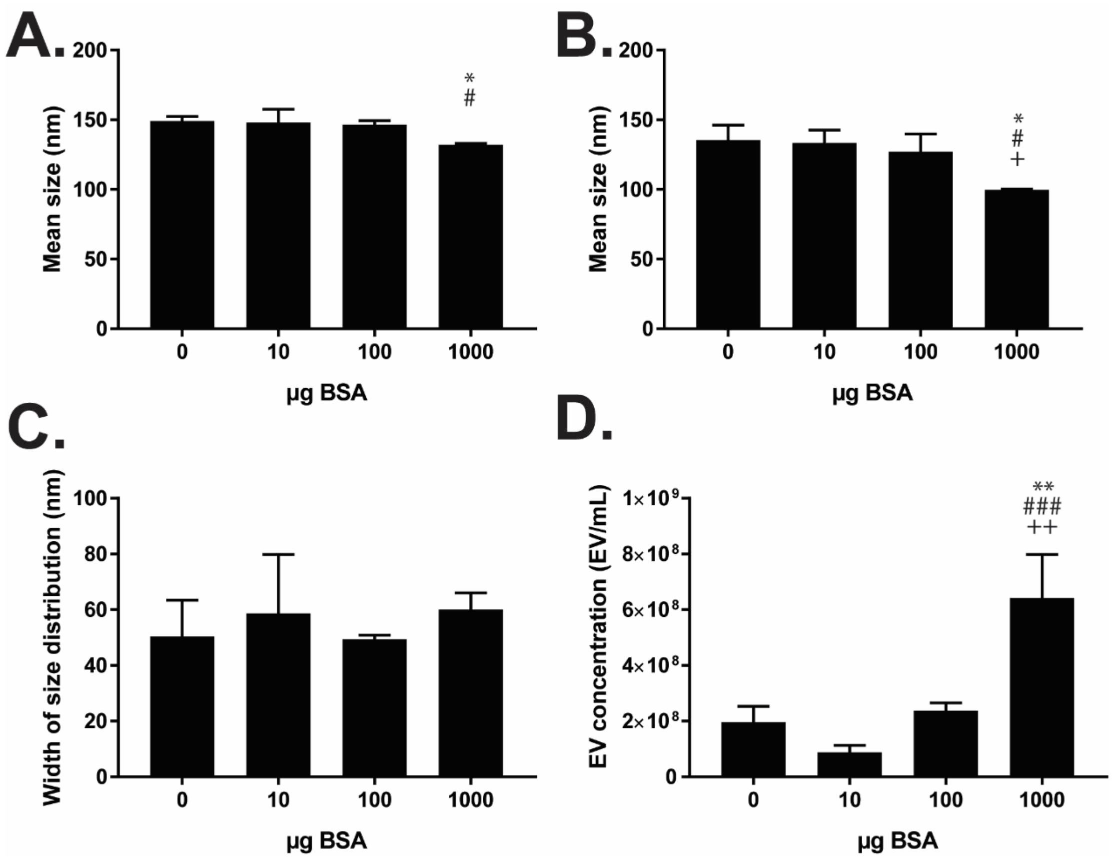

Figure 4.5. The effect of BSA concentration on BDMSC EV concentration measured via NTA. (A) Mean (B) mode and (C) width of the size distribution as well as the (D) concentration of EVs was measured via NTA. Either no BSA, 10 µg, 100 µg, or 1000 µg of BSA were added to the same number of EVs before NTA analysis. N = 1 and each n was measured 3 times at different fields of view. * = significance with respect to 0 µg; # = significance with respect to 10 µg; + = significance with respect to 100 µg.

To evaluate if buffer choice contributed to the changes in EV characterization via NTA, EVs were stored in trehalose. Trehalose is a natural, non-toxic sugar widely used as a protein stabilizer and cryoprotectant by both the food and drug industries. It has been validated as a cryo-preservative for labile proteins, vaccines, and liposomes as well as cells and organs for transplant [118,145,158–160]. Trehalose can stabilize proteins and lipid membranes [116]. It can also decrease intracellular ice formation during freezing and prevent protein aggregation [118]. **Figure 4.6** shows that although the EV size distribution remains relatively unchanged, the concentration measurements for EVs increases with longer durations of freezing.

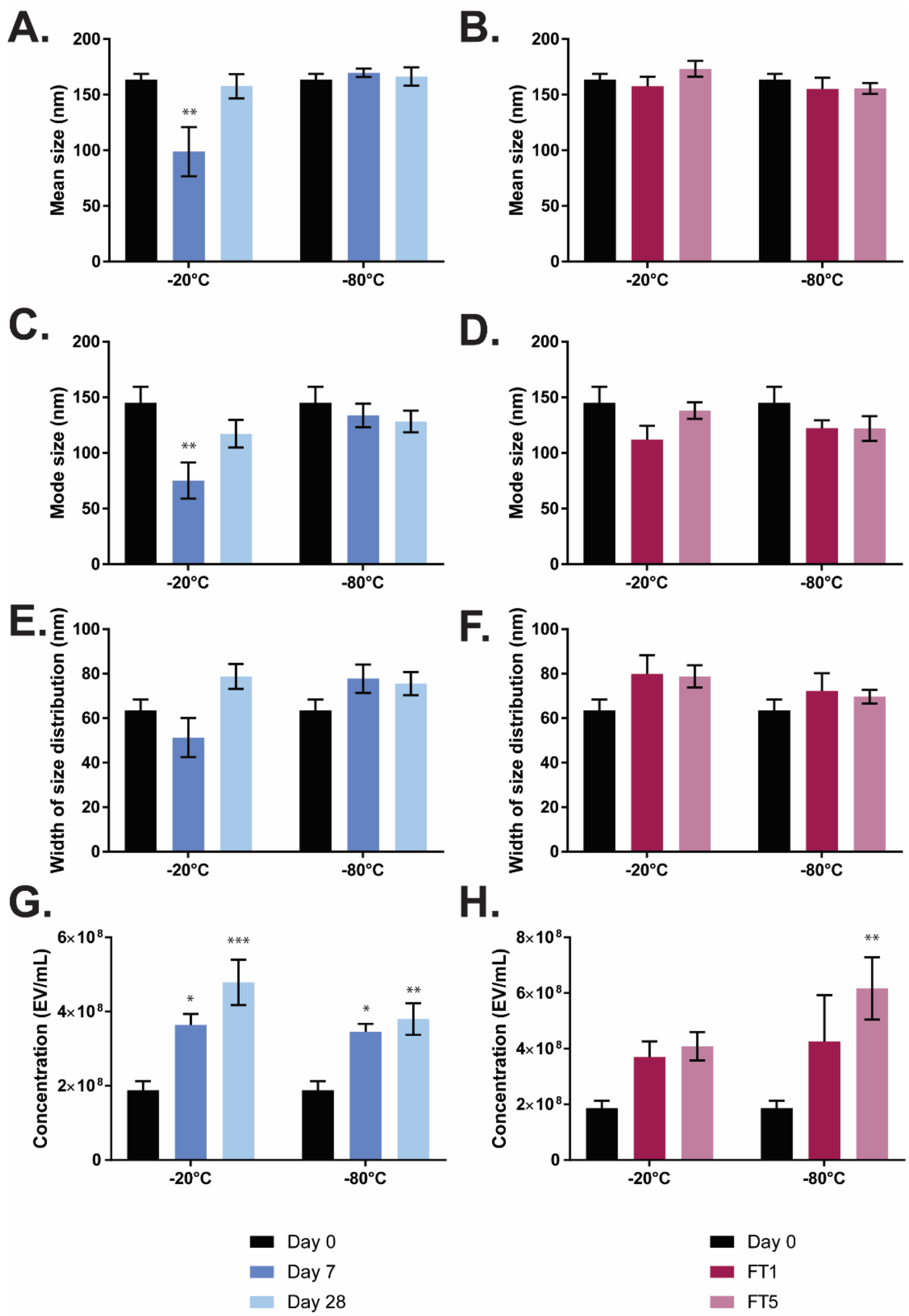

Figure 4.6. Storage effects on size distribution and concentration on BDMSC EVs after storage in trehalose. (A) Mean EV size over 28 days and (B) after freeze-thaw cycles, as well as (C) mode of EV size over 28 days and (D) after freeze-thaw cycles. (E) The width of the size distribution over 28 days and (F) after freeze-thaws. This variation in size is the standard deviation of the size distribution of each sample reading. (G) EV concentration after freezing for 28 days and (H) freeze-thaw cycles increases. N = 3 and each n was measured 3 times at different fields of view. (2 way ANOVA; no matching; simple effects within rows; Dunnett post hoc. * p≤0.05, ** p≤0.01, *** p≤0.001, **** p≤0.0001)

Total protein concentration as well as levels of BDMSC EV associated proteins were evaluated for the same time points and conditions as used in NTA (**Figure 4.7**). A bicinchoninic acid (BCA) assay and total protein gel electrophoresis were used to assess overall protein levels. Both the BCA and total protein results show no significant changes in total protein levels with storage, but after five freeze-thaws there appeared to be a decrease in protein concentration via BCA. Western blot for EV markers (TSG 101 and CD63) demonstrated that neither storage time nor freeze-thaw cycles showed a significant change in the protein levels, regardless of storage type.

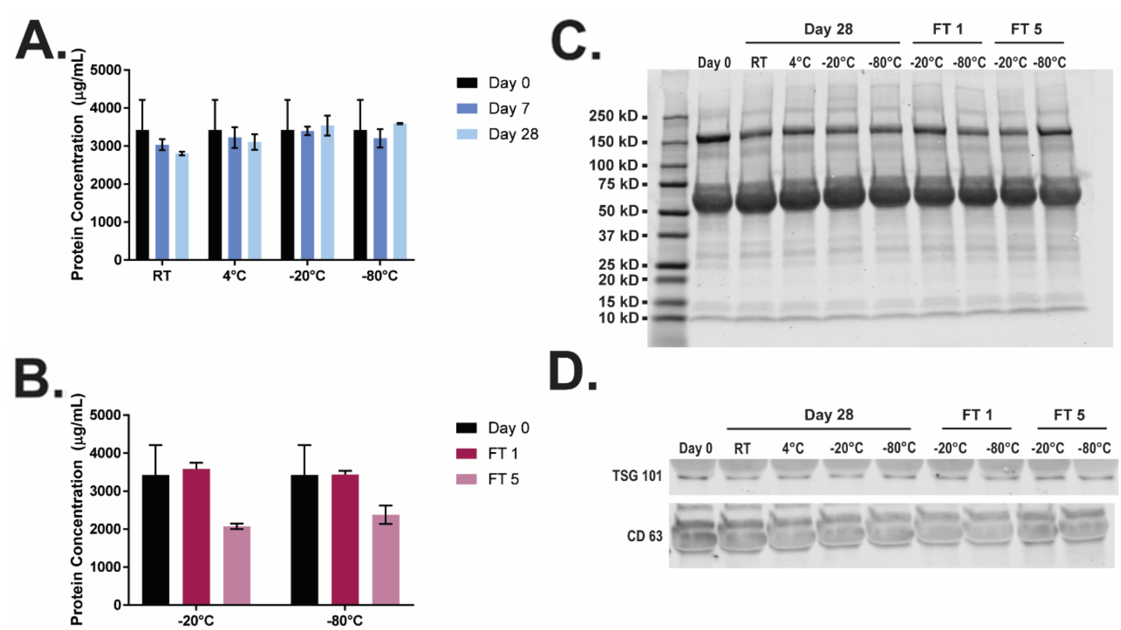

Figure 4.7. BDMSC EV protein content after storage. (A) BCA protein concentration for storage conditions over 28 days and (B) increasing numbers of freeze-thaw cycles show an observable decrease. (C) A total protein blot demonstrates that neither storage over 28 days nor freeze-thaw cycles results in a change of EV protein footprint. (D) Western blot confirms that EV-associated markers, TSG 101 and CD 63, in particular do not degrade with storage. N = 3

4.3.2 Storage effects on endogenous EV bioactivity

Gap closure assays were used to determine the impact of freeze-thaw cycles on the bioactivity of the EVs. Increasing numbers of freeze-thaw cycles induced a trend toward decreasing bioactivity; however, the change after one freeze-thaw cycle was not statistically significant (**Figure 4.8A**). The positive and negative controls, endothelial growth media (EGM) and endothelial basal media (EBM) were not frozen or thawed. The graph represents the combination of three different gap closure experiments that were conducted: on the day of EV isolation (Day 0), after one freeze-thaw cycle, and after five freeze-thaw cycles. All EV samples are represented with black bars while the respective positive (EGM) and negative (EBM) control treatments corresponding to that time point are overlaid in a green square or red circle. For each of the freeze-thaw experiments, samples stored at -20°C are represented with diagonal lines and those stored at -80°C are represented with diamonds. MSC EVs fresh after isolation induced 58% closure of the denuded area after 11 hours. After one freeze-thaw, EVs stored at -20°C and -80°C, resulted in 59% and 56% closure of the wound areas, respectively. This value decreased after five freeze-thaws to 44% gap closure at -20°C and 47% closure at -80°C. To evaluate the impact of storage duration at different conditions, EV bioactivity was evaluated for Day 0 BDMSC P3 EVs and EVs stored for 28 days via gap closure (**Figure 4.8B**). Immediately after isolation, fresh BDMSC EVs induced 37% gap closure of HUVEC cells. After 28 days of storage, EVs at room temperature or 4°C induced a similar level of gap closure to the basal media negative control treatment, indicating a loss of bioactivity. Both storage at -20°C and -80°C, as well as lyophilized samples stored at room temperature, preserved EV bioactivity to similar levels of the fresh sample. To investigate if EVs stored at room temperature or 4°C lose their bioactivity at earlier time points, they were assed in a gap closure assay after storage for 7 days (**Figure 4.8C**). Fresh EVs induced 40% gap closure on day 0, but after storage, the % gap closure was reduced to 26% gap closure for EVs at room temperature and 33% for EVs at 4°C.

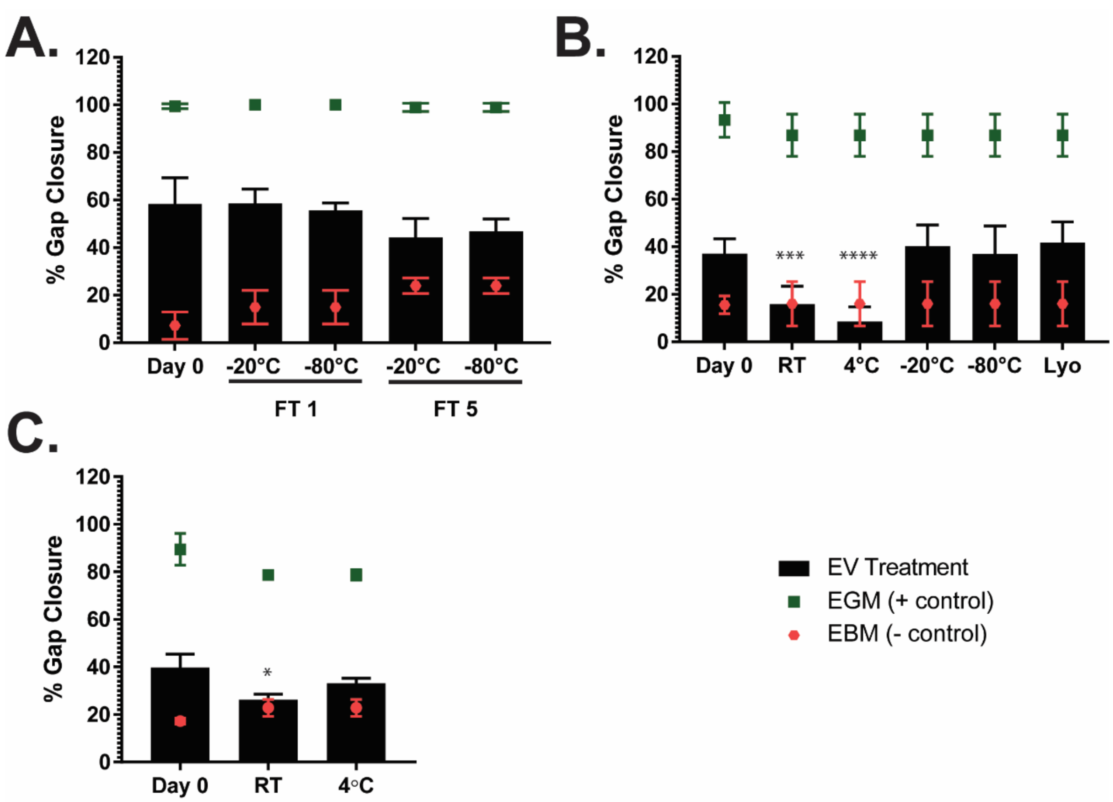

Figure 4.8. Function of BDMSC EVs after storage. (A) Samples were stored at either -20°C or -80°C and subjected to 1 or 5 freeze-thaw cycles before assessing BDMSC bioactivity via gap closure assay.(B) EVs were stored for 28 days at room temperature (RT), 4°C, -20°C, -80°C, or at room temperature after lyophilization (Lyo). For both figures, gap closure assays were performed on the day of isolation (Day 0) or at the indicated time point. Positive (EGM) and negative (EBM) controls for each experiment are shown in as a square or circle, respectively. N=3, representative data shown from 3 independent experiments. Statistical significance is shown with respect to the Day 0 EV Treatment.

4.3.3 Impact of storage on endogenous nucleic acid levels and uptake

Nucleic acid levels were investigated as a potential cause of changes to EV bioactivity after storage. Endogenous nucleic acids were labelled by treating HEK EVs with a cell-permeant stain before extensive washing with a 300 kDa MWCO filter to remove unincorporated dye or nucleic acids on the exterior of the EVs and measuring fluorescence levels. The nucleic acid levels after 7 days of storage were normalized to the average reading for freshly isolated EVs on day 0. Though there is no statistical significance, the fold change in nucleic acid levels decreased with increasing temperature, with a 40% decrease in nucleic acid levels for samples storage at room temperature (**Figure 4.9A**). Levels appear relatively unchanged for EVs frozen at either -20°C or -80°C.

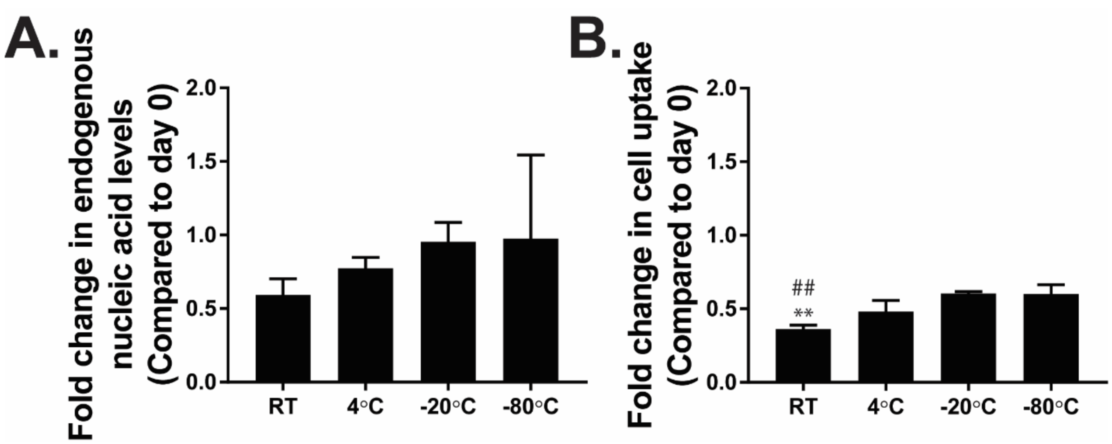

Figure 4.9. Change in HEK EV endogenous nucleic acid levels and cellular uptake after 7 days. EVs were labeled with SYTO™ 60 Red Fluorescent Nucleic Acid Stain either freshly after isolation or after storage at the indicated temperatures. Relative fluorescent units indicated nucleic acid levels. (A) Nucleic acid levels are presented after normalization to EV nucleic acid levels on day 0. Statistical significance is shown with respect to -80°C. N = 3 in 3 independent experiments. Data is combined from the 3 experiments. (B) After measuring fluorescence for nucleic acid levels, EVs were incubated with HUVEC cells for 21 hours before measuring nucleic acid levels taken up into cells to represent uptake. Uptake was first normalized based on fluorescence reading before treating cells before normalizing all data to Day 0 uptake. N = 3 in 1 experiment. * = statistical significance with respect to -20°C. # = statistical significance with respect to -80°C.

HEK EVs with their endogenous nucleic acid content labeled were then used to assess uptake (**Figure 4.9B**). After 21 hours of incubation with EVs, HUVECs were washed and then fluorescence was measured to determine the amount of nucleic acids internalized. This was used to indicate the relative uptake levels of EVs stored at different levels of treatment. There was a 40% decrease in cell uptake after 7 days of storage at both -20°C and -80°C. Uptake levels decreased by 65% when stored at room temperature for the same duration.

4.3.4 Stability of EVs after sonication loading

Though we have shown that endogenous nucleic acids are preserved at -20°C and -80°C for 7 days, this needed to be investigated for exogenously-loaded cargo. HEK EVs were loaded with Cy3-labeled miRNA via sonication and pooled together before quantifying loading. Aliquots stored at RT, 4°C, -20°C, or -80°C were washed extensively after 7 days of storage and fluorescence measurements were taken to evaluate cargo retention. All storage conditions showed a decrease in the amount of cargo retained within EVs, but there is no significant difference between the 4 storage conditions (**Figure 4.10**).

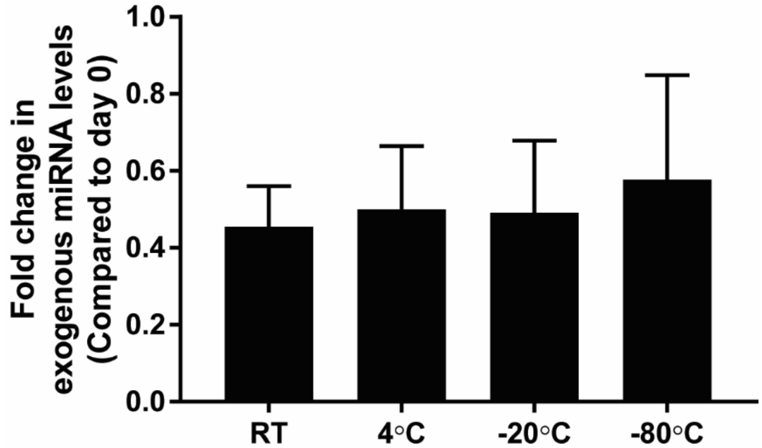

Figure 4.10. Storage of sonication loaded HEK EVs. EVs were loaded with Cy3-labeled miRNA via sonication and then stored for 7 days at the indicated conditions. N=3 for 2 independent experiments. Data is combined from the 2 experiments.

4.4 Discussion

As with any biologically derived therapeutic, understanding the storage stability of EVs is essential for clinical translation and widespread use. This study establishes that while multiple freeze-thaw cycles may lead to a decrease in bioactivity, BDMSC vesicles largely remained preserved in structure and total protein amount. Additionally, EV function is preserved while stored at -20°C, -80°C, or room temperature after lyophilization. The findings are essential to both the reproducibility of work in the lab as well as eventual translatability of EV technology. While most studies to date focus on the storage of a sample prior to EV isolation, Lőrincz et al., obtained a cell-type of interest from venous blood and then detailed the impact of storage on the isolated EVs [113]. Recent studies have emerged further evaluating stability of EVs from cell lines [144–146]. We have expanded on this knowledge by investigating the impact of storage on EVs isolated from MSCs, a widely used cell source of EV production for numerous potential therapeutic applications. It remains to be investigated if these observations are consistent across cell types.

Initial characterization of EVs was done by nanoparticle tracking analysis, one of the most popular techniques of EV size measurements and quantification [161]. Unexpectedly, with both prolonged freezing and multiple freeze-thaw cycles, NTA showed an increase in EV concentration. If the particle sizes were also decreasing, this could be attributed to EVs breaking apart and reforming into smaller vesicles. However, as vesicle size also increased this could not be the case. One potential cause for the artificial increase in concentration via NTA could be disodium salt crystals that can form in phosphate buffers during freezing [162]. The crystallization and aggregation of these salts may also contribute to the increase in observed particle size. It is also important to note that, with larger and more polydisperse samples, increased background signal can lead to an inaccurate count of smaller particles. While this could contribute to some of the increased concentration readings, the videos captured in NTA showed the presence of a larger number of distinct particles. Alternatively, the concentration increase could be due an increase in free protein concentration. In the case that there are any proteins loosely associated with EVs, it is possible that the freezing and thawing process causes them to dissociate from the EVs. In either of these cases NTA would not be able to distinguish between vesicles and these aggregates. This could be remedied by using fluorescent-NTA, in which the EVs are fluorescently labeled to distinguish these vesicles from other debris and aggregates. However, because of their size, achieving adequate EV-labelling efficiency to maximize signal to noise ratio may be difficult [163].

Using an ELISA as an alternative method validate EV concentration results demonstrated that when quantifying EV number based on CD63 expression, there was no significant change. The discrepancy between these results and the NTA data demonstrates the limitations of relying on a sole method of quantification. As with the NTA, it is important to take into considerations the limitations of this method when evaluating the results. This assay indirectly quantifies the number of EVs present based on the amount of CD63 protein present. The ELISA does not take into account if the EVs broke apart and reformed during the process of freezing or rupturing of EVs.

This study demonstrates the importance of understanding the limitations of characterization techniques and supplementing results with appropriate additional methods. A similar issue of discrepancy was reported by Almizraq et al., in their study on the effects of storing red blood cells on their EVs. Comparing various techniques, including NTA, this group observed considerable differences in EV size profile based on the method used. Further, of the three methods they assessed, only tunable resistive pulse sensing showed a change in EV concentration after storing the red blood cells [122]. Therefore, any future standardization of EV characterization must also take into consideration the effects of storage.

Importantly, MSC EV bioactivity can be retained after storage. As protein level appeared not to change significantly, any loss in bioactivity may be due to either changes in uptake efficiency or loss of nucleic acid contents. Though increasing numbers of freeze-thaws lead to decreased bioactivity, some EV function was still retained. In general, storage at both -20°C and -80°C appear comparable after one freeze-thaw, but -80°C retains more activity after 5 freeze-thaw cycles. While this suggests that -80°C may be a safer storage option, -20°C storage is still a viable option. This is promising for therapeutic applications of EVs, as -80°C storage may be limited due to limited availability in clinical settings [123]. However, the effect of multiple freeze-thaws needs to be taken into consideration when storing or transporting EV products. This issue can be resolved by lyophilizing EVs, as our data shows that MSC EV function is retained when lyophilized EVs are stored at room temperature.

Further, this study is the first to evaluate storage stability of EVs loaded with nucleic acid cargo. Within seven days of storage, approximately 40% of miRNA loaded was lost at -80°C. This was the lowest amount of cargo lost among the various storage conditions. As lyophilization of cargo was not explored in this study, this technique can be explored to better preserve cargo within loaded EVs. Another aspect to consider is that the cargo retention may be impacted by loading technique. As sonication depends on perturbation of the EV membrane for cargo loading, this may be affecting the membrane integrity during storage. Thus, loading techniques that don't disrupt the membrane may be advantageous for long-term storage.

Ultimately, storage conditions should always be recorded when analyzing EV samples or using them in experiments. Such information is often not discussed in literature and can be highly variable from group to group. Taking note of this information will allow storage to be taken into account when evaluating any differences in EV analysis or function and also ensure reproducibility of experiments. For experiments comparing EV production or yield using NTA, all samples must be stored at the same temperature for the same duration between isolation and analysis to ensure consistency. Ideally, confirming results with a secondary analysis technique would be preferred, especially in cases were storage time cannot be kept consistent between samples. To retain bioactivity of EVs, multiple freeze-thaws should be avoided.

4.5 Conclusion

Though this study does demonstrate loss of activity with increasing freeze-thaw cycles, this still shows promise for the translation of EVs into clinical use as activity was not completely diminished immediately after storage. Most promising was the potential for storing MSC EVs at room temperature after lyophilization. This can expand the clinical utility of EVs and their potential for widespread use. Future work investigating the impacts of storage technique and buffer on MSC EV activity in vivo will provide further clarity on the optimal storage condition.

Chapter 5: Enhanced loading of functional miRNA cargo via pH-gradient modification of extracellular vesicles‡‡

5.1 Introduction

We have shown in **Chapter 3**, that sonication allows for siRNA loading without significant aggregation, but we also demonstrated nucleic acid degradation with longer exposure times. Thus, there remains a need for further development of cargo loading techniques. Approaches for loading cargo into EVs can be informed by research on liposomal systems, as EVs and liposomes share features of a phospholipid bilayer enclosing an aqueous lumen [73,164,165]. Due to previous work with liposomes showing that a transmembrane pH-gradient can be used to effectively encapsulate weakly basic or negatively-charged small molecule drugs [166–170], we hypothesized that this principle could be translated to loading negatively-charged nucleic acids within EVs. Here, we report the parameter optimization of pH-gradient-mediated loading of miRNAs to HEK293T-derived EVs. We further demonstrate the functionality of these loaded miRNAs via modulation of protein expression in cellular systems as well as the ability to successfully administer pH-gradient-modified EVs to animals.

‡‡ **Jeyaram A**, Lamichhane TN, Wang S, Zou L, Dahal E, Parajuli B, Knudsen DR, Chao W, Jay SM. "Enhanced loading of functional miRNA cargo via pH-gradient modification of extracellular vesicles." *Molecular Therapy*. (Submitted)

5.2 Methods

5.2.1 Cell culture

Human Embryonic Kidney Cells (HEK 293T; ATCC CRL-3216; Manassas, VA) were cultured in Dulbecco's Modification of Eagle's Medium (DMEM) [+] 4.5 g/L glucose, L-glutamine, sodium pyruvate (Corning 10-013-CV; Corning, NY) supplemented with 10% FBS in T175 tissue culture polystyrene flasks in the presence of EV-depleted serum. Human umbilical vein endothelial cells (HUVEC; Lonza C2519A) were cultured in endothelial cell growth media (PromoCell C-22121; Heidelberg, Germany) in flasks coated with 0.1% gelatin. Bone marrow cells were harvested from mouse tibias and femurs, cultured, and differentiated into macrophages (Mϕs) in the presence of M-CSF (10 ng/mL). In brief, bone marrow cells were cultured in RPMI 1640 culture medium (Thermo Fisher Scientific; Waltham, MA) with 10% FBS (Thermo Fisher Scientific), 5% horse serum (Thermo Fisher Scientific), and penicillin (100 U/mL)/streptomycin (100 μg/mL) (Thermo Fisher Scientific) in a CO_2 incubator at 37°C. Three days later, culture media were changed, and Mϕs were ready for experiments at day 4.

5.2.2 EV isolation and characterization

Conditioned media from HEK293T cells grown in EV-depleted media was collected and subjected to differential ultracentrifugation with a 118,000 x *g* final centrifugation step as previously described [76,104]. Pelleted EVs were resuspended in 1XPBS and washed using Nanosep 300 kDa MWCO spin columns (Pall OD300C35; Port

Washington, NY). The washed EVs were resuspended in 1XPBS and filtered using an 0.2 μm syringe filter. EV size distribution and concentration were evaluated by nanoparticle tracking analysis (NTA) via a NanoSight LM10 using NTA analytical software version 2.4. Each sample was analyzed in triplicate using different fields of view with a 30 second video acquisition time. The camera level and threshold were set consistently at 13 and 3, respectively for all samples. Total EV protein concentration was measured using a bicinchoninic acid assay (BCA) following the manufacturer's protocol. Relative levels of EV-associated proteins were assessed via total protein and western blotting. The membrane was imaged using a LI-COR Odyssey CLX Imager. Specific EV-associated protein marker levels and control proteins were quantified using immunoblot analysis for Alix (Abcam ab186429; Cambridge, MA), TSG101 (Abcam ab125011), CD9 (Abcam ab92726), Calnexin (Cell Signaling Technology 2679S; Danvers, MA), and GAPDH (Cell Signaling Technology 2118L). Primary antibodies were added at 1:1000 dilution, besides anti-GAPDH which was added at 1:2000 dilution. Secondary antibody IRDye 800CW anti-Mouse and anti-Rabbit (LI-COR Biosciences 926-32210 and 926-32211; Lincoln, Nebraska) were added at 1:10000 dilutions.

5.2.3 Preparation of pH-gradient modified EVs

To create the pH-gradient, EVs were first dehydrated in 70% ethanol at a concentration of 300 μg/mL. The dehydration was allowed to proceed for 12 hours in a 24-well plate with 1 mL of the dehydration solution per well. Once most of the liquid evaporated, the EVs were rehydrated in 1mL of citrate buffer (150 mM, pH 2.5 for 1 hour). After rehydration, EVs were resuspended and transferred to 300 kDa Spectra/Por Float-A-Lyzer G2 dialysis tubes (Spectrum Labs G235072; Waltham, MA) and dialyzed in 1X HEPES buffered saline (HBS) at pH 7.0. EVs were dialyzed for 24 hours with buffer changes every 2 hours for the first 6 hours and then left overnight. After dialysis, the volume of EV solution was concentrated down using 100 kDa MWCO centrifuge tubes and filtered through 0.2 μm syringe filters. EVs were then characterized as above. For cargo loading, unless otherwise described, $3x10^9$ EVs were incubated with 1000 pmol of miRNA cargo for 2 hours before washing in a 300 kDa MWCO filter with 1X HBS.

To optimize maximum loading efficiency, pH-EVs or unmodified EVs were incubated with equal amounts of miR-93 labeled immediately prior to each set of experiments. To determine the optimal temperature for miRNA incubation, miRNA was incubated with EVs at 4°C, 22°C, 37°C and 60°C. Unincorporated excess cargo was removed by washing with 1X HBS buffer after one hour of incubation. To determine the optimal length of incubation with cargo, the labeled miRNA was incubated with the EVs for 0 minutes, 30 minutes, 1 hour, 2 hours, 6 hours, and 24 hours. After each time point, excess miRNA was removed by washing, as described previously. To evaluate the effect of the citrate buffer pH, the buffer was prepared at pH 2.5, 3, 4, and 7. For all optimization experiments, the unincorporated excess cargo was removed by washing with 1X HBS. Fluorescence was quantified by comparing the values measured at 480 excitation and 520 emission to a standard curve.

miR-93: Dharmacon custom sequence; Chicago, IL; 5' –
CAAAGUGCUGUUCGUGCAGGUAG

5.2.4 Sonication

1000 pmol of nucleic acids were incubated with 100 μg of EVs in 100 μL total volume for 30 minutes. EVs were sonicated in a water bath sonicator (VWR® symphony™; cat# 97043-964, 2.8 L capacity, dimensions 24 L × 14 W × 10 D cm) twice for 30 s at 35 Hz, resting on ice for 1 minute in between. After sonication, EVs were washed in a 300 kDa MWCO filter with 1X PBS. For loading comparison by EV number, $6x10^9$ EVs were used in each loading volume.

5.2.5 Quantification of EV loading

EV loading quantification was performed by labeling nucleic acids with picogreen Quant-iT™ PicoGreen Assay Kits (ThermoFisher Scientific, cat# P11496) Nucleic acids were pre-labeled for detection by mixing 1000 pmol of nucleic acids with 10 μL dye reagent at room temperature for 5 minutes according to manufacturer's instructions for Quant-iT™ PicoGreen Assay Kits. This dye was used in cases where RNA loading was compared to other nucleic acids. The EV samples were washed using 300 kDa MWCO filter tubes to ensure all unincorporated nucleic acids are washed through. To quantify loading of doxorubicin, loading was performed as described above and the fluorescence intensity was measured after washing using excitation 470nm and emission 570nm.

miRNA (miR-93): Dharmacon; 5' -CAAAGUGCUGUUCGUGCAGGUAG

siRNA: Dharmacon; 5′-GGUGCCAGUUCUCCAAGAUUdTdT ssDNA: Integrated DNA Technologies (IDT); Skokie, Illinois; 5′-TGCTAGCTATCTAGTAGCCTAGTTA

5.2.6 Gel to evaluate RNA integrity

RNA (miR-93) was incubated for the indicated number of pH-loading cycles in 1XHBS or incubated with RNase I (Thermo Fisher Scientific EN0601) at 37°C for 45 min. RNA was subsequently incubated at 70°C for 10 min after 1:1 dilution in RNA loading buffer (1 mM EDTA, 96% formamide) before running on a polyacrylamide gel at 100 V for 10 min. After staining with SYBR™ Gold Nucleic Acid Gel Stain, gels were imaged using a FluorChem E System Gel Imaging System.

5.2.7 EV uptake and cytotoxicity

HUVECs were plated in black-walled 96-well plated coated with 0.1% gelatin at a seeding density of 6,000 cells/well the day before the experiment. 200 µg of EVs were labeled with BODIPY™ TR Ceramide (Thermo Fisher D7540) at a 10 µM concentration in a total volume of 100 µL. The solution was incubated at 37°C for 20 minutes, protected from light. Excess unincorporated dye was removed by washing in 300 kDa MWCO filter tubes. Fluorescence of the labeled EVs was measured at excitation 592 nm and emission 618 nm before treatment. HUVECs were then treated with 200 µg of labeled EVs and incubated at 37°C for 24 hours. Cells were washed and fluorescence of the cells was measured and normalized to the initial fluorescence intensity. Fold change of uptake is shown with respect to unmodified EVs. For cytotoxicity assessment, $3x10^5$ HEK293T cells were plated per well in a 6-well plate. At ~50% confluence, cells were treated with EVs (added in a range of doses from 10 µg/mL to 200 µg/mL) for 24 hours. After incubation, cells were trypsinized and counted to determine cell count. The cell count data for each treatment is represented as a percentage of the untreated control cell count.

5.2.8 In vivo cytotoxicity

The in vivo study was performed in 9 to 10-week-old male wild-type (C57BL/6J) mice (The Jackson Laboratories, Bar Harbor, ME). Mice were housed in an animal facility of University of Maryland School of Medicine (Baltimore, Maryland) for 1 week before the study under specific pathogen-free environment. They were fed with autoclaved bacteria-free diet, and the housing facilities were temperature-controlled and air-conditioned with 12-h/12-h light/dark cycles. All animal protocols were approved by the Institutional Animal Care and Use Committees of University of Maryland School of Medicine and the University of Maryland, College Park. For the in vivo experiments, mice were randomly assigned into three groups (5 mice/group) and intraperitoneally (i.p.) injected with either buffer (HBS), unmodified EV, or pH-EV (5.26×10^9 EV/mouse/day in 250 µl volume) for three days.

All animals were sacrificed on day 4. Peritoneal lavage was collected following anesthetizing by Ketamine (100 mg/kg) and Xylazine (4 mg/kg) subcutaneous injection and centrifuged to prepare cell-free peritoneal lavage supernatant and peritoneal cell pellets. Whole blood was collected by cardiac puncture using a 26G needle and transferred to an EDTA coated blood collection tube (Beckton Dickinson), and a 100 μl aliquot was used for complete blood count analysis (Beckman COULTER Ac-T diffTM Analyzer, Brea, CA). Plasma was harvested by centrifugation and stored at -80°C for cytokine analysis. Kidneys were collected, snap frozen in liquid nitrogen, and stored at -80°C for future analysis. Peritoneal and blood cells were further analyzed by flow cytometry as described below.

IL-6 in the plasma and peritoneal lavage supernatant was measured using commercially available DuoSet ELISA kits (R&D systems, Minneapolis, MN) following the manufacturer's instructions.

Total RNA was extracted from the kidney using Trizol (Sigma, St. Louis, MO). Reverse transcription was performed using the M-MLV reverse transcriptase (Promega, Madison, WI). qPCR was performed on a QuantStudio 3 real-time PCR system (Applied Biosystems, Foster City, CA) using the GoTaq qPCR master mix (Promega, Madison, WI). The transcripts of neutrophil gelatinase-associated lipocalin (NGAL), and kidney injury molecule-1 (KIM-1) were quantified with glyceraldehyde 3-phosphate dehydrogenase (GAPDH) as the internal control. The PCR primer sequences are listed below: GAPDH (Forward: 5′-AACTTT GGCATTGTGGAAGG-3′, Reverse: 5′-GGATGCAGGGATGATGTTCT-3′); NGAL (Forward: 5′-CTCAGAACTTGATCCCTGCC-3′, Reverse: 5′-TCCTTGAGGCCCAGAGACTT-3′); KIM-1 (Forward: 5′-CATTTAGGCCTCATACTGC-3′, Reverse: 5′-ACAAGCAGAAGATGGGCATT-3′). Transcript expression was calculated using the comparative Ct method normalized to GAPDH (2-ΔΔCt) and expressed as the fold changed in the EV injected group over the buffer (HBS) treated group.

Peritoneal cells were manually counted using a hemocytometer and a fraction of cells (1×10^6) were stained with the surface marker CD45-PE (BD Biosciences, San Jose, CA), F4/80-Alexa Fluro 647 (BD Biosciences, San Jose, CA) and Ly6G-BV421 (BD Biosciences, San Jose, CA). After red blood cell lysis, cells from 100 µL blood sample was stained with CD45-PE (BD Biosciences, San Jose, CA), Ly6C- BV510 (BioLegend, San Diego, CA), CD3-FITC (BioLegend, San Diego, CA) and CD19-PE-cy7 (BioLegend, San Diego, CA). Cells were incubated with antibodies in the dark at 4°C for 30 min and then washed once with 4 mL PBS. Cell pellets were resuspended in PBS containing 5% FBS and analyzed using a BD LSR II flow cytometer. Data analysis was performed with FlowJo software.

5.2.9 Functional evaluation of loaded RNA cargo

To assess function of loaded siRNA, pH-gradient or unmodified EVs were incubated at room temperature for one hour with GAPDH siRNA, washed and isolated as described above, and then added to HEK293T cells (plated the day before in a 6-well plate with 3×10^5 cells per well). 100 µg of each EV sample (unmodified EVs, pH-EVs, pH-EVs + scrambled siRNA, pH-EVs + GAPDH siRNA) were added to the cells dropwise. As a positive control, 20nM GAPDH siRNA was applied to cells with HiPerFect transfection reagent (Qiagen 301705; Germantown, MD) and a PBS only negative control. After 2 days of incubation, total RNA was isolated (Qiagen RNeasy

Kit 74104) from the cells. 1 μg of total RNA from each type of sample was converted into cDNA and mRNA level of GAPDH was confirmed by q-PCR. The change in mRNA level was normalized by using Ct value from B-actin mRNA[38].

GAPDH siRNA: Dharmacon ON-TARGETplus GAPDH Control siRNA D-001830-01-20;

Scrambled siRNA: Dharmacon; 5′-GGUGCCAGUUCUCCAAGAUUdTdT

To assess cytokine regulation by loaded miRNAs, BMDMs seeded in a 96-well plate ($2x10^5$ cells/well) were treated with single-stranded miR-146a-5p mimic loaded EVs (doses ranging from $1.5x10^8$ to $1.5x10^9$ EV/ml) overnight. Cells were incubated in serum-free culture medium containing 0.05% BSA for 1 hour before treatment with EVs. Medium was collected for detection of MIP-2 using ELISA kits (R&D Systems, Minneapolis, MN) according to the manufacturer's instructions. Final cytokine concentrations were calculated based on a standard curve.

ss-miR-146-5p: IDT; 5'-UGAGAACUGAAUUCCAUGGGUU

ss-miR146 (U→A) mutant: IDT; 5'-AGAGAACAGAAAACCAAGGGAA

Additionally, BMDMs seeded in a 12-well plate (4×10^6 cells/well) were treated double-stranded miR-146a-mimic-loaded EVs (100 μg/ml) for 2 days. Cell culture media were collected from cultures and stored at -80°C for ELISA analysis. Cells were lysed using NP-40 lysis buffer and protein concentration was determined using Bradford assay (Bio-Rad). 20 μg of protein from each sample was separated using 4–12% gradient gel, transferred to PVDF membrane and blotted with primary Abs (anti-IRAK1, anti-

GAPDH, 1:1000, Cell Signaling Technology) overnight at 4°C. After incubation with secondary Abs, protein bands were visualized using Luminata Forte Western HRP substrate (Millipore) and imaged in a ChemiDoc system (Bio-Rad Laboratories, Hercules, CA). The band intensity was quantified using Image J. IL-6 levels in the media were measured via ELISA (R&D Systems) according the manufacturer's instructions.

ds-miR-146a-5p mimic: Qiagen Syn-mmu-miR-146a-5p miScript miRNA Mimic 219600; 5'-UGAGAACUGAAUUCCAUGGGUU

ds-miR-146a scramble: IDT; 5' – ACGAGUUACGUGGUACGUUAAU

5.2.10 Statistical analysis

Data were analyzed using GraphPad Prism software version 7.04. Analysis of variance (one or two-way as appropriate) was used with Tukey's post hoc test unless otherwise stated. Statistical significance was shown with the following notation: ns (not significant), $p > 0.05$, * or # $p \leq 0.05$, ** or ## $p \leq 0.01$, *** or ### $p \leq 0.001$, **** or #### $p \leq 0.0001$. Data are plotted as mean ± standard error.

5.3 Results

5.3.1 Preparation and characterization of EVs

To promote the loading of negatively-charged cargo, a pH-gradient was utilized to render the interior of HEK293T-derived EVs acidic. This was accomplished by first dehydrating the EVs in 70% ethanol and then rehydrating them in an acidic citrate buffer (pH 2.5). To replace the surrounding acidic buffer with a more neutral buffer, EVs were dialyzed in HBS (pH 7), resulting in a pH-gradient between the intravesicular and extravesicular environments (**Figure 5.1A**). The effects of this process on EV yield and integrity were assessed by nanoparticle tracking analysis (NTA), bicinchoninic acid (BCA) assay and immunoblotting. The results showed that both unmodified and pH-gradient-modified EVs (pH-EVs) fall within a similar size range (**Figure 5.1B**). Additionally, the total protein content associated with pH-EVs decreased in comparison to unmodified EVs, and thus the amount of EVs per µg of protein increased (**Figure 5.1C**). Dialysis of EV samples that were not pH-gradient-modified led to similar effects, suggesting that dialysis of the samples is leading to this decrease in protein content (**Figure 5.2**). Alternatively, some EV-associated proteins may be degraded during the procedure. Supporting this latter possibility, a total protein gel showed some bands with decreased intensity (**Figure 5.1D**) and levels of EV-associated proteins Alix and TSG101 decreased after pH-gradient modification (**Figure 5.1E,F**). However, the expression of EV-associated marker CD9 was enriched in the pH-EV sample (**Figure 5.1E,F**). Thus, there may be a combination of increased sample purity with some EV protein degradation during the pH-gradient process. The absence of expression of the endoplasmic reticulum-associated protein calnexin further verified the absence of intracellular contaminants within the EV samples [171] (**Figure 5.1E,F**).

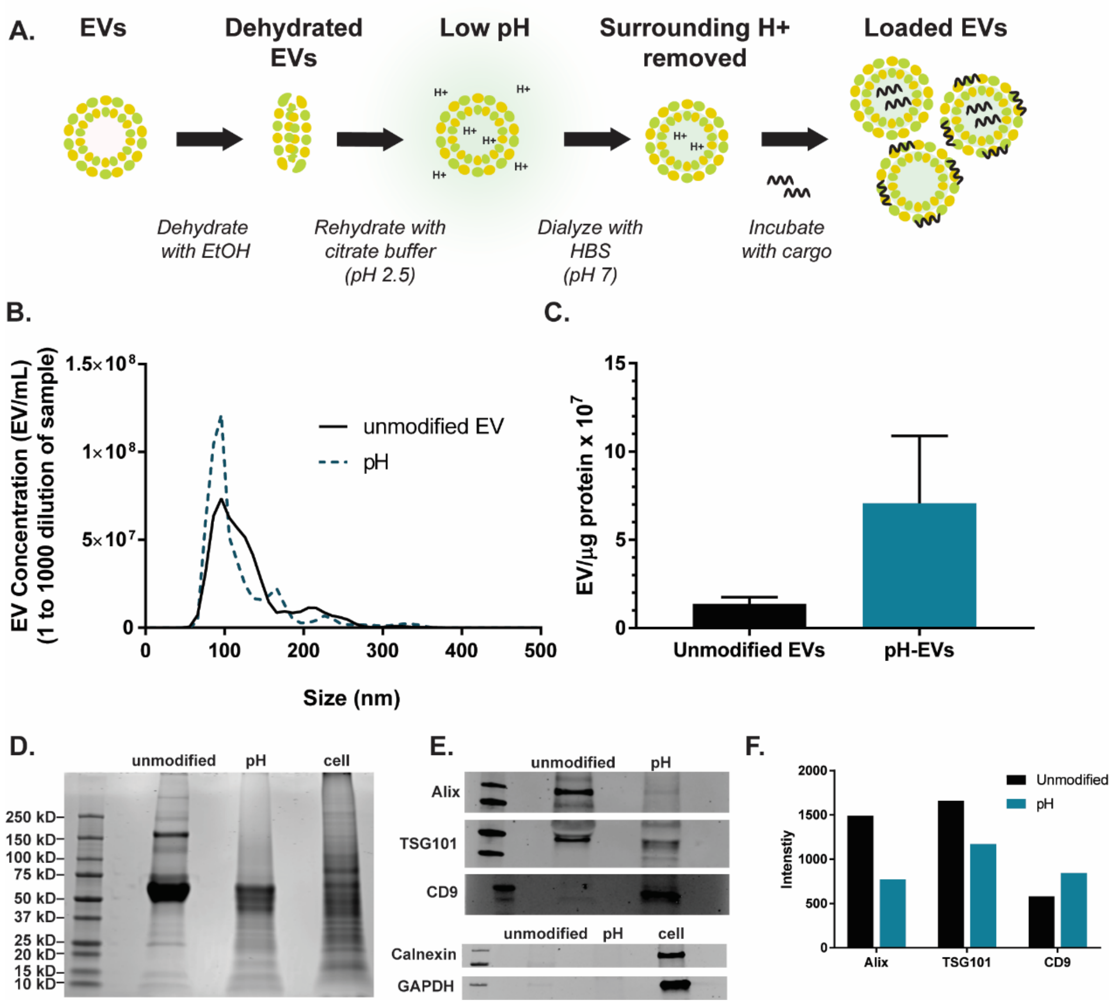

Figure 5.1. Preparation and characterization of pH-EVs. (A) Schematic describing the steps to prepare and load pH-EVs. (B) The concentration of HEK293T EVs vs. size was determined by nanoparticle tracking analysis via Nanosight. Samples were diluted 1000-fold before analysis. (C) The amount of HEK293T EVs associated per µg of protein with or without pH-gradient modification was determined by the ratio of NTA and BCA results. (D) Total protein and (E) immunoblotting of unmodified and pH-gradient modified HEK293T EVs. (F) Densitometry of the immunoblot of EV-associated markers.

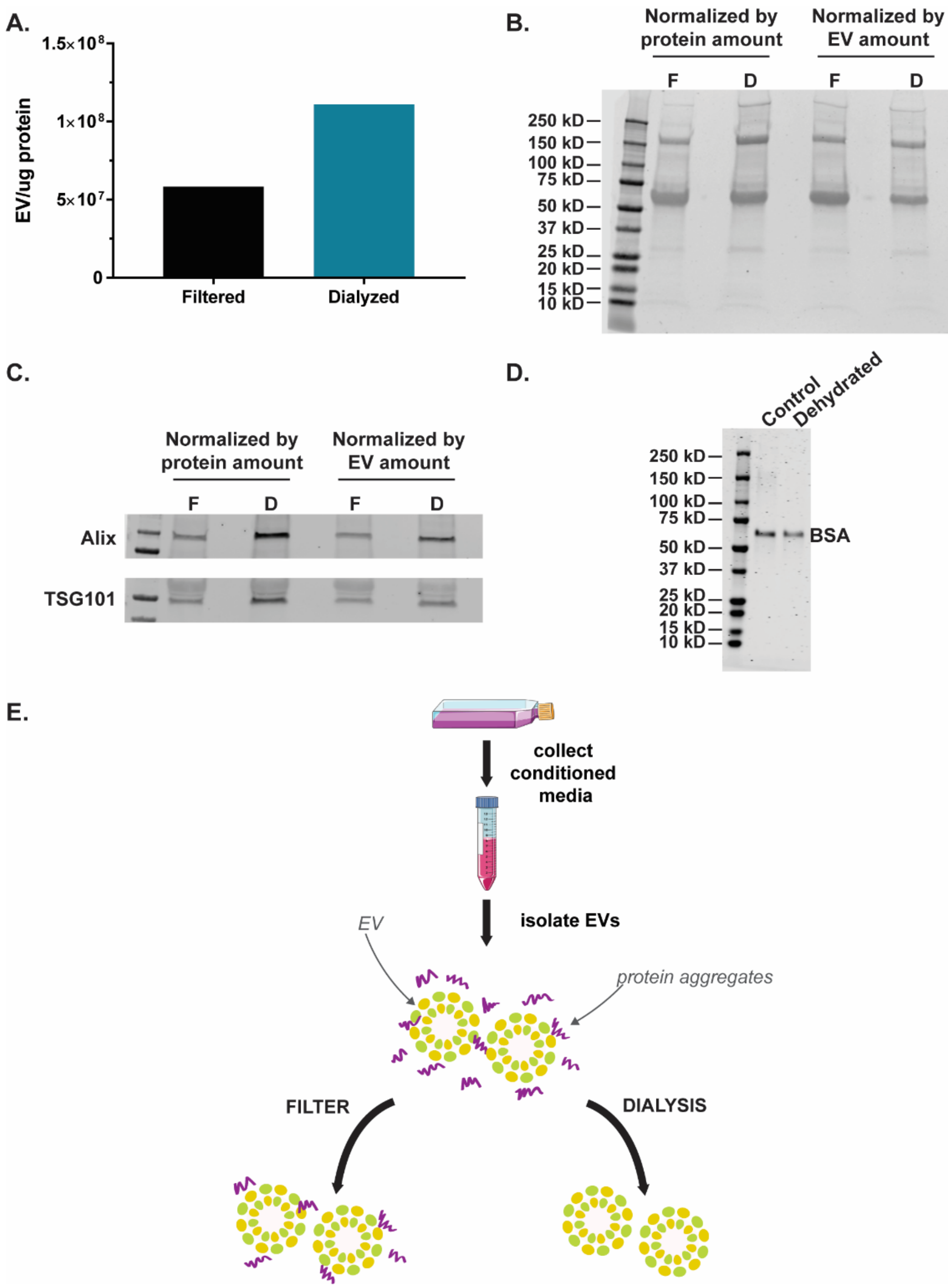

Figure 5.2. Investigating the source of protein loss in pH-EVs. (A) The amount of EVs associated per ug of protein in EVs that are washed by dialysis in comparison to EVs washed by filtering. (B) Total protein and (C) immunoblotting show that when samples are normalized by total protein amount, EV associated protein intensities appear higher in dialyzed samples. The intensities are more similar when normalized by EV amount, as determined by NTA. (D) A potential explanation for some loss of protein is that external proteins are not completely washed away and loosely associated with EVs after isolation. These proteins are likely better removed with dialysis. (E) Dehydration of bovine serum albumin (BSA, Sigma Aldrich 5000206, Darmstadt, Germany) in ethanol overnight did not result in degradation of the protein as shown by total protein.

5.3.2 Parameter optimization to enhance cargo incorporation

The process variables of incubation temperature, time, and pH were all investigated to promote the optimal loading of nucleic acid cargo. Comparing a range of temperatures from 4°C to 60°C, incubation at room temperature (22°C) was optimal for maximum observed incorporation of miRNA (**Figure 5.3A**). Cargo incorporation was found to be the lowest at 4°C or 60°C incubation. Varying the duration of EV incubation with cargo revealed that maximum observed incorporation was achieved after 2 hours (**Figure 5.3B**). With longer incubation times, a decrease in cargo incorporation was observed, with a 57% decrease in total miRNA loaded between 2 and 6 hours of incubation. This could be potentially due to the degradation of miRNA in the buffer over time or to a loss of the pH-gradient over time as negative cargo is entering the vesicles. Based on liposomal studies [167], the degree of acidity of the intravesicular compartment was expected to significantly impact loading efficiency. Using citrate buffers of varying acidic strengths, we observed that miRNA association with EVs increased with an increase in acidity of the internal pH, with the highest cargo loading achieved at pH 2.5, an ~6-fold increase compared to loading without a pH-gradient (**Figure 5.3C**). The optimal observed combination of loading parameters was thus a 2-hour incubation time at room temperature with EVs that had an internal pH of 2.5. Using the optimized protocol for pH-EV loading, loading via this technique was compared to sonication loading. Since, we observed a change in protein content between unmodified and pH-EV populations, loading was done based on EV number. Loading via pH-gradient leads to a higher encapsulation of miRNA than sonication (**Figure 5.3D**).

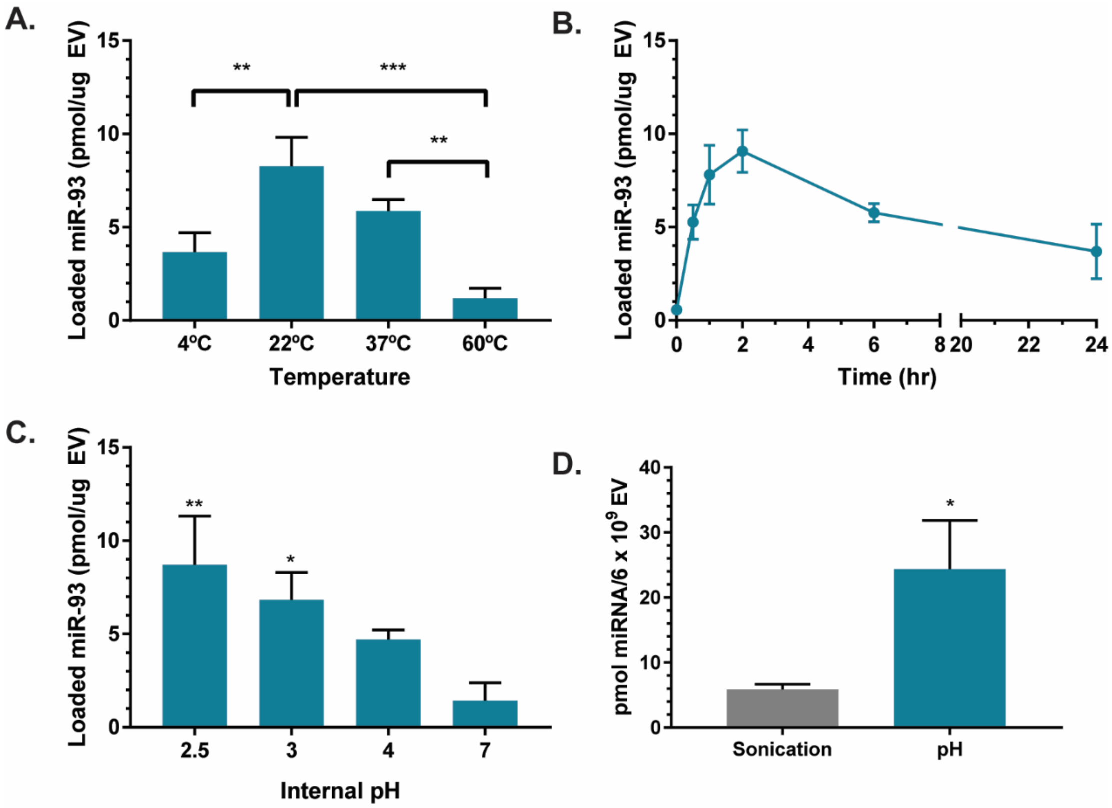

Figure 5.3. Parameter optimization and miRNA loading into pH-EVs. Loading of unmodified and pH-gradient-modified HEK293T EVs with miR-93 was assessed by fluorescence quantification after (A) 1 hour incubation at the indicated temperatures; (B) incubation at 22°C for the indicated times; and (C) 2 hour incubation at 22°C with the indicated internal pH values. (D) Loading EVs via sonication vs pH-gradient. Panel D statistics determined via two-tailed t-test, ANOVA for other panels.

5.3.3 Reusability of excess nucleic acid cargo

EV loading methods such as electroporation, sonication, and heat shock that ultimately rely on cargo diffusion are inherently limited in terms of efficiency. In these cases, the maximum possible loading efficiency is dictated by the volumetric ratio between the cargo-containing solution and the total intravesicular volume of EVs in suspension. Solubility considerations and practical working volume limitations often lead to this ratio being 20:1 or greater in favor of the cargo solution volume, meaning that a maximum of 5% or less of the total cargo in solution would be expected to associate with or be encapsulated by EVs, even assuming perfect conditions for diffusion.

Previous studies have shown that loading by electroporation or sonication can damage nucleic acid cargo through aggregation and/or degradation[79,104,115], rendering any non EV-associated cargo useless. In contrast, we hypothesized that the pH-gradient method may allow for non EV-associated cargo to be reused in additional loading processes, thus increasing overall cargo utilization efficiency. Testing this hypothesis with siRNA, non EV-associated cargo was isolated by filtration with 300 kDa MWCO filters after 2-hour incubation with pH-EVs. The recovered siRNA was then added to fresh pH-EVs and successful loading was confirmed by fluorescence measurements of labeled siRNA (**Table 5.1**). Iterations of this process were continued until we could no longer detect RNA after washing steps, showing that we could re-use the same RNA to load four additional sets of EVs. Cargo miRNA integrity was evaluated after 2 cycles of loading in pH-buffer (**Figure 5.4A**) by visualization after gel electrophoresis.

Table 5.1. Reusability of nucleic acids after cargo loading with pH-EVs. After incubation with pH-EVs, the amount of siRNA was calculated via fluorescence measurements. The remaining loading buffer (filtrate after washing loaded EVs) was then used to load a fresh set of EVs and the measurements were repeated until RNA could no longer be loaded.

Amount of siRNA in loading buffer	Amount of pH-EVs used	Amount of siRNA loaded in EVs	% of siRNA loaded	Theoretical unused siRNA	siRNA recovered after washing
1000 pmole	10 µg	65 pmole	6.5%	935 pmole	720 pmole (Filtrate 1)
720 pmole (Filtrate 1)	10 µg	41 pmole	5.6 %	679 pmole	543 pmole (Filtrate 2)
543 pmole (Filtrate 2)	10 µg	32 pmole	5.8%	511 pmole	420 pmole (Filtrate 3)
420 pmole (Filtrate 3)	10 µg	23 pmole	5.4%	397 pmole	280 pmole (Filtrate 4)
280 pmole (Filtrate 4)	10 µg	7 pmole	3.2%	273 pmole	198 pmole (Filtrate 5)
198 pmole (Filtrate 5)	10 µg	~0 pmole	~0%	~198 pmole	125 pmole (Filtrate 6)

5.3.4 pH-EVs are effectively taken up an exhibit no significant toxicity

One potential pitfall of the pH-gradient method was the possibility of inhibited EV uptake via damage to surface proteins or lipids during the dehydration/rehydration process. However, there was no significant difference in uptake between pH-gradient-modified and unmodified HEK293T EVs by HUVECs in culture was observed (**Figure 5.4B**) as evaluated by measuring the amount of florescence signal present in the cells after treating with fluorescently labeled EVs. Further, doses up to 200µg/mL of pH-EVs showed no significant toxicity HEK293T cells (**Figure 5.4C**).

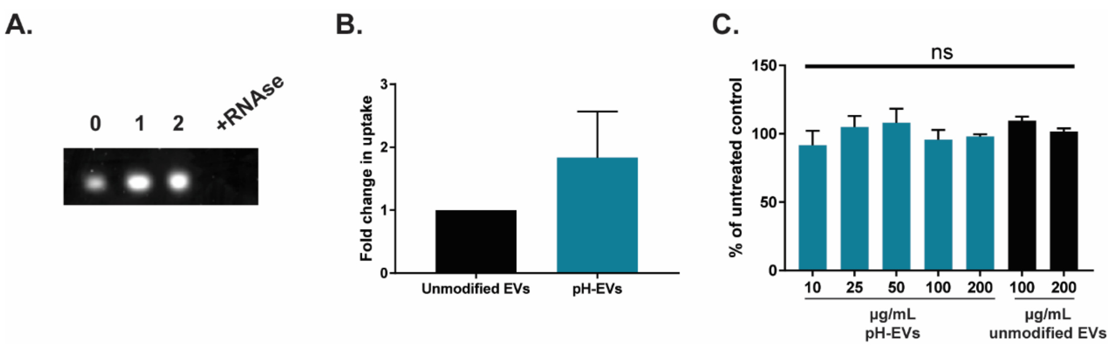

Figure 5.4. pH-EV uptake and cytotoxicity. (A) RNA integrity was evaluated by subjecting RNA to 0, 1, or 2 cycles of loading by pH-gradient process; RNase I treatment was used as a control. (B) Uptake of BODIPY™ TR Ceramide-labelled unmodified and pH-gradient-modified HEK293T EVs by HUVECs was assessed by fluorescence quantification. Uptake is shown as fold change in comparison to unmodified EVs. (C) Cytotoxicity of pH-gradient-modified HEK293T EVs on HEK293T cells was assessed by cell counting and compared to untreated cells. There was no statistical significance between any samples (t-test for B; one-way ANOVA for C).

Toxicity was also evaluated *in vivo* by assessing lavage fluid in the peritoneal cavity and plasma after multiple EV injections into C57BL/6J mice. $4.5x10^9$ of either unmodified or pH-modified HEK293T-derived EVs were injected i.p. daily for 3 days, and kidney injury, inflammation and peritoneal/blood cell population were carefully examined. qPCR results indicated no effect of the pH-gradient process on EV-induced expression of acute kidney injury markers KIM-1 and NGAL (**Figure 5.5A**), while levels of pro-inflammatory cytokine IL-6 in plasma and peritoneal lavage supernatant were also unaffected (**Figure 5.5B**).

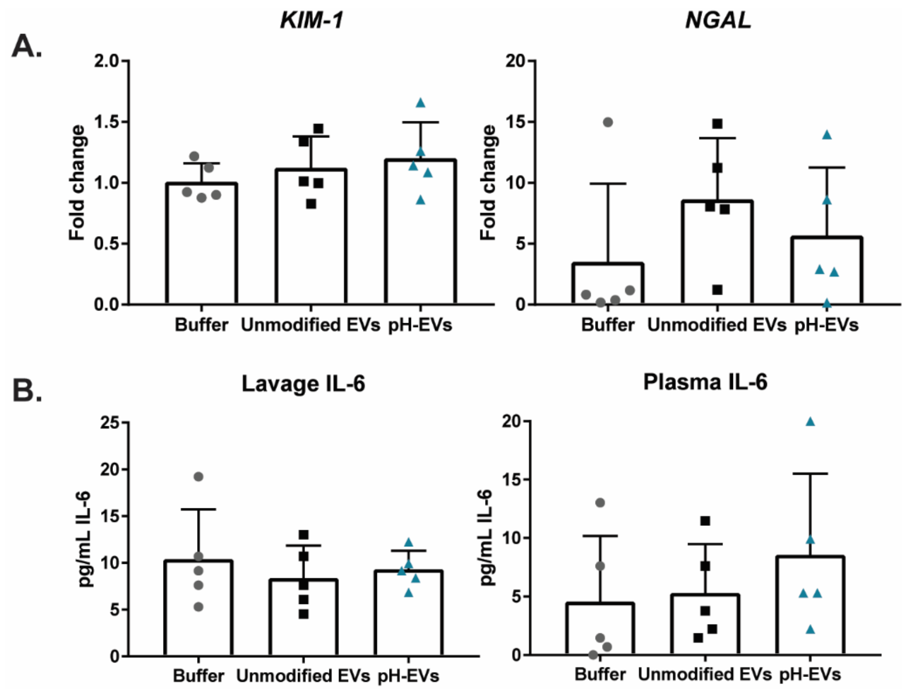

Figure 5.5. Markers of inflammation and cytotoxicity in the peritoneal lavage and plasma. (A) Acute kidney injury marker KIM-1 and NGAL were measured in the kidney using qRT-PCR. n=5/group. (B) Plasma and peritoneal lavage IL-6. n=5/group.

To investigate whether pH-EV injection would impact host immune cell composition, we performed immunophenotyping experiments both locally in the peritoneal cavity where the EVs were delivered and systemically in the blood circulation. No significant differences between EV treatments were observed in total cell numbers, resident macrophages (F4/80^{high}/ Ly6G^{-}) or monocytes (F4/80^{middle}/ Ly6G^{-}), while a slight increase of neutrophil population ($F4/80^-/Ly6G^+$) in the peritoneal cavity was seen following administration of unmodified EVs compared to control (**Figure 5.6A**). These data suggest that pH-EVs did not significantly affect immune cell composition in the peritoneal cavity. Further, the percentages of monocytes ($Ly6C^+/Ly6G^-$), neutrophils ($Ly6C^+/Ly6G^+$), T cells ($CD3^+/CD19^-$) and B cells ($CD3^-/CD19^+$) in the blood as measured by flow cytometry analysis suggested no significant systemic immunogenicity following repeated administration of unmodified or pH-EVs (**Figure 5.6B**). EV treatment also had little effect on hemoglobin levels as well as leukocyte and platelet counts (**Table 5.2**).

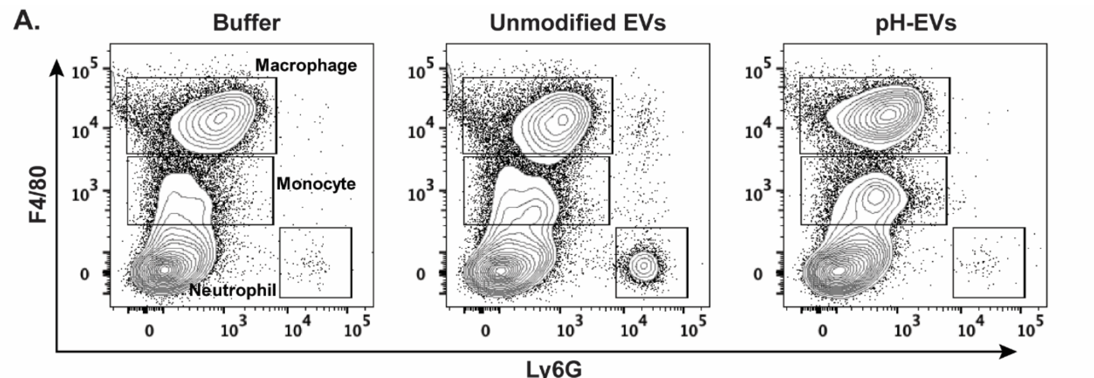

	Total cell number (x 10^6)	% leukocyte	% macrophage	% monocyte	% neutrophil
Buffer	2.83 ± 1.45	94.78 ± 2.44	20.04 ± 5.26	8.67 ± 0.88	0.39 ± .35
Unmodified	3.42 ± 0.67	98.98 ± 1.12	14.76 ± 2.23	11.86 ± 2.37	4.23 ± 1.69***
pH	2.13 ± 0.39	96.24 ± 2.74	17.80 ± 4.58	11.94 ± 3.45	0.49 ± 0.69

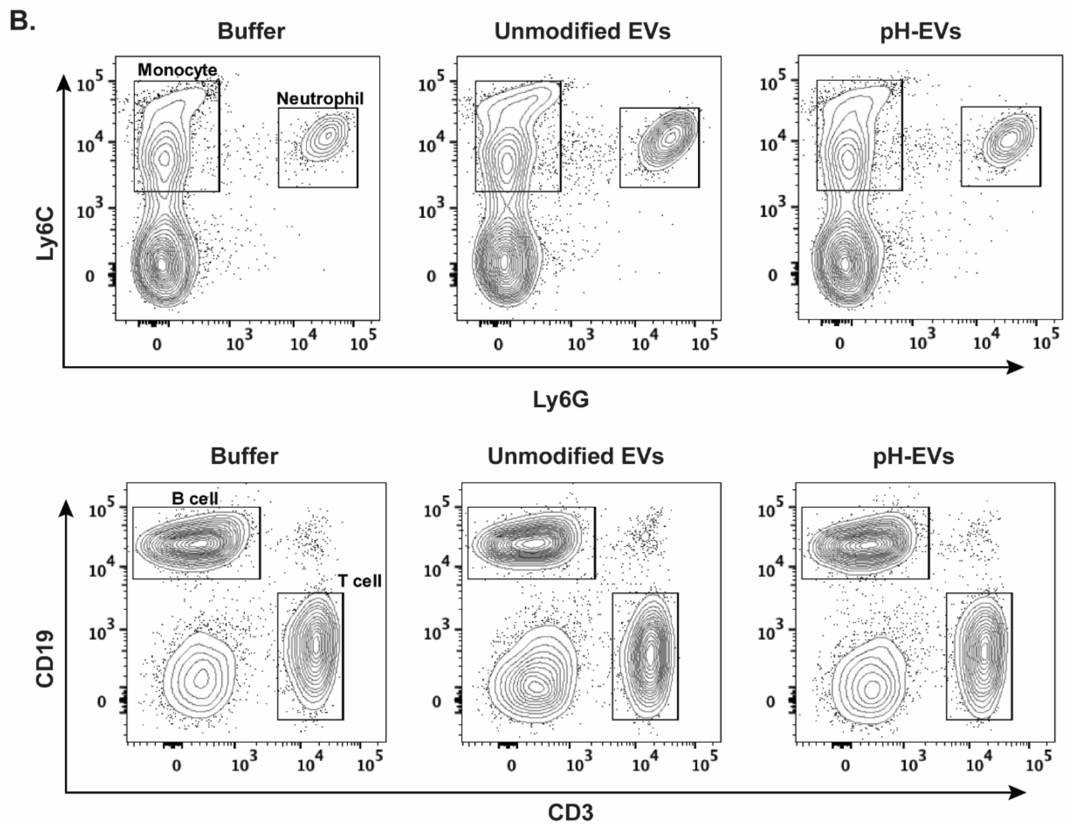

	% B cell	% T cell	% monocyte	% neutrophil
Buffer	54.96 ± 6.24	27.22 ± 4.89	16.36 ± 1.76	10.20 ± 4.77
Unmodified	51.02 ± 8.36	29.56 ± 4.64	16.92 ± 3.49	10.66 ± 3.04
pH	52.06 ± 4.27	29.86 ± 2.72	17.16 ± 1.86	9.34 ± 2.80

Figure 5.6. Host immune cell composition. (A) Representative flow cytometry of gated macrophage (F4/80high/Ly6G-), monocyte (F4/80middle/Ly6G-) and neutrophil (F4/80-/Ly6G+) in the peritoneal cavity. The percentage of each cell population over leukocyte (CD45+) was listed in the table. n=5/group. (B) Representative flow cytometry of gated monocyte (Ly6C+/Ly6G-), neutrophil (Ly6C+/Ly6G+), B cell (CD19+/CD3-) and T cell (CD19-/CD3+) in the blood. Percentage to total leukocyte (CD45+) was calculated. n=5/group.

Table 5.2. Blood cell count. Whole blood was collected following 3 days of EV administration and transferred to EDTA-coated blood collection tube. Leukocyte, platelet, and hemoglobin levels were analyzed using an automated cell counter.

	White blood cell (x 103/µL)	Hemoglobin (g/dL)	Platelet (x 103/ µL)
Buffer	3.76 ± 1.14	12.78 ± 0.31	1111 ± 49.87
Unmodified EVs	3.18 ± 0.36	13.04 ± 0.50	1121 ± 47.64
pH-EVs	3.90 ± 1.15	12.94 ± 0.46	1096 ± 58.41

5.4.4 pH-EVs deliver functionally active RNA cargo

After evaluating that the pH-gradient process did not induce significant effects counter to productive therapeutic cargo delivery, we next assessed the ability of pH-EVs to deliver functionally active RNA to cells. Delivery by pH-EVs of siRNA targeted to the protein GAPDH in HEK293T cells resulted in 54% knockdown compared to scrambled RNA or PBS controls (**Figure 5.7A**), while unmodified EVs did not induce significant knockdown.

We next examined the potential of pH-EVs to modulate the production of inflammatory cytokines known to be important in sepsis, a condition for which EVs have been both proposed as a treatment [156,172–174] and implicated as a contributing factor [175,176]. In one experiment, pH-EVs were loaded with the pro-inflammatory ss-miR-146 [175] and exposed to bone marrow-derived macrophage cells. In this case, loaded pH-EVs induced dose-dependent cellular production of MIP-2 (macrophage inflammatory protein 2; CXCL2), a classical inflammatory cytokine, compared to a minimal response from pH-EVs alone or pH-EVs with a mutant sequence (**Figure**

5.7B). In another experiment, pH-EVs were loaded with anti-inflammatory ds-miR-146 [172,177]. Here, loaded pH-EVs induced a decrease in inflammatory protein expression, as evidenced by immunoblotting for IRAK1 (**Figure 5.7C**), a proinflammatory enzyme. ELISA-based detection also revealed loaded pH-EV-induced decrease in levels of IL-6 (**Figure 5.7D**), a pro-inflammatory cytokine whose inhibition has previously been shown to improve survival in sepsis models [178–180]. Thus, these results suggest therapeutic potential for utilizing pH-EVs in sepsis treatment.

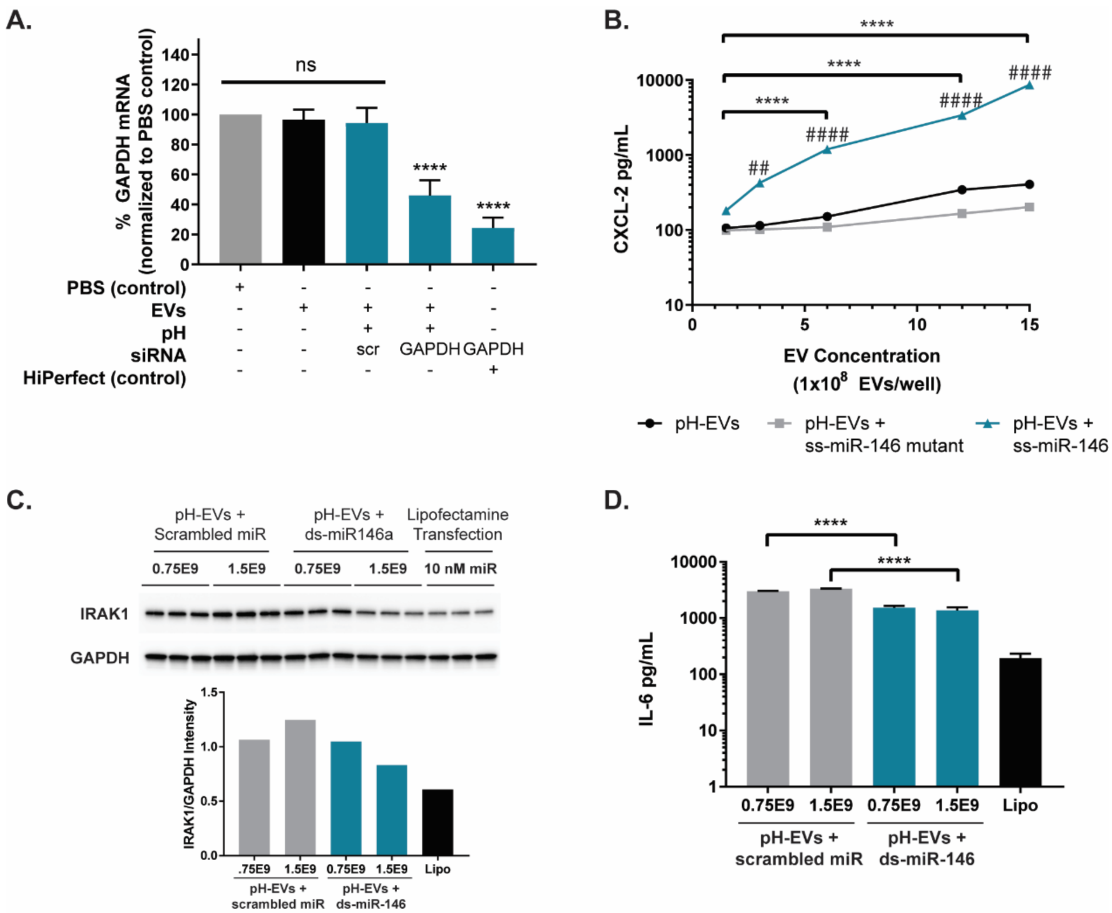

Figure 5.7. Delivery of functionally active cargo. (A) GAPDH mRNA in cells after 48 hour incubation with pH-gradient-modified HEK293T EVs or controls as indicated was evaluated by qPCR; statistical significance is shown with respect to the PBS control. (B) MIP-2 release by BMDMs after 16 hour incubation with the indicated EV groups was determined by ELISA; * indicates statistical significance as shown by the bars, # indicates statistical significance with respect to the corresponding EV only sample for each corresponding time point. Effects of scramble control of ds-miR-146a delivery by pH-gradient-modified HEK293T EVs at the indicated doses on (C) IRAK1 (by immunoblot and densitometry quantification) and (D) IL-6 (by ELISA) production by BMDMs were assessed; * indicates significance with respect to 0.75E9 EVs + scramble, # indicates significance with respect to Lipofectamine treatment.

5.4 Discussion

In this study, we demonstrated versatile loading potential and functional delivery of miRNA cargo using a pH-gradient-based method. Using this approach, we were able to load an estimated ~4000-5000 copies of miRNA per EV, comparable to what has been reported for other EV loading methods such as sonication [104], electroporation [76], chemical modification of cargo [71,134], and others [78,129]. Additionally, this strategy enabled preservation of unloaded nucleic acid cargo such that it could be reused in subsequent loading operations, resulting in more efficient use of valuable biological therapeutic molecules (**Table 5.1**).

Despite exposing EVs to dehydration by ethanol during the loading process, cell uptake and functional cargo delivery were still achieved (**Figure 5.4**, **Figure 5.7**). This suggests that any proteins and lipids critical to cell uptake of EVs were not critically negatively impacted by the pH-gradient process. This finding echoes prior work that showed that exposure of EVs to proteinase K, which would be expected to degrade surface proteins, has little effect on EV physicochemical properties [181]. This same study found that after injection in mice, the half-life and mean residence time of EVs did not change based on proteinase K exposure. However, the area under the curve increased significantly for proteinase K-treated EVs, indicating an increased percent of EV dose in the blood and decreased clearance. In our study, levels of Alix and TSG101 decreased after pH-modification, while CD9 was increased (**Figure 5.1**). It is possible that the pH-gradient process results in rearrangement and differential exposure of surface proteins and lipids on EVs, which could impact uptake in unpredictable ways. Overall, further dedicated study of EV uptake mechanisms would shed light on how this and other methods might be optimized to reduce any detrimental effects on EV cargo delivery.

The possibility of different loading levels in different EV subsets should also be considered. Studies have shown that the composition and function of small and large EVs can differ in morphology as well as protein and lipid content [182,183]; these differences in the surface composition of EV subtypes may make them more or less conducive to loading via the pH method. Further, the roles of EV-associated proteins differ depending on the parent cell type, and thus the method described here may not be universally appropriate for EV loading.

The results of this study also have implications for the field with regard to normalization of EV amount for functional studies, a subject on which there is not yet a consensus best practice [171]. Many studies determine EV dose based on total protein content of EVs; however, as shown here, processing can dramatically impact the relationship between EVs and their associated proteins. Thus, in cases where EVs undergo downstream modification, dosage on the basis of number of EVs may be more accurate. Of course, since proteins could be the active cargo of interest, dosing by protein amount may be more relevant for some studies.

Ultimately, the utility of the method described here was shown by functional delivery of both siRNA and miRNA cargoes. Treating bone marrow-derived macrophage cells with pro- or anti-inflammatory miRNA led to regulation of corresponding cytokine levels. Specifically, we observed that delivery of pro-inflammatory ss-miR-146a resulted in increased MIP-2 secretion by bone marrow derived macrophage cells. This suggests that pH-EVs can be employed in further studies exploring the roles of miRNAs in inflammatory diseases, such as sepsis. Further, we showed that delivery of ds-miR-146a reduced IL-6 production by the same cells, a potentially anti-inflammatory outcome, as endogenous EV-associated miR-146 has been shown to reduce inflammatory gene expression and inhibit endotoxin-induced inflammation in mice [172]. This same study showed that there was approximately one copy of miR-146 per EV and an average 370 copies per cell after treatment. It has been reported that at least 100 copies of miRNA per cell is necessary for regulatory capacity [184]. These results suggest that pH-gradient-based loading of EVs may be a promising approach to achieve functional therapeutic effects of miRNA delivery.

5.5 Conclusion

Here, we have established a novel method for cargo loading by modifying the internal pH, and thus the charge, of EVs. Any modifications induced by this method do not result in *in vitro* or *in vivo* cytotoxicity. miRNA delivery via loaded pH-EVs was successfully used to modulate inflammatory cytokines. The simplicity of this method as well as the ability to reuse unincorporated cargo makes this an attractive technique for eventual scalability and manufacturing.

Chapter 6: Conclusions and outlook

6.1 Conclusions and summary of work

EVs are an exciting new platform for therapeutic gene and drug delivery that has gained momentum after the discovery that they can induce a function by transporting RNA [41]. A number of promising studies have demonstrated the potential of EVs to shift the paradigm of disease treatment. However, studies focusing on the fundamental questions of how to load cargo and preserve EV function are limited, with no consensus on best practices. Without proper understanding and development of EV cargo manipulation and stability, they will face obstacles in manufacturing and translation. Studies focusing on understanding basic principles such as these will also contribute to better understanding of how to treat this modality when considering FDA approval pathways.

Thus, the research described in this dissertation has focused on methods to either enhance or preserve the potency of EV therapeutics. This goal is achieved by developing novel loading techniques and better understanding the stability of EVs after storage (**Figure 6.1**). These methods are intended to create a platform that can be used in developing EV therapeutics for any application and help propel the field forward toward clinical use.

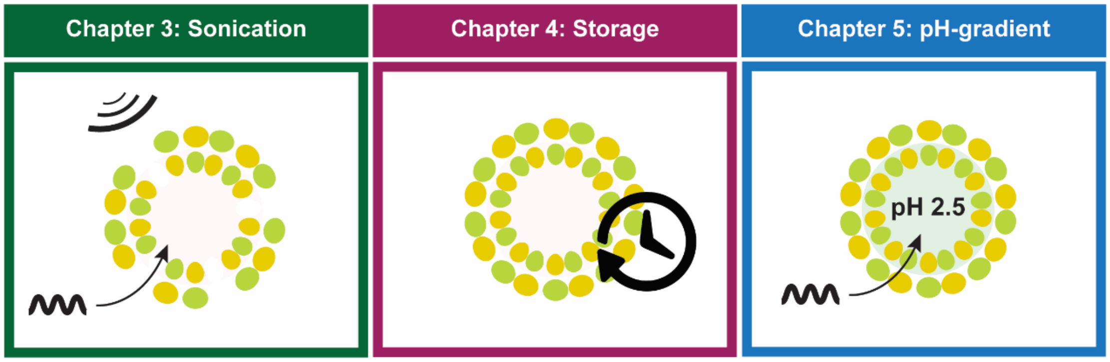

Figure 6.1. Summary of work. Chapter 3 focuses on loading cargo after using sonication to disrupt the membrane. Chapter 4 investigates the impact of storage duration and type on EV stability. Chapter 5 presents a loading method based on creating a pH-gradient between EVs and the surrounding buffer.

Chapter 3, introduces sonication as potential method for cargo loading into EVs. Prior to this work, there were limited studies showing the utility of sonication for loading small molecule drugs [136] or protein cargo [82], but none evaluating its potential for nucleic acid loading. This work successfully demonstrated that sonication can be used to load various nucleic acid cargos without any observed negative effect on the EVs or cargo aggregation. However, increased exposure was shown to degrade nucleic acids. This poses a problem for practical scalability of the method. In **Chapter 4**, the impact of storage on MSC EVs as well as cargo sonicated into EVs is explored. At the time of this work, there was limited precedence on proper EV storage. The International Society of Extracellular Vesicles (ISEV) recommends storage at -80°C, but cost and access would then restrict the usage of EV-based therapeutics. We have shown that function can still be effectively preserved at -20°C or at room temperature after lyophilization indicating that -80°C can be avoided. However, when looking at certain analysis techniques, such as nanoparticle tracking analysis, storage methods that can best preserve function resulted in inaccurate concentration measurements. This indicates that the application is an important consideration when determining storage method and that there is a need to use multiple modes of characterization. This is also the first study to assess the storage of EVs after exogenously loading with cargo. The work we have presented here suggests that with current storage techniques, EVs loaded via sonication stored at any condition will start to lose some of their cargo within 7 days. **Chapter 5**, presents a novel loading technique based on creating a pH-gradient. Unlike sonication, this technique did not result in degradation of cargo and also resulted in increased cargo loading. However, the protein profile of samples after undergoing pH treatment did differ. This did not result in any adverse effects in *in vitro* uptake or cytotoxicity studies or in *in vivo* cytotoxicity studies. We were able to successfully use this technique to deliver miRNAs to modulate inflammatory cytokines *in vitro*. This work also provided knowledge about the nature of EVs, emphasizing the robustness of these carriers.

In developing the two loading techniques described, I have established platforms that can be used toward any application. Based on the data presented here, the technique for loading can be determined based on the cargo used (sonication for non-nucleic acid cargo or pH-gradient for negatively charged cargo including nucleic acids).

6.2 Future research directions

6.2.1 Sonication loading

While the research encompassed in this dissertation provides fundamental information for EV loading and storage, further work is required before they can make clinical impact. Based on the results shown here, sonication is most practical for loading small molecule and protein drugs. Currently, our loading technique uses nucleic acid cargo in excess. Although cargo remains intact during this loading process, additional exposure to sonication can degrade the cargo. Thus, all the excess unloaded cargo cannot be used. This poses a problem for cost-effective scalability. Thus, there are two main avenues that future research in this area can continue. One direction to explore is further method optimization to minimize damage to nucleic acid cargo. Future studies to reduce wasted excess cargo will make sonication more practical for gene delivery. The sonicator used in the data shown here has a fixed frequency at 35 kHz. Studies evaluating loading efficiencies with different frequencies may limit damage.

Another direction for future studies is to focus on using EVs for protein and small molecule delivery. Although I have shown that sonication induces no loss of intrinsic EV function (**Figure 3.6**, **Figure 3.7**), this may change when loading large cargo. It is possible that with the introduction of such cargo, that certain endogenous cargos are expelled from the vesicle. Thus, these studies will need to be repeated under these conditions. Additionally, future studies will need to develop an understanding of size restrains for loading cargo. In the case of electroporation, exogenous DNA loading was shown to be size dependent [76], potentially due to the size of pore formation. Thus, we have reason to expect that there will be a size limitation for effective small molecule or protein loading.

6.2.2 Storage

The stability studies conducted here provided useful information for the field. Further studies can further elucidate the mechanism of loss of activity and provide an optimal storage protocol for loaded EVs.

We have shown that after 7 days of storing sonication loaded EVs, there is a decrease in retained cargo regardless of storage temperature. This suggests the need to explore lyophilization as well as buffer choice for the storage of exogenously loaded EVs. Preliminary data pertaining to lyophilization of sonicated EV (**Figure 6.2**) shows that after sonication we are able to retain 74% of the initially loaded cargo. This initial result is a promising alternative to the existing methods shown in **Figure 4.10**. Future work developing the lyophilization of loaded EVs will be useful in broad usage of EV therapeutics.

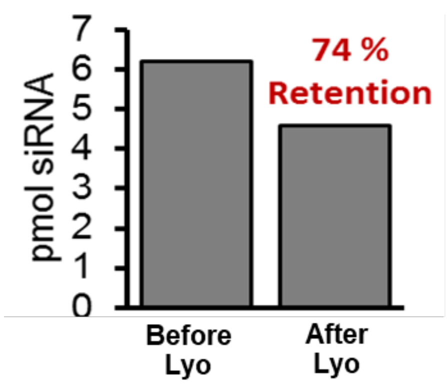

Figure 6.2. Cargo retention in sonicated EVs after lyophilization. Fluorescently labeled siRNA loaded into EVs via sonication were quantified before and after lyophilization.

Another avenue to explore for preservation of EV bioactivity is excipient and buffer choice. Trehalose was explored as an alternative to PBS in **Chapter 4**, but like PBS, it showed an increasing EV concentration via NTA. Studies have suggested that using trehalose instead of PBS may better preserve biologic function after freezing or lyophlization. In our studies, lyophilization with PBS did not result in any degrading effects in lyophilization of MSC EVs *in vitro* (**Figure 4.8**), but it is possible that aggregation effects may be higher when lyophilizing in PBS [119,145]. Differences in aggregation may in turn impact *in vivo* bioactivity of EV treatments. Thus, a combination of *in vivo* studies and experiments evaluating buffer choice will be essential.

Ongoing work is also investigating the impact of storage on EVs loaded by a pH-gradient. Since the pH-gradient loading method does not involve perturbing the membrane in the same way as sonication, this may change how well the EVs are able to retain cargo. Studies have shown that sonication decreases the microviscosity of exosomal membranes [136]. This change in membrane fluidity may be the mechanism for cargo loss.

<u>6.3.3 pH-gradient loading</u>

This section of work has specifically provided preliminary work for developing EV therapies towards treating sepsis. Current research involving EVs and sepsis is focused on the impact of the pathological state on EVs in the body. As mentioned in **Chapter 5**, endogenously anti-inflammatory EVs required only one copy of miR-146 per EV to have a functional effect. Thus, our technique may be a promising method to treat sepsis with low EV dosage. However, to further this as a therapy with sepsis, *in vivo* delivery of cargo via pH-EV must be explored. Along with this, we must evaluate is the scalability of this technique.

6.3 Contributions

I have contributed to the field two techniques to load cargo into EVs and knowledge of how storage can impair potency. Sonication is a rapid method for loading, while the pH-gradient based loading technique in particular can be used by any group, without the need for any specialized equipment. In understanding the impact of storage, I have provided guidelines for storage that can be tailored toward the type of analysis that will be performed. Ultimately these accomplishments contribute to platform technologies that can be used in any therapeutic application. Information on storage may also prove to be essential in the diagnostics field.

My work has led to a number of publications, conference proceedings, and awards. I am a co-author on a portion of the work in **Chapter 3**, published in Cellular and Molecular Bioengineering (CMBE). I also published the first review article discussing the preservation and stability of EVs for therapeutic applications (**Chapter 2.4**), which showed how severely limited research in the field was and motivated the work presented in **Chapter 4**. This research in this chapter is currently being prepared for publication. The studies pertaining to pH-gradient loading of EVs in **Chapter 5** are in revision with Molecular Therapy. Additionally, I am a co-author on four accepted or published manuscripts, with others in preparation. I have also had the honor of presenting my work at seven conferences, with one of them winning the judges choice for Best Poster (World Preclinical Congress 2018). Additionally, I have presented talks multiple times at the University level. My accomplishments have been recognized with three travel awards from the University of Maryland, a Career Development Award from the Biomedical Engineering Society, and a 2-year pre-doctoral fellowship from the Pharmaceutical Researchers and Manufacturers of America (PhRMA) Foundation.

Appendix A: Depot delivery of EVs[§§]

Thus far, strategies that have been employed for *in vivo* EV delivery are highly variable [185]. Understanding the effects that delivery mechanisms have on EV potency and off-target effects are essential for eventual translation and commercialization of this therapeutic product. One mechanism of enhancing uptake of EVs at the site of disease or injury is through the incorporation of targeting moieties. Most studies focused on EV targeting, demonstrate the ability to modify EVs for specificity to cancerous cells. EVs modified with peptides that are ligands for the epidermal growth factor receptor (EGFR) were shown to target breast cancer cells in RAG2$^{-/-}$ mice [77]. Other approaches use the C1C2 domain of lactadherin to direct HER2 or EGFR targeting moieties to the EV surface during biogenesis or after EV isolation [186,187]. In a non-cancer example, dendritic cell EVs modified to express Lamp2b, an EV membrane protein, fused to the neuron-specific RVG peptide were able to deliver their cargo to neurons in the brain after systemic injection [14]. Although these targeting moieties appear promising, there has generally been limited success in translating targeted nanoparticles. In particular, as many applications focus on systemic injection of the vesicles, the EVs may not interact with the desired target cells since they would have to pass through vessel walls first and enter the tissue.

While in some cases, systemic delivery has been successfully used to show a functional effect, sequestering these vesicles at the target site will allow for increased potency and

[§§] The experiments in this section were done with the help of Chris Kuffner and Eli Pottash. In particular, they designed the vector for protein expression and purified the protein.

may allow for a decrease in total dosage. Recent studies have shown that controlled delivery via a biomaterial scaffold may overcome potential limitations of non-specific toxicity or high dosage requirements [188–191]. Further, the use of such hybrid systems can allow for differential delivery of multiple types of cargo. Despite promising initial studies, the use of biomaterial carriers compared to free EV administration is not yet well characterized [185] and there remains significant room for advancement in this area.

A number of groups have demonstrated that liposomes and nanoparticles can be used as cross-linkers for hydrogel formation. For example, polyethylene glycol (PEG) modified at either end, has been used to allow liposomes to self-assemble in to shear thinning hydrogels [192,193]. Such models allow for self-assembly and simple manufacturing. Based on these studies, we propose a novel method for an EV-based hydrogel. However, instead of using a PEG linker, we have investigated a protein linker to create a fully biologic depot.

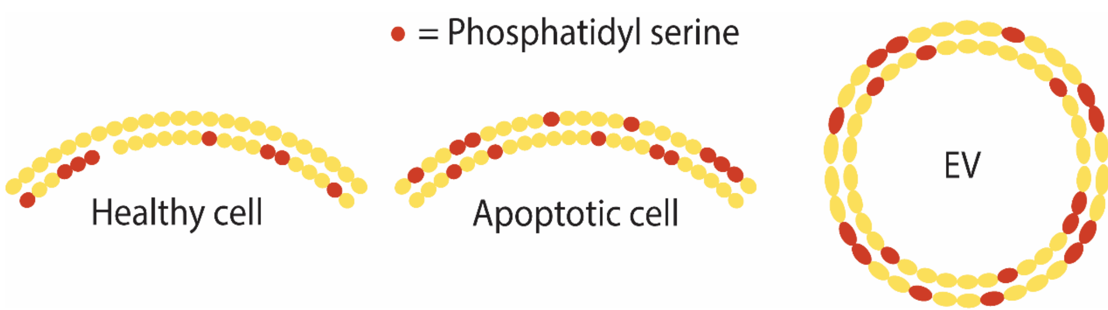

Figure A.1. Phosphatidyl serine distribution in cells and EVs. Apoptotic cells and EVs have a higher level of phosphatidyl serine display on the outer surface.

The design of this structure is based on studies which use the C1C2 domain of lactadherin for targeting purposes. As mentioned above, the C1C2 domain of lactadherin selectively associates with phosphatidyl serine, with a preference for highly curved, small diameter membrane surfaces (**Figure A.1**) [194]. Thus, we propose that introducing a bivalent C1C2, which can bind two EVs and contribute to forming a network (**Figure A.2**).

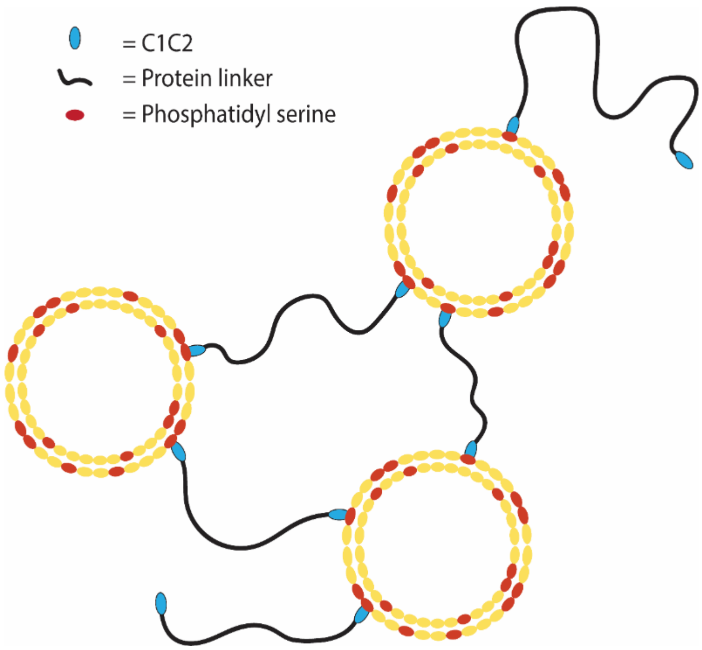

Figure A.2. Schematic of hydrogel structure using a bivalent C1C2 molecule to link EVs. C1C2 associated with phosphatidyl serine and can be used to connect multiple EVs.

Before developing the gel, initial work focused on evaluating the ability to express C1C2 in bacterial cells and confirming binding to EVs. These pilot studies were executed by expressing a C1C2 protein with a green fluorescent protein (GFP) instead of a second C1C2. This allows for ease of validation. C1C2 was expressed in E. coli and purified via affinity chromatography. In short, the protein coding sequence was inserted into the pET45b plasmid (Merck Millipore) via Hifi DNA Assembly (New England Biolabs). The plasmid encoded for a fusion protein (estimated MW ~ 91 kDA), containing: a histidine tag, glutathione S-transferase (GST), a thrombin-cleavage site, enhanced green fluorescent protein (eGFP), and C1C2 (sequence originally obtained as a gift from Ding Xue). After transformation of BL21 (DE3) E. coli (New England Biolabs) with the pET45b-hGST-GFP-C1C2 plasmid, cultures were grown to an OD600 of 0.6 and induced with 0.4 mM IPTG, followed by 19 hour expression at room temperature. Subsequently, the C1C2 protein was purified using a glutathione resin column (GenScript) following the manufacturer's protocol. In the future, the GST tag can be removed through incubation with thrombin.

Western blot results for GFP suggest that the protein effectively is able to bind to EVs (**Figure A.3**). Looking at the protein alone lane in the blot, we can see that we likely are co-purifying fragments of GST and GFP along with the full construct. The band around 37 kD is likely a GST-GFP fragment and close to 20 kD is likely GFP alone. After mixing the protein with EVs for 30 minutes at room temperature and washing through a 300 kD MWCO filter, the smaller molecular weight fractions are washed through. The band expected to contain C1C2 is retained with the EVs, suggesting that the protein has bound to the EVs.

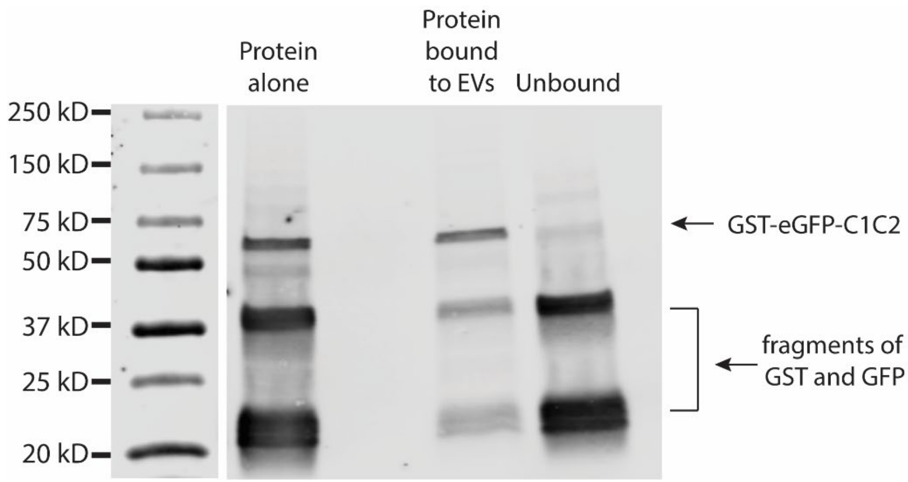

Figure A.3. Western blot for GFP shows that GST-eGFP-C1C2 is able to bind to EVs. The first lane shows the protein purified from bacterial cells. Intact protein is expected to be at 96 kDa. Protein was incubated with EVs for 30 minutes at room temperature and the complex is then washed through a 300 kDa MWCO filter tube. EVs and anything bound to them is retained above the filter. Everything retained above the filter is shown in the lane "Protein bound to EVs." The flow through is in the lane labeled "unbound." Primary antibody for GFP was used

Preliminary studies show that the protein does not induce cell cytotoxicity (**Figure A.4**) when treating HEK293T cells in an alamarBlue assay.

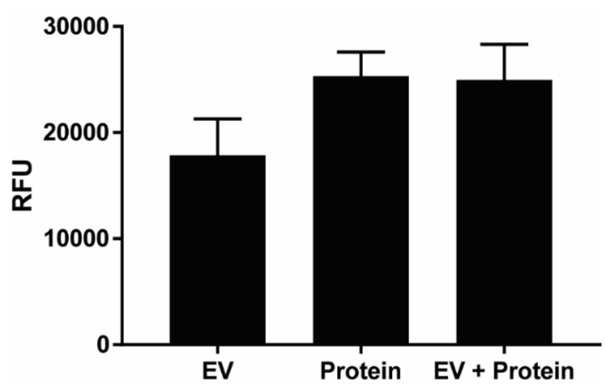

Figure A.4. *In vitro* cytotoxicity. Cytotoxicity is evaluated using an alamarBlue assay. HEK cells were treated with either EVs, protein, or protein bound to EVs. After incubation for five days, alamarBlue reagent was added to each well. Fluorescence measurement were made after incubation.

Ongoing work is focused on further confirming protein binding to EVs as well as evaluating gel formation. Part of this will involve evaluating different lengths of amino acid linker between the two C1C2 domains. An alternative strategy if this bivalent C1C2 approach is not successful is to use this construct to bind EVs into a gel such as fibrin or chitosan for more tunable release. In this case, instead of making a bivalent C1C2 structure, we can have one end of the protein linker be C1C2 and the other end be a peptide with affinity for the gel being used. By modulating the ratio of high and low affinity peptides, we hypothesize that the release profile from gels can be more controllably tuned based on therapeutic need. Upon completion, this delivery technique can then be used in combination with the other methods developed in dissertation to enhance therapeutic potency of EV therapeutics.

Bibliography

1. Pecot C V., Calin GA, Coleman RL, Lopez-Berestein G, Sood AK. RNA interference in the clinic: challenges and future directions. Nat Rev Cancer. 2011 Jan 16;11(1):59–67.
2. Barba AA, Bochicchio S, Dalmoro A, Lamberti G. Lipid Delivery Systems for Nucleic-Acid-Based-Drugs: From Production to Clinical Applications. Pharmaceutics. 2019 Jul 24;11(8):360.
3. Deng Y, Wang CC, Choy KW, Du Q, Chen J, Wang Q, Li L, Chung TKH, Tang T. Therapeutic potentials of gene silencing by RNA interference: Principles, challenges, and new strategies. Gene. 2014 Apr 1;538(2):217–27.
4. Elsabahy M, Nazarali A, Foldvari M. Non-Viral Nucleic Acid Delivery: Key Challenges and Future Directions. Curr Drug Deliv. 2012;
5. Saffari M, Moghimi HR, Dass CR. Barriers to Liposomal Gene Delivery: from Application Site to the Target. Iran J Pharm Res IJPR. 2016;15(Suppl):3–17.
6. Hergenreider E, Heydt S, Tréguer K, Boettger T, Horrevoets AJG, Zeiher AM, Scheffer MP, Frangakis AS, Yin X, Mayr M, Braun T, Urbich C, Boon RA, Dimmeler S. Atheroprotective communication between endothelial cells and smooth muscle cells through miRNAs. Nat Cell Biol. 2012 Feb 12;14(3):249–56.
7. Maria Chiara Deregibus, Vincenzo Cantaluppi, Raffaele Calogero, Marco Lo Iacono, Ciro Tetta, Luigi Biancone, Stefania Bruno, Benedetta Bussolati GC. Endothelial progenitor cell derived microvesicles activate an angiogenic program in endothelial cells by a horizontal transfer of mRNA. Blood. 2007

Oct 1;110(7):2440–8.

8. Chevillet JR, Kang Q, Ruf IK, Briggs HA, Vojtech LN, Hughes SM, Cheng HH, Arroyo JD, Meredith EK, Gallichotte EN, Pogosova-Agadjanyan EL, Morrissey C, Stirewalt DL, Hladik F, Yu EY, Higano CS, Tewari M. Quantitative and stoichiometric analysis of the microRNA content of exosomes. Proc Natl Acad Sci. 2014 Oct 14;111(41):14888–93.

9. Sercombe L, Veerati T, Moheimani F, Wu SY, Sood AK, Hua S. Advances and Challenges of Liposome Assisted Drug Delivery. Front Pharmacol. 2015;6:286.

10. Pattni BS, Chupin V V., Torchilin VP. New Developments in Liposomal Drug Delivery. Chem Rev. 2015 Oct 14;115(19):10938–66.

11. Bulbake U, Doppalapudi S, Kommineni N, Khan W, Bulbake U, Doppalapudi S, Kommineni N, Khan W. Liposomal Formulations in Clinical Use: An Updated Review. Pharmaceutics. 2017 Mar 27;9(4):12.

12. Sahoo S, Klychko E, Thorne T, Misener S, Schultz KM, Millay M, Ito A, Liu T, Kamide C, Agrawal H, Perlman H, Qin G, Kishore R, Losordo DW. Exosomes From Human CD34+ Stem Cells Mediate Their Proangiogenic Paracrine Activity. Circ Res. 2011 Sep 16;109(7):724–8.

13. Zhou Y, Zhou G, Tian C, Jiang W, Jin L, Zhang C, Chen X. Exosome-mediated small RNA delivery for gene therapy. Wiley Interdiscip Rev RNA. 2016 Nov 1;7(6):758–71.

14. Alvarez-Erviti L, Seow Y, Yin H, Betts C, Lakhal S, Wood MJA. Delivery of siRNA to the mouse brain by systemic injection of targeted exosomes. Nat

Biotechnol. 2011 Apr;29(4):341–5.

15. Tominaga N, Kosaka N, Ono M, Katsuda T, Yoshioka Y, Tamura K, Lötvall J, Nakagama H, Ochiya T. Brain metastatic cancer cells release microRNA-181c-containing extracellular vesicles capable of destructing blood–brain barrier. Nat Commun. 2015 Nov 1;6(1):6716.

16. Zhu X, Badawi M, Pomeroy S, Sutaria DS, Xie Z, Baek A, Jiang J, Elgamal OA, Mo X, Perle K La, Chalmers J, Schmittgen TD, Phelps MA. Comprehensive toxicity and immunogenicity studies reveal minimal effects in mice following sustained dosing of extracellular vesicles derived from HEK293T cells. J Extracell Vesicles. 2017 Dec 6;6(1):1324730.

17. Clayton A, Harris CL, Court J, Mason MD, Morgan BP. Antigen-presenting cell exosomes are protected from complement-mediated lysis by expression of CD55 and CD59. Eur J Immunol. 2003 Feb 1;33(2):522–31.

18. Pan B-T, Johnstone RM. Fate of the transferrin receptor during maturation of sheep reticulocytes in vitro: Selective externalization of the receptor. Cell. 1983;33(3):967–78.

19. Abels ER, Breakefield XO. Introduction to Extracellular Vesicles: Biogenesis, RNA Cargo Selection, Content, Release, and Uptake. Cell Mol Neurobiol. 2016 Apr 6;36(3):301–12.

20. EL Andaloussi S, Mäger I, Breakefield XO, Wood MJA. Extracellular vesicles: biology and emerging therapeutic opportunities. Nat Rev Drug Discov. 2013 May;12(5):347–57.

21. Kim KM, Abdelmohsen K, Mustapic M, Kapogiannis D, Gorospe M. RNA in

extracellular vesicles. Wiley Interdiscip Rev RNA. 2017 Jan;e1413.

22. Kalra H, Drummen G, Mathivanan S. Focus on Extracellular Vesicles: Introducing the Next Small Big Thing. Int J Mol Sci. 2016 Feb 6;17(2):170.

23. Maas SLN, Breakefield XO, Weaver AM. Extracellular Vesicles: Unique Intercellular Delivery Vehicles. Trends Cell Biol. 2017 Mar;27(3):172–88.

24. Desrochers LM, Antonyak MA, Cerione RA. Extracellular Vesicles: Satellites of Information Transfer in Cancer and Stem Cell Biology. Dev Cell. 2016 May;37(4):301–9.

25. Ventimiglia LN, Alonso MA. Biogenesis and Function of T Cell-Derived Exosomes. Front cell Dev Biol. 2016;4:84.

26. Colombo M, Raposo G, Théry C. Biogenesis, Secretion, and Intercellular Interactions of Exosomes and Other Extracellular Vesicles. Annu Rev Cell Dev Biol. 2014 Oct 11;30(1):255–89.

27. Ostrowski M, Carmo NB, Krumeich S, Fanget I, Raposo G, Savina A, Moita CF, Schauer K, Hume AN, Freitas RP, Goud B, Benaroch P, Hacohen N, Fukuda M, Desnos C, Seabra MC, Darchen F, Amigorena S, Moita LF, Thery C. Rab27a and Rab27b control different steps of the exosome secretion pathway. Nat Cell Biol. 2010 Jan 6;12(1):19–30.

28. Colombo M, Moita C, van Niel G, Kowal J, Vigneron J, Benaroch P, Manel N, Moita LF, Théry C, Raposo G. Analysis of ESCRT functions in exosome biogenesis, composition and secretion highlights the heterogeneity of extracellular vesicles. J Cell Sci. 2013 Dec 15;126(Pt 24):5553–65.

29. Christ L, Raiborg C, Wenzel EM, Campsteijn C, Stenmark H. Cellular

Functions and Molecular Mechanisms of the ESCRT Membrane-Scission Machinery. Trends Biochem Sci. 2017 Jan;42(1):42–56.

30. Kowal J, Tkach M, Théry C. Biogenesis and secretion of exosomes. Curr Opin Cell Biol. 2014;29:116–25.

31. Stuffers S, Sem Wegner C, Stenmark H, Brech A. Multivesicular Endosome Biogenesis in the Absence of ESCRTs. Traffic. 2009 Jul;10(7):925–37.

32. Gulbins E, Kolesnick R. Raft ceramide in molecular medicine. Oncogene. 2003 Oct 13;22(45):7070–7.

33. van Niel G, Charrin S, Simoes S, Romao M, Rochin L, Saftig P, Marks MS, Rubinstein E, Raposo G. The Tetraspanin CD63 Regulates ESCRT-Independent and -Dependent Endosomal Sorting during Melanogenesis. Dev Cell. 2011 Oct 18;21(4):708–21.

34. Stenmark H. Rab GTPases as coordinators of vesicle traffic. Nat Rev Mol Cell Biol. 2009 Aug 15;10(8):513–25.

35. Iavello A, Frech VSL, Gai C, Deregibus MC, Quesenberry PJ, Camussi G. Role of Alix in miRNA packaging during extracellular vesicle biogenesis. Int J Mol Med. 2016 Apr 12;37(4):958–66.

36. Santangelo L, Giurato G, Cicchini C, Montaldo C, Mancone C, Tarallo R, Battistelli C, Alonzi T, Weisz A, Tripodi M. The RNA-Binding Protein SYNCRIP Is a Component of the Hepatocyte Exosomal Machinery Controlling MicroRNA Sorting. Cell Rep. 2016 Oct 11;17(3):799–808.

37. Villarroya-Beltri C, Baixauli F, Gutiérrez-Vázquez C, Sánchez-Madrid F, Mittelbrunn M. Sorting it out: Regulation of exosome loading. Semin Cancer

Biol. 2014 Oct;28:3–13.

38. Witwer KW, Buzás EI, Bemis LT, Bora A, Lässer C, Lötvall J, Nolte-‘t Hoen EN, Piper MG, Sivaraman S, Skog J, Théry C, Wauben MH, Hochberg F. Standardization of sample collection, isolation and analysis methods in extracellular vesicle research. J Extracell Vesicles. 2013 Jan 24;2(1):20360.

39. Lötvall J, Hill AF, Hochberg F, Buzás EI, Di Vizio D, Gardiner C, Gho YS, Kurochkin I V., Mathivanan S, Quesenberry P, Sahoo S, Tahara H, Wauben MH, Witwer KW, Théry C. Minimal experimental requirements for definition of extracellular vesicles and their functions: a position statement from the International Society for Extracellular Vesicles. J Extracell Vesicles. 2014 Jan 24;3(1):26913.

40. Teixeira JH, Silva AM, Almeida MI, Barbosa MA, Santos SG. Circulating extracellular vesicles: Their role in tissue repair and regeneration. Transfus Apher Sci. 2016;

41. Valadi H, Ekström K, Bossios A, Sjöstrand M, Lee JJ, Lötvall JO. Exosome-mediated transfer of mRNAs and microRNAs is a novel mechanism of genetic exchange between cells. Nat Cell Biol. 2007 Jun 7;9(6):654–9.

42. Mickleburgh I, Burtle B, Hollås H, Campbell G, Chrzanowska-Lightowlers Z, Vedeler A, Hesketh J. Annexin A2 binds to the localization signal in the 3′ untranslated region of c-myc mRNA. FEBS J. 2005 Jan;272(2):413–21.

43. Hollås H, Aukrust I, Grimmer S, Strand E, Flatmark T, Vedeler A. Annexin A2 recognises a specific region in the 3′-UTR of its cognate messenger RNA. Biochim Biophys Acta - Mol Cell Res. 2006;1763(11):1325–34.

44. Filipenko NR, MacLeod TJ, Yoon C-S, Waisman DM. Annexin A2 is a novel RNA-binding protein. J Biol Chem. 2004 Mar 5;279(10):8723–31.

45. Lobb RJ, Lima LG, Möller A. Exosomes: Key mediators of metastasis and pre-metastatic niche formation. Semin Cell Dev Biol. 2017 Jan;

46. Costa-Silva B, Aiello NM, Ocean AJ, Singh S, Zhang H, Thakur BK, Becker A, Hoshino A, Mark MT, Molina H, Xiang J, Zhang T, Theilen T-M, García-Santos G, Williams C, Ararso Y, Huang Y, Rodrigues G, Shen T-L, Labori KJ, Lothe IMB, Kure EH, Hernandez J, Doussot A, Ebbesen SH, Grandgenett PM, Hollingsworth MA, Jain M, Mallya K, Batra SK, Jarnagin WR, Schwartz RE, Matei I, Peinado H, Stanger BZ, Bromberg J, Lyden D. Pancreatic cancer exosomes initiate pre-metastatic niche formation in the liver. Nat Cell Biol. 2015 May 18;17(6):816–26.

47. Antonyak MA, Cerione RA. Microvesicles as Mediators of Intercellular Communication in Cancer. In: Methods in molecular biology (Clifton, NJ). 2014 [cited 2017 Mar 10]. p. 147–73.

48. Santos JC, Ribeiro ML, Sarian LO, Ortega MM, Derchain SF. Exosomes-mediate microRNAs transfer in breast cancer chemoresistance regulation. Am J Cancer Res. 2016;6(10):2129–39.

49. Fujita Y, Yoshioka Y, Ito S, Araya J, Kuwano K, Ochiya T. Intercellular communication by extracellular vesicles and their microRNAs in asthma. Clin Ther. 2014 Jun 1;36(6):873–81.

50. Zhang X, Abels ER, Redzic JS, Margulis J, Finkbeiner S, Breakefield XO. Potential Transfer of Polyglutamine and CAG-Repeat RNA in Extracellular

Vesicles in Huntington's Disease: Background and Evaluation in Cell Culture. Cell Mol Neurobiol. 2016 Apr 7;36(3):459–70.

51. Waldenström A, Ronquist G. Role of Exosomes in Myocardial Remodeling. Circ Res. 2014;114(2).

52. Théry C, Amigorena S, Raposo G, Clayton A, Théry C, Amigorena S, Raposo G, Clayton A. Isolation and Characterization of Exosomes from Cell Culture Supernatants and Biological Fluids. In: Current Protocols in Cell Biology. Hoboken, NJ, USA: John Wiley & Sons, Inc.; 2006 [cited 2017 Mar 10]. p. 3.22.1-3.22.29.

53. Nordin JZ, Lee Y, Vader P, Mäger I, Johansson HJ, Heusermann W, Wiklander OPB, Hällbrink M, Seow Y, Bultema JJ, Gilthorpe J, Davies T, Fairchild PJ, Gabrielsson S, Meisner-Kober NC, Lehtiö J, Smith CIE, Wood MJA, El Andaloussi S. Ultrafiltration with size-exclusion liquid chromatography for high yield isolation of extracellular vesicles preserving intact biophysical and functional properties. Nanomedicine. 2015 May;11(4):879–83.

54. Linares R, Tan S, Gounou C, Arraud N, Brisson AR. High-speed centrifugation induces aggregation of extracellular vesicles. J Extracell vesicles. 2015;4:29509.

55. Böing AN, Pol E van der, Grootemaat AE, Coumans FAWW, Sturk A, Nieuwland R, van der Pol E, Grootemaat AE, Coumans FAWW, Sturk A, Nieuwland R. Single-step isolation of extracellular vesicles by size-exclusion chromatography. J Extracell Vesicles. 2014 Sep 8;3.

56. Stremersch S, De Smedt SC, Raemdonck K. Therapeutic and diagnostic applications of extracellular vesicles. J Control Release. 2016 Dec;244:167–83.

57. Zitvogel L, Regnault A, Lozier A, Wolfers J, Flament C, Tenza D, Ricciardi-Castagnoli P, Raposo G, Amigorena S. Eradication of established murine tumors using a novel cell-free vaccine: dendritic cell derived exosomes. Nat Med. 1998 May;4(5):594–600.

58. Pitt JM, Charrier M, Viaud S, André F, Besse B, Chaput N, Zitvogel L. Dendritic cell-derived exosomes as immunotherapies in the fight against cancer. J Immunol. 2014 Aug 1;193(3):1006–11.

59. Vrijsen KR, Sluijter JPG, Schuchardt MWL, Van Balkom BW., Noort WA, Chamuleau SAJ, Doevendans PAF. Cardiomyocyte progenitor cell-derived exosomes stimulate migration of endothelial cells. J Cell Mol Med. 2010 May;14(5):no-no.

60. Lai RC, Arslan F, Lee MM, Sze NSK, Choo A, Chen TS, Salto-Tellez M, Timmers L, Lee CN, El Oakley RM, Pasterkamp G, de Kleijn DPV, Lim SK. Exosome secreted by MSC reduces myocardial ischemia/reperfusion injury. Stem Cell Res. 2010 May;4(3):214–22.

61. Marote A, Teixeira FG, Mendes-Pinheiro B, Salgado AJ. MSCs-Derived Exosomes: Cell-Secreted Nanovesicles with Regenerative Potential. Front Pharmacol. 2016;7:231.

62. Arslan F, Lai RC, Smeets MB, Akeroyd L, Choo A, Aguor ENE, Timmers L, van Rijen H V., Doevendans PA, Pasterkamp G, Lim SK, de Kleijn DP. Mesenchymal stem cell-derived exosomes increase ATP levels, decrease

oxidative stress and activate PI3K/Akt pathway to enhance myocardial viability and prevent adverse remodeling after myocardial ischemia/reperfusion injury. Stem Cell Res. 2013;10(3):301–12.

63. Pascucci L, Coccè V, Bonomi A, Ami D, Ceccarelli P, Ciusani E, Viganò L, Locatelli A, Sisto F, Doglia SM, Parati E, Bernardo ME, Muraca M, Alessandri G, Bondiolotti G, Pessina A. Paclitaxel is incorporated by mesenchymal stromal cells and released in exosomes that inhibit in vitro tumor growth: A new approach for drug delivery. J Control Release. 2014 Oct;192:262–70.

64. Mizrak A, Bolukbasi MF, Ozdener GB, Brenner GJ, Madlener S, Erkan EP, Ströbel T, Breakefield XO, Saydam O. Genetically Engineered Microvesicles Carrying Suicide mRNA/Protein Inhibit Schwannoma Tumor Growth. Mol Ther. 2013 Jan 1;21(1):101–8.

65. Manfredi F, Di Bonito P, Arenaccio C, Anticoli S, Federico M. Incorporation of Heterologous Proteins in Engineered Exosomes. In Humana Press, New York, NY; 2016 [cited 2016 Jul 8]. p. 249–60.

66. Hartman ZC, Wei J, Glass OK, Guo H, Lei G, Yang X-Y, Osada T, Hobeika A, Delcayre A, Le Pecq J-B, Morse MA, Clay TM, Lyerly HK. Increasing vaccine potency through exosome antigen targeting. Vaccine. 2011 Nov;29(50):9361–7.

67. Yim N, Ryu S-W, Choi K, Lee KR, Lee S, Choi H, Kim J, Shaker MR, Sun W, Park J-H, Kim D, Do Heo W, Choi C. Exosome engineering for efficient intracellular delivery of soluble proteins using optically reversible protein–

protein interaction module. Nat Commun. 2016 Dec 22;7(1):12277.

68. Saari H, Lázaro-Ibáñez E, Viitala T, Vuorimaa-Laukkanen E, Siljander P, Yliperttula M. Microvesicle- and exosome-mediated drug delivery enhances the cytotoxicity of paclitaxel in autologous prostate cancer cells. J Control Release. 2015 Sep 18;220:727–37.

69. Sun D, Zhuang X, Xiang X, Liu Y, Zhang S, Liu C, Barnes S, Grizzle W, Miller D, Zhang H-G. A Novel Nanoparticle Drug Delivery System: The Anti-inflammatory Activity of Curcumin Is Enhanced When Encapsulated in Exosomes. Mol Ther. 2010 Sep;18(9):1606–14.

70. Hadla M, Palazzolo S, Corona G, Caligiuri I, Canzonieri V, Toffoli G, Rizzolio F. Exosomes increase the therapeutic index of doxorubicin in breast and ovarian cancer mouse models. Nanomedicine. 2016 Sep;11(18):2431–41.

71. Didiot M-C, Hall LM, Coles AH, Haraszti RA, Godinho BM, Chase K, Sapp E, Ly S, Alterman JF, Hassler MR, Echeverria D, Raj L, Morrissey D V, DiFiglia M, Aronin N, Khvorova A. Exosome-mediated Delivery of Hydrophobically Modified siRNA for Huntingtin mRNA Silencing. Mol Ther. 2016 Oct 1;24(10):1836–47.

72. O'Loughlin AJ, Mäger I, de Jong OG, Varela MA, Schiffelers RM, El Andaloussi S, Wood MJA, Vader P. Functional Delivery of Lipid-Conjugated siRNA by Extracellular Vesicles. Mol Ther. 2017;

73. Stremersch S, Vandenbroucke RE, Van Wonterghem E, Hendrix A, De Smedt SC, Raemdonck K. Comparing exosome-like vesicles with liposomes for the functional cellular delivery of small RNAs. J Control Release. 2016 Apr

9;232:51–61.

74. El-Andaloussi S, Lee Y, Lakhal-Littleton S, Li J, Seow Y, Gardiner C, Alvarez-Erviti L, Sargent IL, Wood MJA. Exosome-mediated delivery of siRNA in vitro and in vivo. Nat Protoc. 2012 Dec 15;7(12):2112–26.

75. Wahlgren J, De L Karlson T, Brisslert M, Vaziri Sani F, Telemo E, Sunnerhagen P, Valadi H, Karlson TDL, Brisslert M, Vaziri Sani F, Telemo E, Sunnerhagen P, Valadi H. Plasma exosomes can deliver exogenous short interfering RNA to monocytes and lymphocytes. Nucleic Acids Res. 2012 Oct 1;40(17):e130.

76. Lamichhane TN, Raiker RS, Jay SM. Exogenous DNA Loading into Extracellular Vesicles via Electroporation is Size-Dependent and Enables Limited Gene Delivery. Mol Pharm. 2015 Oct 5;12(10):3650–7.

77. Ohno S, Takanashi M, Sudo K, Ueda S, Ishikawa A, Matsuyama N, Fujita K, Mizutani T, Ohgi T, Ochiya T, Gotoh N, Kuroda M. Systemically Injected Exosomes Targeted to EGFR Deliver Antitumor MicroRNA to Breast Cancer Cells. Mol Ther. 2013 Jan;21(1):185–91.

78. Sutaria DS, Badawi M, Phelps MA, Schmittgen TD. Achieving the Promise of Therapeutic Extracellular Vesicles: The Devil is in Details of Therapeutic Loading. Pharm Res. 2017;34(5):1053–66.

79. Kooijmans SAA, Stremersch S, Braeckmans K, de Smedt SC, Hendrix A, Wood MJA, Schiffelers RM, Raemdonck K, Vader P. Electroporation-induced siRNA precipitation obscures the efficiency of siRNA loading into extracellular vesicles. J Control Release. 2013 Nov;172(1):229–38.

80. Aqil F, Munagala R, Jeyabalan J, Agrawal AK, Kyakulaga A-H, Wilcher SA, Gupta RC. Milk exosomes - Natural nanoparticles for siRNA delivery. Cancer Lett. 2019 May 1;449:186–95.

81. Shtam TA, Kovalev RA, Varfolomeeva E, Makarov EM, Kil Y V, Filatov M V. Exosomes are natural carriers of exogenous siRNA to human cells in vitro. Cell Commun Signal. 2013 Nov 18;11(1):88.

82. Haney MJ, Klyachko NL, Zhao Y, Gupta R, Plotnikova EG, He Z, Patel T, Piroyan A, Sokolsky M, Kabanov A V., Batrakova E V. Exosomes as drug delivery vehicles for Parkinson's disease therapy. J Control Release. 2015 Jun;207:18–30.

83. Fuhrmann G, Serio A, Mazo M, Nair R, Stevens MM. Active loading into extracellular vesicles significantly improves the cellular uptake and photodynamic effect of porphyrins. J Control Release. 2015 May;205:35–44.

84. Welch JL, Madison MN, Margolick JB, Galvin S, Gupta P, Martínez-Maza O, Dash C, Okeoma CM. Effect of prolonged freezing of semen on exosome recovery and biologic activity. Sci Rep. 2017 Mar 24;7:45034.

85. Oosthuyzen W, Sime NEL, Ivy JR, Turtle EJ, Street JM, Pound J, Bath LE, Webb DJ, Gregory CD, Bailey MA, Dear JW. Quantification of human urinary exosomes by nanoparticle tracking analysis. J Physiol. 2013 Dec 1;591(23):5833–42.

86. Zhou H, Yuen PST, Pisitkun T, Gonzales PA, Yasuda H, Dear JW, Gross P, Knepper MA, Star RA. Collection, storage, preservation, and normalization of human urinary exosomes for biomarker discovery. Kidney Int.

2006;69(8):1471–6.

87. Zonneveld MI, Brisson AR, van Herwijnen MJC, Tan S, van de Lest CHA, Redegeld FA, Garssen J, Wauben MHM, Hoen EN t. NM. Recovery of extracellular vesicles from human breast milk is influenced by sample collection and vesicle isolation procedures. J Extracell Vesicles. 2014;3(1):24215.

88. Agrawal AK, Aqil F, Jeyabalan J, Spencer WA, Beck J, Gachuki BW, Alhakeem SS, Oben K, Munagala R, Bondada S, Gupta RC. Milk-derived exosomes for oral delivery of paclitaxel. Nanomedicine Nanotechnology, Biol Med. 2017;13(5):1627–36.

89. Zhou Q, Li M, Wang X, Li Q, Wang T, Zhu Q, Zhou X, Wang X, Gao X, Li X. Immune-related microRNAs are abundant in breast milk exosomes. Int J Biol Sci. 2012;8(1):118–23.

90. Munagala R, Aqil F, Jeyabalan J, Gupta RC. Bovine milk-derived exosomes for drug delivery. 2016 Feb 1;371(1):48–61.

91. Revenfeld ALS, Bæk R, Nielsen MH, Stensballe A, Varming K, Jørgensen M. Diagnostic and prognostic potential of extracellular vesicles in peripheral blood. Clin Ther. 2014 Jun 1;36(6):830–46.

92. Jin Y, Chen K, Wang Z, Wang Y, Liu J, Lin L, Shao Y, Gao L, Yin H, Cui C, Tan Z, Liu L, Zhao C, Zhang G, Jia R, Du L, Chen Y, Liu R, Xu J, Hu X, Wang Y. DNA in serum extracellular vesicles is stable under different storage conditions. BMC Cancer. 2016 Sep 23;16(1):753.

93. Tegegn TZ, De Paoli SH, Orecna M, Elhelu OK, Woodle SA, Tarandovskiy

ID, Ovanesov M V., Simak J. Characterization of procoagulant extracellular vesicles and platelet membrane disintegration in DMSO-cryopreserved platelets. J Extracell Vesicles. 2016 Jan 4;5(1):30422.

94. Enderle D, Spiel A, Coticchia CM, Berghoff E, Mueller R, Schlumpberger M, Sprenger-Haussels M, Shaffer JM, Lader E, Skog J, Noerholm M. Characterization of RNA from Exosomes and Other Extracellular Vesicles Isolated by a Novel Spin Column-Based Method. Bouma GJ, editor. PLoS One. 2015 Aug 28;10(8):e0136133.

95. Ge Q, Zhou Y, Lu J, Bai Y, Xie X, Lu Z. miRNA in Plasma Exosome is Stable under Different Storage Conditions. Molecules. 2014 Jan 27;19(2):1568–75.

96. Sarker S, Scholz-Romero K, Perez A, Illanes SE, Mitchell MD, Rice GE, Salomon C. Placenta-derived exosomes continuously increase in maternal circulation over the first trimester of pregnancy. J Transl Med. 2014;12(1):204.

97. Ayers L, Kohler M, Harrison P, Sargent I, Dragovic R, Schaap M, Nieuwland R, Brooks SA, Ferry B. Measurement of circulating cell-derived microparticles by flow cytometry: Sources of variability within the assay. Thromb Res. 2011;127(4):370–7.

98. Muller L, Hong C-S, Stolz DB, Watkins SC, Whiteside TL. Isolation of biologically-active exosomes from human plasma. J Immunol Methods. 2014;411:55–65.

99. Maroto R, Zhao Y, Jamaluddin M, Popov VL, Wang H, Kalubowilage M, Zhang Y, Luisi J, Sun H, Culbertson CT, Bossmann SH, Motamedi M, Brasier AR. Effects of storage temperature on airway exosome integrity for diagnostic

and functional analyses. J Extracell Vesicles. 2017 Jan 13;6(1):1359478.

100. Dubois L, Stridsberg M, Kharaziha P, Chioureas D, Meersman N, Panaretakis T, Ronquist KG. Malignant cell-derived extracellular vesicles express different chromogranin epitopes compared to prostasomes. Prostate. 2015 Jul 1;75(10):1063–73.

101. Madison MN, Roller RJ, Okeoma CM. Human semen contains exosomes with potent anti-HIV-1 activity. Retrovirology. 2014 Nov 19;11(1):102.

102. Madison MN, Jones PH, Okeoma CM. Exosomes in human semen restrict HIV-1 transmission by vaginal cells and block intravaginal replication of LP-BM5 murine AIDS virus complex. Virology. 2015;482:189–201.

103. Lamichhane TN, Sokic S, Schardt JS, Raiker RS, Lin JW, Jay SM. Emerging Roles for Extracellular Vesicles in Tissue Engineering and Regenerative Medicine. Tissue Eng Part B Rev. 2015 Feb 23;21(1):45–54.

104. Lamichhane TN, Jeyaram A, Patel DB, Parajuli B, Livingston NK, Arumugasaamy N, Schardt JS, Jay SM. Oncogene Knockdown via Active Loading of Small RNAs into Extracellular Vesicles by Sonication. Cell Mol Bioeng. 2016;

105. van Balkom BWM, Pisitkun T, Verhaar MC, Knepper MA. Exosomes and the kidney: prospects for diagnosis and therapy of renal diseases. Kidney Int. 2011 Dec;80(11):1138–45.

106. Samuel M, Chisanga D, Liem M, Keerthikumar S, Anand S, Ang C-S, Adda CG, Versteegen E, Jois M, Mathivanan S. Bovine milk-derived exosomes from colostrum are enriched with proteins implicated in immune response and

growth. Sci Rep. 2017 Jul 19;7(1):5933.

107. Jakobsen KR, Paulsen BS, Bæk R, Varming K, Sorensen BS, Jørgensen MM. Exosomal proteins as potential diagnostic markers in advanced non-small cell lung carcinoma. http://dx.doi.org/103402/jev.v426659. 2015;

108. Bæk R, Søndergaard EKL, Varming K, Jørgensen MM. The impact of various preanalytical treatments on the phenotype of small extracellular vesicles in blood analyzed by protein microarray. J Immunol Methods. 2016 Nov;438:11–20.

109. Kalra H, Adda CG, Liem M, Ang CS, Mechler A, Simpson RJ, Hulett MD, Mathivanan S. Comparative proteomics evaluation of plasma exosome isolation techniques and assessment of the stability of exosomes in normal human blood plasma. Proteomics. 2013;

110. Long Tuan Kechik TBZSW. Establishment of the collection, storage and preservation methods and their influence on stability of human salivary exosome. J Biomed Clin Sci. 2018;3(1):44–52.

111. Kreke M, Smith R, Hanscome P, Peck K, Ibrahim A. Processes for producing stable exosome formulations. USPTO; 14/958804, 2016.

112. Szcześ A, Jurak M, Chibowski E. Stability of binary model membranes—Prediction of the liposome stability by the Langmuir monolayer study. J Colloid Interface Sci. 2012 Apr;372(1):212–6.

113. Lőrincz ÁM, Timár CI, Marosvári KA, Veres DS, Otrokocsi L, Kittel Á, Ligeti E. Effect of storage on physical and functional properties of extracellular vesicles derived from neutrophilic granulocytes. J Extracell Vesicles. 2014 Jan

22;3(1):25465.

114. György B, Hung ME, Breakefield XO, Leonard JN. Therapeutic Applications of Extracellular Vesicles: Clinical Promise and Open Questions. Annu Rev Pharmacol Toxicol. 2015 Jan 6;55(1):439–64.

115. Johnsen KB, Gudbergsson JM, Skov MN, Christiansen G, Gurevich L, Moos T, Duroux M. Evaluation of electroporation-induced adverse effects on adipose-derived stem cell exosomes. Cytotechnology. 2016 Oct 8;68(5):2125–38.

116. Leslie SB, Israeli E, Lighthart B, Crowe JH, Crowe LM. Trehalose and sucrose protect both membranes and proteins in intact bacteria during drying. Appl Environ Microbiol. 1995 Oct;61(10):3592–7.

117. Crowe JH, Crowe LM, Carpenter JF, Aurell Wistrom C. Stabilization of dry phospholipid bilayers and proteins by sugars. Biochem J. 1987 Feb 15;242(1):1–10.

118. Jain NK, Roy I. Effect of trehalose on protein structure [Internet]. Vol. 18, Protein Science. Wiley Subscription Services, Inc., A Wiley Company; 2009 [cited 2017 Apr 12]. p. 24–36.

119. Bosch S, de Beaurepaire L, Allard M, Mosser M, Heichette C, Chrétien D, Jegou D, Bach J-M. Trehalose prevents aggregation of exosomes and cryodamage. Sci Rep. 2016 Dec 8;6(1):36162.

120. Sokolova V, Ludwig A-K, Hornung S, Rotan O, Horn PA, Epple M, Giebel B. Characterisation of exosomes derived from human cells by nanoparticle tracking analysis and scanning electron microscopy. Colloids Surf B

Biointerfaces. 2011 Oct 1;87(1):146–50.

121. Jayachandran M, Miller VM, Heit JA, Owen WG. Methodology for isolation, identification and characterization of microvesicles in peripheral blood. J Immunol Methods. 2012;375(1):207–14.

122. Almizraq RJ, Seghatchian J, Holovati JL, Acker JP. Extracellular vesicle characteristics in stored red blood cell concentrates are influenced by the method of detection. Transfus Apher Sci. 2017;56(2):254–60.

123. Grasedieck S, Schöler N, Bommer M, Niess JH, Tumani H, Rouhi A, Bloehdorn J, Liebisch P, Mertens D, Döhner H, Buske C, Langer C, Kuchenbauer F. Impact of serum storage conditions on microRNA stability. Leukemia. 2012;26(11):2414–6.

124. Wiklander OPB, Brennan MÁ, Lötvall J, Breakefield XO, Andaloussi S EL. Advances in therapeutic applications of extracellular vesicles. Sci Transl Med. 2019 May 15;11(492):eaav8521.

125. Kamerkar S, LeBleu VS, Sugimoto H, Yang S, Ruivo CF, Melo SA, Lee JJ, Kalluri R. Exosomes facilitate therapeutic targeting of oncogenic KRAS in pancreatic cancer. Nature. 2017 Jun 7;546(7659):498.

126. Mendt M, Kamerkar S, Sugimoto H, McAndrews KM, Wu C-C, Gagea M, Yang S, Blanko EVR, Peng Q, Ma X, Marszalek JR, Maitra A, Yee C, Rezvani K, Shpall E, LeBleu VS, Kalluri R. Generation and testing of clinical-grade exosomes for pancreatic cancer. JCI insight. 2018 Apr 19;3(8).

127. Vader P, Mol EA, Pasterkamp G, Schiffelers RM. Extracellular vesicles for drug delivery. Adv Drug Deliv Rev. 2016 Feb 26;

128. Armstrong JPK, Stevens MM. Strategic design of extracellular vesicle drug delivery systems. Adv Drug Deliv Rev. 2018;130:12–6.

129. Ferguson SW, Wang J, Lee CJ, Liu M, Neelamegham S, Canty JM, Nguyen J. The microRNA regulatory landscape of MSC-derived exosomes: a systems view. Sci Rep. 2018 Dec 23;8(1):1419.

130. Shimbo K, Miyaki S, Ishitobi H, Kato Y, Kubo T, Shimose S, Ochi M. Exosome-formed synthetic microRNA-143 is transferred to osteosarcoma cells and inhibits their migration. Biochem Biophys Res Commun. 2014 Mar 7;445(2):381–7.

131. Lee J, Lee H, Goh U, Kim J, Jeong M, Lee J, Park J-H. Cellular Engineering with Membrane Fusogenic Liposomes to Produce Functionalized Extracellular Vesicles. ACS Appl Mater Interfaces. 2016 Mar 23;8(11):6790–5.

132. Kao C-Y, Papoutsakis ET. Engineering human megakaryocytic microparticles for targeted delivery of nucleic acids to hematopoietic stem and progenitor cells. Sci Adv. 2018 Nov 7;4(11):eaau6762.

133. Zhang D, Lee H, Zhu Z, Minhas JK, Jin Y. Enrichment of selective miRNAs in exosomes and delivery of exosomal miRNAs in vitro and in vivo. Am J Physiol Cell Mol Physiol. 2017 Jan;312(1):L110–21.

134. Haraszti RA, Miller R, Didiot M-C, Biscans A, Alterman JF, Hassler MR, Roux L, Echeverria D, Sapp E, DiFiglia M, Aronin N, Khvorova A. Optimized Cholesterol-siRNA Chemistry Improves Productive Loading onto Extracellular Vesicles. Mol Ther. 2018 Aug 1;26(8):1973–82.

135. Didiot M-C, Haraszti RA, Aronin N, Khvorova A. Loading of Extracellular

Vesicles with Hydrophobically Modified siRNAs. In Humana Press, New York, NY; 2018 [cited 2018 Dec 17]. p. 199–214.

136. Kim MS, Haney MJ, Zhao Y, Mahajan V, Deygen I, Klyachko NL, Inskoe E, Piroyan A, Sokolsky M, Okolie O, Hingtgen SD, Kabanov A V., Batrakova E V. Development of exosome-encapsulated paclitaxel to overcome MDR in cancer cells. Nanomedicine Nanotechnology, Biol Med. 2016 Apr;12(3):655–64.

137. Nahta R, Yu D, Hung M-C, Hortobagyi GN, Esteva FJ. Mechanisms of Disease: understanding resistance to HER2-targeted therapy in human breast cancer. Nat Clin Pract Oncol. 2006 May;3(5):269–80.

138. Ma L, Kohli M, Smith A. Nanoparticles for Combination Drug Therapy. ACS Nano. 2013 Nov 26;7(11):9518–25.

139. Chakraborty C, Sharma AR, Sharma G, Sarkar BK, Lee SS. The novel strategies for next-generation cancer treatment: miRNA combined with chemotherapeutic agents for the treatment of cancer. Oncotarget. 2018.

140. Huang W, Tian S-S, Hang P-Z, Sun C, Guo J, Du Z-M. Combination of microRNA-21 and microRNA-146a Attenuates Cardiac Dysfunction and Apoptosis During Acute Myocardial Infarction in Mice. Mol Ther Nucleic Acids. 2016 Mar 15;5:e296.

141. Squadrito ML, Baer C, Burdet F, Maderna C, Gilfillan GD, Lyle R, Ibberson M, De Palma M. Endogenous RNAs modulate microRNA sorting to exosomes and transfer to acceptor cells. Cell Rep. 2014 Sep 11;8(5):1432–46.

142. Li J, Chen X, Yi J, Liu Y, Li D, Wang JJ, Hou D, Jiang X, Zhang J, Wang JJ,

Zen K, Yang F, Zhang C-Y, Zhang Y. Identification and Characterization of 293T Cell-Derived Exosomes by Profiling the Protein, mRNA and MicroRNA Components. Gerber AP, editor. PLoS One. 2016 Sep 20;11(9):e0163043.

143. Jeyaram A, Jay SM. Preservation and Storage Stability of Extracellular Vesicles for Therapeutic Applications. AAPS J. 2018;20(1):1.

144. Frank J, Richter M, de Rossi C, Lehr CM, Fuhrmann K, Fuhrmann G. Extracellular vesicles protect glucuronidase model enzymes during freeze-drying. Sci Rep. 2018;

145. Charoenviriyakul C, Takahashi Y, Nishikawa M, Takakura Y. Preservation of exosomes at room temperature using lyophilization. Int J Pharm. 2018 Dec 20;553(1–2):1–7.

146. Park SJ, Jeon H, Yoo S-M, Lee M-S. The effect of storage temperature on the biological activity of extracellular vesicles for the complement system. Vitr Cell Dev Biol - Anim. 2018 Jun 10;54(6):423–9.

147. Quesenberry PJ, Aliotta J, Camussi G, Abdel-Mageed AB, Wen S, Goldberg L, Zhang H-G, Tetta C, Franklin J, Coffey RJ, Danielson K, Subramanya V, Ghiran I, Das S, Chen CC, Pusic KM, Pusic AD, Chatterjee D, Kraig RP, Balaj L, Dooner M. Potential functional applications of extracellular vesicles: a report by the NIH Common Fund Extracellular RNA Communication Consortium [Internet]. Vol. 4, Journal of Extracellular Vesicles. 2015 [cited 2015 Sep 3].

148. Rani S, Ritter T. The Exosome - A Naturally Secreted Nanoparticle and its Application to Wound Healing. Adv Mater. 2015 Dec 17;28(27):5542–52.

149. Katsuda T, Kosaka N, Takeshita F, Ochiya T. The therapeutic potential of mesenchymal stem cell-derived extracellular vesicles. Proteomics. 2013;13(10–11):1637–53.

150. Rani S, Ryan AE, Griffin MD, Ritter T. Mesenchymal Stem Cell-derived Extracellular Vesicles: Toward Cell-free Therapeutic Applications. Mol Ther. 2015;23(5):812–23.

151. Liang X, Zhang L, Wang S, Han Q, Zhao RC. Exosomes secreted by mesenchymal stem cells promote endothelial cell angiogenesis by transferring miR-125a. J Cell Sci. 2016;129(11):2182–9.

152. Bruno S, Grange C, Collino F, Deregibus MC, Cantaluppi V, Biancone L, Tetta C, Camussi G. Microvesicles derived from mesenchymal stem cells enhance survival in a lethal model of acute kidney injury. Câmara NOS, editor. PLoS One. 2012 Jan 14;7(3):e33115.

153. Lee C, Mitsialis SA, Aslam M, Vitali SH, Vergadi E, Konstantinou G, Sdrimas K, Fernandez-Gonzalez A, Kourembanas S. Exosomes mediate the cytoprotective action of mesenchymal stromal cells on hypoxia-induced pulmonary hypertension. Circulation. 2012 Nov 27;126(22):2601–11.

154. Xin H, Li Y, Buller B, Katakowski M, Zhang Y, Wang X, Shang X, Zhang ZG, Chopp M. Exosome-mediated transfer of miR-133b from multipotent mesenchymal stromal cells to neural cells contributes to neurite outgrowth. Stem Cells. 2012 Jul 1;30(7):1556–64.

155. Lee J-K, Park S-R, Jung B-K, Jeon Y-K, Lee Y-S, Kim M-K, Kim Y-G, Jang J-Y, Kim C-W. Exosomes Derived from Mesenchymal Stem Cells Suppress

Angiogenesis by Down-Regulating VEGF Expression in Breast Cancer Cells. PLoS One. 2013;8(12):e84256.

156. Wang X, Gu H, Qin D, Yang L, Huang W, Essandoh K, Wang Y, Caldwell CC, Peng T, Zingarelli B, Fan G-CC. Exosomal MIR-223 Contributes to Mesenchymal Stem Cell-Elicited Cardioprotection in Polymicrobial Sepsis. Sci Rep. 2015 Nov 8;5(1):13721.

157. Liang C-C, Park AY, Guan J-L. In vitro scratch assay: a convenient and inexpensive method for analysis of cell migration in vitro. Nat Protoc. 2007 Jan;2(2):329–33.

158. Luyckx J, Baudouin C. Trehalose: an intriguing disaccharide with potential for medical application in ophthalmology. Clin Ophthalmol. 2011;5:577–81.

159. Yokomise H, Inui K, Wada H, Hasegawa S, Ohno N, Hitomi S. Reliable cryopreservation of trachea for one month in a new trehalose solution. J Thorac Cardiovasc Surg. 1995 Aug 1;110(2):382–5.

160. Taylor MJ, Weegman BP, Baicu SC, Giwa SE. New Approaches to Cryopreservation of Cells, Tissues, and Organs. Transfus Med Hemother. 2019 Jun;46(3):197–215.

161. Chia BS, Low YP, Wang Q, Li P, Gao Z. Advances in exosome quantification techniques. TrAC - Trends Anal Chem. 2017;86:93–106.

162. Pikal-Cleland KA, Cleland JL, Anchordoquy TJ, Carpenter JF. Effect of glycine on pH changes and protein stability during freeze-thawing in phosphate buffer systems. J Pharm Sci. 2002;91(9):1969–79.

163. Gardiner C, Ferreira YJ, Dragovic RA, Redman CWG, Sargent IL.

Extracellular vesicle sizing and enumeration by nanoparticle tracking analysis. J Extracell Vesicles. 2013 Jan;2(1):19671.

164. Antimisiaris S, Mourtas S, Papadia K. Targeted si-RNA with liposomes and exosomes (extracellular vesicles): How to unlock the potential. Int J Pharm. 2017;525(2):293–312.

165. Lane RE, Korbie D, Anderson W, Vaidyanathan R, Trau M. Analysis of exosome purification methods using a model liposome system and tunable-resistive pulse sensing. Sci Rep. 2015;

166. Maurer-Spurej E, Wong KF, Maurer N, Fenske DB, Cullis PR. Factors influencing uptake and retention of amino-containing drugs in large unilamellar vesicles exhibiting transmembrane pH gradients. Biochim Biophys Acta - Biomembr. 1999 Jan 12;1416(1–2):1–10.

167. Bertrand N, Bouvet CC, Moreau P, Leroux J-C. Transmembrane pH-Gradient Liposomes To Treat Cardiovascular Drug Intoxication. ACS Nano. 2010 Dec 28;4(12):7552–8.

168. Li X, Hirsh DJ, Cabral-Lilly D, Zirkel A, Gruner SM, Janoff AS, Perkins WR. Doxorubicin physical state in solution and inside liposomes loaded via a pH gradient. Biochim Biophys Acta - Biomembr. 1998;1415(1):23–40.

169. Harrigan PR, Wong KF, Redelmeier TE, Wheeler JJ, Cullis PR. Accumulation of doxorubicin and other lipophilic amines into large unilamellar vesicles in response to transmembrane pH gradients. BBA - Biomembr. 1993;

170. Qiu L, Jing N, Jin Y. Preparation and in vitro evaluation of liposomal chloroquine diphosphate loaded by a transmembrane pH-gradient method. Int J

Pharm. 2008;

171. Théry C, Witwer KW, Aikawa E, Alcaraz MJ, Anderson JD, Andriantsitohaina R, Antoniou A, Arab T, Archer F, Atkin-Smith GK, Ayre DC, Bach J-M, Bachurski D, Baharvand H, Balaj L, Baldacchino S, Bauer NN, Baxter AA, Bebawy M, Beckham C, Bedina Zavec A, Benmoussa A, Berardi AC, Bergese P, Bielska E, Blenkiron C, Bobis-Wozowicz S, Boilard E, Boireau W, Bongiovanni A, Borràs FE, Bosch S, Boulanger CM, Breakefield X, Breglio AM, Brennan MÁ, Brigstock DR, Brisson A, Broekman ML, Bromberg JF, Bryl-Górecka P, Buch S, Buck AH, Burger D, Busatto S, Buschmann D, Bussolati B, Buzás EI, Byrd JB, Camussi G, Carter DR, Caruso S, Chamley LW, Chang Y-T, Chen C, Chen S, Cheng L, Chin AR, Clayton A, Clerici SP, Cocks A, Cocucci E, Coffey RJ, Cordeiro-da-Silva A, Couch Y, Coumans FA, Coyle B, Crescitelli R, Criado MF, D’Souza-Schorey C, Das S, Datta Chaudhuri A, de Candia P, De Santana EF, De Wever O, del Portillo HA, Demaret T, Deville S, Devitt A, Dhondt B, Di Vizio D, Dieterich LC, Dolo V, Dominguez Rubio AP, Dominici M, Dourado MR, Driedonks TA, Duarte F V, Duncan HM, Eichenberger RM, Ekström K, EL Andaloussi S, Elie-Caille C, Erdbrügger U, Falcón-Pérez JM, Fatima F, Fish JE, Flores-Bellver M, Försönits A, Frelet-Barrand A, Fricke F, Fuhrmann G, Gabrielsson S, Gámez-Valero A, Gardiner C, Gärtner K, Gaudin R, Gho YS, Giebel B, Gilbert C, Gimona M, Giusti I, Goberdhan DC, Görgens A, Gorski SM, Greening DW, Gross JC, Gualerzi A, Gupta GN, Gustafson D, Handberg A, Haraszti RA, Harrison P, Hegyesi H, Hendrix A, Hill AF, Hochberg FH, Hoffmann KF,

Holder B, Holthofer H, Hosseinkhani B, Hu G, Huang Y, Huber V, Hunt S, Ibrahim AG-E, Ikezu T, Inal JM, Isin M, Ivanova A, Jackson HK, Jacobsen S, Jay SM, Jayachandran M, Jenster G, Jiang L, Johnson SM, Jones JC, Jong A, Jovanovic-Talisman T, Jung S, Kalluri R, Kano S, Kaur S, Kawamura Y, Keller ET, Khamari D, Khomyakova E, Khvorova A, Kierulf P, Kim KP, Kislinger T, Klingeborn M, Klinke DJ, Kornek M, Kosanović MM, Kovács ÁF, Krämer-Albers E-M, Krasemann S, Krause M, Kurochkin I V, Kusuma GD, Kuypers S, Laitinen S, Langevin SM, Languino LR, Lannigan J, Lässer C, Laurent LC, Lavieu G, Lázaro-Ibáñez E, Le Lay S, Lee M-S, Lee YXF, Lemos DS, Lenassi M, Leszczynska A, Li IT, Liao K, Libregts SF, Ligeti E, Lim R, Lim SK, Linē A, Linnemannstöns K, Llorente A, Lombard CA, Lorenowicz MJ, Lörincz ÁM, Lötvall J, Lovett J, Lowry MC, Loyer X, Lu Q, Lukomska B, Lunavat TR, Maas SL, Malhi H, Marcilla A, Mariani J, Mariscal J, Martens-Uzunova ES, Martin-Jaular L, Martinez MC, Martins VR, Mathieu M, Mathivanan S, Maugeri M, McGinnis LK, McVey MJ, Meckes DG, Meehan KL, Mertens I, Minciacchi VR, Möller A, Møller Jørgensen M, Morales-Kastresana A, Morhayim J, Mullier F, Muraca M, Musante L, Mussack V, Muth DC, Myburgh KH, Najrana T, Nawaz M, Nazarenko I, Nejsum P, Neri C, Neri T, Nieuwland R, Nimrichter L, Nolan JP, Nolte-'t Hoen EN, Noren Hooten N, O'Driscoll L, O'Grady T, O'Loghlen A, Ochiya T, Olivier M, Ortiz A, Ortiz LA, Osteikoetxea X, Østergaard O, Ostrowski M, Park J, Pegtel DM, Peinado H, Perut F, Pfaffl MW, Phinney DG, Pieters BC, Pink RC, Pisetsky DS, Pogge von Strandmann E, Polakovicova I, Poon IK, Powell BH, Prada I, Pulliam L, Quesenberry P, Radeghieri A, Raffai RL, Raimondo S, Rak J, Ramirez MI, Raposo G, Rayyan MS, Regev-Rudzki N, Ricklefs FL, Robbins PD, Roberts DD, Rodrigues SC, Rohde E, Rome S, Rouschop KM, Rughetti A, Russell AE, Saá P, Sahoo S, Salas-Huenuleo E, Sánchez C, Saugstad JA, Saul MJ, Schiffelers RM, Schneider R, Schøyen TH, Scott A, Shahaj E, Sharma S, Shatnyeva O, Shekari F, Shelke GV, Shetty AK, Shiba K, Siljander PR-M, Silva AM, Skowronek A, Snyder OL, Soares RP, Sódar BW, Soekmadji C, Sotillo J, Stahl PD, Stoorvogel W, Stott SL, Strasser EF, Swift S, Tahara H, Tewari M, Timms K, Tiwari S, Tixeira R, Tkach M, Toh WS, Tomasini R, Torrecilhas AC, Tosar JP, Toxavidis V, Urbanelli L, Vader P, van Balkom BW, van der Grein SG, Van Deun J, van Herwijnen MJ, Van Keuren-Jensen K, van Niel G, van Royen ME, van Wijnen AJ, Vasconcelos MH, Vechetti IJ, Veit TD, Vella LJ, Velot É, Verweij FJ, Vestad B, Viñas JL, Visnovitz T, Vukman K V, Wahlgren J, Watson DC, Wauben MH, Weaver A, Webber JP, Weber V, Wehman AM, Weiss DJ, Welsh JA, Wendt S, Wheelock AM, Wiener Z, Witte L, Wolfram J, Xagorari A, Xander P, Xu J, Yan X, Yáñez-Mó M, Yin H, Yuana Y, Zappulli V, Zarubova J, Žėkas V, Zhang J, Zhao Z, Zheng L, Zheutlin AR, Zickler AM, Zimmermann P, Zivkovic AM, Zocco D, Zuba-Surma EK. Minimal information for studies of extracellular vesicles 2018 (MISEV2018): a position statement of the International Society for Extracellular Vesicles and update of the MISEV2014 guidelines. J Extracell Vesicles. 2018 Jan 23;7(1):1535750.

172. Alexander M, Hu R, Runtsch MC, Kagele DA, Mosbruger TL, Tolmachova T,

Seabra MC, Round JL, Ward DM, O'Connell RM, O'Connell RM. Exosome-delivered microRNAs modulate the inflammatory response to endotoxin. Nat Commun. 2015 Jan 18;6(1):7321.

173. Wu J, Wang Y, Li L. Functional significance of exosomes applied in sepsis: A novel approach to therapy. Biochim Biophys Acta - Mol Basis Dis. 2017 Jan 1;1863(1):292–7.

174. Miksa M, Wu R, Dong W, Komura H, Amin D, Ji Y, Wang Z, Wang H, Ravikumar TS, Tracey KJ, Wang P. Immature dendritic cell-derived exosomes rescue septic animals via milk fat lobule epidermal growth factor-factor VIII. J Immunol. 2009 Nov 1;183(9):5983–90.

175. Xu J, Feng Y, Jeyaram A, Jay SM, Zou L, Chao W. Circulating Plasma Extracellular Vesicles from Septic Mice Induce Inflammation via MicroRNA- and TLR7-Dependent Mechanisms. J Immunol. 2018 Dec 1;201(11):3392–400.

176. Essandoh K, Yang L, Wang X, Huang W, Qin D, Hao J, Wang Y, Zingarelli B, Peng T, Fan G-C. Blockade of exosome generation with GW4869 dampens the sepsis-induced inflammation and cardiac dysfunction. Biochim Biophys Acta - Mol Basis Dis. 2015 Nov 1;1852(11):2362–71.

177. Boldin MP, Taganov KD, Rao DS, Yang L, Zhao JL, Kalwani M, Garcia-Flores Y, Luong M, Devrekanli A, Xu J, Sun G, Tay J, Linsley PS, Baltimore D. miR-146a is a significant brake on autoimmunity, myeloproliferation, and cancer in mice. J Exp Med. 2011 Jun 6;208(6):1189–201.

178. Damas P, Ledoux D, Nys M, Vrindts Y, De Groote D, Franchimont P, Lamy

M. Cytokine serum level during severe sepsis in human IL-6 as a marker of severity. Ann Surg. 1992 Apr;215(4):356–62.

179. Shalova IN, Lim JY, Chittezhath M, Zinkernagel AS, Beasley F, Hernández-Jiménez E, Toledano V, Cubillos-Zapata C, Rapisarda A, Chen J, Duan K, Yang H, Poidinger M, Melillo G, Nizet V, Arnalich F, López-Collazo E, Biswas SK. Human Monocytes Undergo Functional Re-programming during Sepsis Mediated by Hypoxia-Inducible Factor-1α. Immunity. 2015 Mar 17;42(3):484–98.

180. Kalbitz M, Fattahi F, Herron TJ, Grailer JJ, Jajou L, Lu H, Huber-Lang M, Zetoune FS, Sarma JV, Day SM, Russell MW, Jalife J, Ward PA. Complement Destabilizes Cardiomyocyte Function In Vivo after Polymicrobial Sepsis and In Vitro. J Immunol. 2016 Aug 12;1600091.

181. Charoenviriyakul C, Takahashi Y, Morishita M, Nishikawa M, Takakura Y. Role of Extracellular Vesicle Surface Proteins in the Pharmacokinetics of Extracellular Vesicles. Mol Pharm. 2018 Mar 5;15(3):1073–80.

182. Tkach M, Kowal J, Théry C. Why the need and how to approach the functional diversity of extracellular vesicles. Philos Trans R Soc B Biol Sci. 2018 Jan 5;373(1737):20160479.

183. Durcin M, Fleury A, Taillebois E, Hilairet G, Krupova Z, Henry C, Truchet S, Trötzmüller M, Köfeler H, Mabilleau G, Hue O, Andriantsitohaina R, Martin P, Le Lay S. Characterisation of adipocyte-derived extracellular vesicle subtypes identifies distinct protein and lipid signatures for large and small extracellular vesicles. J Extracell Vesicles. 2017 Dec 10;6(1):1305677.

184. Mullokandov G, Baccarini A, Ruzo A, Jayaprakash AD, Tung N, Israelow B, Evans MJ, Sachidanandam R, Brown BD. High-throughput assessment of microRNA activity and function using microRNA sensor and decoy libraries. Nat Methods. 2012 Aug 1;9(8):840–6.

185. Pinheiro A, Silva AM, Teixeira JH, Gonçalves RM, Almeida MI, Barbosa MA, Santos SG. Extracellular vesicles: intelligent delivery strategies for therapeutic applications. J Control Release. 2018 Nov 10;289:56–69.

186. Longatti A, Schindler C, Collinson A, Jenkinson L, Matthews C, Fitzpatrick L, Blundy M, Minter R, Vaughan T, Shaw M, Tigue N. High affinity single-chain variable fragments are specific and versatile targeting motifs for extracellular vesicles. Nanoscale. 2018 Jul 26;10(29):14230–44.

187. Kooijmans SAA, Gitz-Francois JJJM, Schiffelers RM, Vader P. Recombinant phosphatidylserine-binding nanobodies for targeting of extracellular vesicles to tumor cells: a plug-and-play approach. Nanoscale. 2018 Feb 1;10(5):2413–26.

188. Tao S-C, Guo S-C, Li M, Ke Q-F, Guo Y-P, Zhang C-Q. Chitosan Wound Dressings Incorporating Exosomes Derived From MicroRNA-126-Overexpressing Synovium Mesenchymal Stem Cells Provide Sustained Release of Exosomes and Heal Full-Thickness Skin Defects in a Diabetic Rat Model. Stem Cells Transl Med. 2016 Oct 26;sctm.2016-0275.

189. Li M, Ke Q-FF, Tao S-C, Guo S-CC, Rui B-Y, Guo Y-PY-J, Moura LI, Dias AM, Leal EC, Carvalho L, Sousa HC de, Carvalho E, Martin P, Parkhurst SM, Martin P, Li JY, Zhai D, Lv F, Yu QQ, Ma HS, Yin JB, Yi ZF, Liu MY, Chang J, Wu CT, Falanga V, Eming SA, Martin P, Tomic-Canic M, Loot MA,

Kenter SB, Au FL, Galen WJ van, Middelkoop E, Bos JD, Mekkes JR, Ferrier TM, Zuk PA, Zhu M, Ashjian P, Ugarte DA De, Huang JI, Mizuno H, Alfonso ZC, Fraser JK, Benhaim P, Hedrick MH, Bari C De, Dell'Accio F, Tylzanowski P, Luyten FP, Bari C De, Dell'Accio F, Vandenabeele F, Vermeesch JR, Raymackers JM, Luyten FP, Shao Z, Zhang X, Pi Y, Yin L, Li L, Chen H, Zhou C, Ao Y, Jones BA, Pei M, Miranda KC, Huynh T, Tay Y, Ang YS, Tam WL, Thomson AM, Lim B, Rigoutsos I, Ardekani AM, Naeini MM, Ha M, Kim VN, Fish JE, Santoro MM, Morton SU, Yu S, Yeh RF, Wythe JD, Ivey KN, Bruneau BG, Stainier DY, Srivastava D, Kuhnert F, Mancuso MR, Hampton J, Stankunas K, Asano T, Chen CZ, Kuo CJ, Wang S, Aurora AB, Johnson BA, Qi X, McAnally J, Hill JA, Richardson JA, Bassel-Duby R, Olson EN, Nicoli S, Standley C, Walker P, Hurlstone A, Fogarty KE, Lawson ND, Chakraborty C, Sharma AR, Patra B, C., Bhattacharya M, Sharma G, Lee SSH, Li Y, Li Y, Ge P, Ma C, Pitzler L, Auler M, Probst K, Frie C, Bergmeier V, Holzer T, Belluoccio D, Bergen J van den, Etich J, Ehlen H, Zhou Z, Bielke W, Pöschl E, Paulsson M, Brachvogel B, Chistiakov DA, Orekhov AN, Bobryshev Y V., Wu K, Yang Y, Zhong Y, Ammar HM, Zhang P, Guo R, Liu H, Cheng C, Koroscil TM, Chen Y, Liu S, Bihl JC, Rani S, Ritter T, Ozcan G, Ozpolat B, Coleman RL, Sood AK, Lopez-Berestein G, Soutschek J, Akinc A, Bramlage B, Charisse K, Constien R, Donoghue M, Elbashir S, Geick A, Hadwiger P, Harborth J, John M, Kesavan V, Lavine G, Pandey RK, Racie T, Rajeev KG, Röhl I, Toudjarska I, Wang G, Wuschko S, Bumcrot D, Koteliansky V, Limmer S, Manoharan M, Vornlocher HP, Pecot C

V., Calin GA, Coleman RL, Lopez-Berestein G, Sood AK, Chen SH, Zhaori G, Andaloussi S El, Lakhal S, Mager I, Wood MJ, Zhou YS, Zhou G, Tian C, Jiang W, Jin L, Zhang CQY, Chen XG, Zhou J, Wang S, Sun K, Chng WJ, Cocucci E, Meldolesi J, Thery C, Boussac M, Veron P, Ricciardi-Castagnoli P, Raposo G, Garin J, Amigorena S, Xiao D, Ohlendorf J, Chen Y, Taylor DD, Rai SN, Waigel S, Zacharias W, Hao H, McMasters KM, Keerthikumar S, Chisanga D, Ariyaratne D, Saffar H Al, Anand S, Zhao K, Samuel M, Pathan M, Jois M, Chilamkurti N, Gangoda L, Mathivanan S, Valadi H, Ekstrom K, Bossios A, Sjostrand M, Lee JJ, Lotvall JO, Xu H, Lv F, Zhang YL, Yi ZF, Ke Q-FF, Wu CT, Liu MY, Chang J, Pyun DG, Yoon HS, Chung HY, Choi HJ, Heidari F, Razavi M, Bahrololoom ME, Bazargan-Lari R, Vashaee D, Kotturi H, Tayebi L, Rogina A, Rico P, Ferrer GG, Ivankovic M, Ivankovic H, Takei T, Nakahara H, Ijima H, Kawakami K, Shi YY, Li M, Liu Q, Jia ZJ, Xu XC, Cheng Y, Zheng YF, Zhao S, Li L, Wang H, Zhang YL, Cheng X, Zhou N, Rahaman MN, Liu Z, Huang W, Zhang CQY, Meagher MJ, Weiss-Bilka HE, Best ME, Boerckel JD, Wagner DR, Roeder RK, Lee SSH, Elias PM, Proksch E, Menon GK, Mao-Quiang M, Feingold KR, Hu GW, Li Q, Niu X, Hu B, Liu J, Zhou SM, Guo S-CC, Lang HL, Zhang CQY, Wang Y, Deng ZF, Kosaka N, Yoshioka Y, Hagiwara K, Tominaga N, Ochiya T, Montecalvo A, Larregina AT, Morelli AE, Nakamura Y, Ishikawa H, Kawai K, Tabata Y, Suzuki S, Liu YS, Ou ME, Liu H, Gu M, Lv LW, Fan C, Chen T, Zhao XH, Jin CY, Zhang X, Ding Y, Zhou YS, Bello SA, Agunsoye JO, Hassan SB, Li Y, Yuan D, Dong M, Chai Z, Fu G, Müller WEG, Tolba E, Schröder HC, Muñoz-Espí R,

Diehl-Seifert B, Wang X, Chang MC, Ko CC, Douglas WH, Yan W, Zhang CQY, Xia LL, Zhang T, Fang QF, Long T, Guo Y-PY-J, Tang S, Guo Y-PY-J, Zhu Z-A, Coelho TC, Laus R, Mangrich AS, Fávere VT de, Laranjeira MCM, Lawrie G, Keen I, Drew B, Chandler-Temple A, Rintoul L, Fredericks P, Grøndahl L, Muzzarelli R, Tarsi R, Filippini O, Giovanetti E, Biagini G, Varaldo PE, Chen XG, Wang Z, Liu WS, Park HJ, Xie H, Cui Z, Wang L, Xia Z, Hu Y, Xian L, Li C, Xie L, Crane J, Wan M, Zhen G, Bian Q, Yu B, Chang W, Qiu T, Pickarski M, Duong LT, Windle JJ, Luo X, Liao E, Cao X, Ma XY, Feng YF, Ma ZS, Li X, Wang J, Wang L, Lei W, Qi W, Yang C, Dai Z, Che D, Feng J, Mao Y, Cheng R, Wang Z, He X, Zhou T, Gu X, Yan L, Yang X, Ma JX, Gao G. Fabrication of hydroxyapatite/chitosan composite hydrogels loaded with exosomes derived from miR-126-3p overexpressed synovial mesenchymal stem cells for diabetic chronic wound healing. J Mater Chem B. 2016;4(42):6830–41.

190. Zhang K, Zhao X, Chen X, Wei Y, Du W, Wang Y, Liu L, Zhao W, Han Z, Kong D, Zhao Q, Guo Z, Han Z, Liu N, Ma F, Li Z. Enhanced Therapeutic Effects of Mesenchymal Stem Cell-Derived Exosomes with an Injectable Hydrogel for Hindlimb Ischemia Treatment. ACS Appl Mater Interfaces. 2018 Sep 12;10(36):30081–91.

191. Liu X, Yang Y, Li Y, Niu X, Zhao B, Wang Y, Bao C, Xie Z, Lin Q, Zhu L. Integration of stem cell-derived exosomes with in situ hydrogel glue as a promising tissue patch for articular cartilage regeneration. Nanoscale. 2017 Mar 30;9(13):4430–8.

192. Rao Z, Inoue M, Matsuda M, Taguchi T. Quick self-healing and thermo-reversible liposome gel. Colloids Surfaces B Biointerfaces. 2011 Jan;82(1):196–202.

193. Liang Y, Kiick KL. Liposome-Cross-Linked Hybrid Hydrogels for Glutathione-Triggered Delivery of Multiple Cargo Molecules. Biomacromolecules. 2016 Feb 8;17(2):601–14.

194. Shi J, Heegaard CW, Rasmussen JT, Gilbert GE. Lactadherin binds selectively to membranes containing phosphatidyl-l-serine and increased curvature. Biochim Biophys Acta - Biomembr. 2004 Nov 17;1667(1):82–90.